
Daylighting – HVAC Interaction Tests for the Empirical Validation of Building Energy Analysis Tools

**A Report of Task 22, Subtask D
Building Energy Analysis Tools
Project D Empirical Validation**

**Gregory M. Maxwell and Peter G. Loutzenhiser
Department of Mechanical Engineering
Iowa State University
Ames, Iowa**

**Curtis J. Klaassen
Iowa Energy Center
Ames, Iowa**

April 2003



Table of Contents

List of Tables	iv
List of Figures	vi
PREFACE: INTRODUCTION TO THE INTERNATIONAL ENERGY AGENCY	vii
PREFACE: INTRODUCTION TO THE INTERNATIONAL ENERGY AGENCY	vii
BACKGROUND	vii
SOLAR HEATING AND COOLING PROGRAM	vii
Task 22: Building Energy Analysis Tools	ix
Goal and objectives of the task	ix
Scope of the task	ix
Means	x
Participants	x
Executive Summary	xi
1 Introduction	1
1.1 Background and motivation for the work	1
1.2 Overview of the Energy Resource Station	1
1.3 Overview of the testing conducted	2
1.4 Overview of the simulation tools used in the study and participating organizations	3
1.5 Analysis procedure	4
1.5.1 Standard numerical summary	4
1.5.2 Comparative statistics	5
1.5.3 Experimental Uncertainty	6
2 Daylighting Test 1	8
2.1 Description of the exercise	8
2.1.1 Run period and general weather conditions	8
2.1.2 Test rooms operation and control parameters	9
2.1.2.1 Internal loads and general room conditions	9
2.1.2.2 Daylighting controls specifications	9
2.1.2.3 Room-level HVAC controls specifications	12
2.1.3 System-level HVAC operation and control	13
2.1.3.1 Air handling unit controls specifications	13
2.1.3.2 System air specifications	14
2.1.3.3 System fans specifications	14
2.2 Comparison between experimental results and simulation results	15
2.2.1 Weather data	15
2.2.2 Comparison with non-daylight controlled “A” test rooms	17
2.2.2.1 System level results for the “A” system	17
2.2.2.2 Zone level results for the “A” test rooms	20
2.2.2.2.1 Lighting electrical power	20
2.2.3 Comparison with daylight controlled “B” test rooms	33
2.2.3.1 System level results for the “B” system	33
2.2.3.2 Zone level results for the “B” test rooms	35
3 Daylighting Test 2	47
3.1 Description of the exercise	47
3.1.1 Run period and general weather conditions	48

3.1.2 Test rooms operation and control parameters	48
3.1.2.1 Internal loads and general room conditions	48
3.1.2.2 Daylighting controls specifications	50
3.1.2.3 Room-level HVAC controls specifications	52
3.1.3 System-level HVAC operation and control	53
3.1.3.1 Air handling unit controls specifications	53
3.1.3.2 System air specifications	54
3.1.3.3 System fans specifications	54
3.2 Comparison between experimental results and simulation results	55
3.2.1 Weather data	55
3.2.2 Comparison with non-daylight controlled “A” test rooms	57
3.2.2.1 System level results for the “A” system	57
3.2.2.2 Zone level results for the “A” test rooms	59
3.2.3 Comparison with daylight controlled “B” test rooms	71
3.2.3.1 System level results for the “B” system	71
3.2.3.2 Zone level results for the “B” test rooms	73
4 Summary	85
4.1 Thermal stratification	85
4.2 Energy usage with and without daylight	85
4.3 Experimental error	85
4.4 Future work	86
Appendix A Energy Resource Station Specification	87
A.1 INPUT FOR LOAD CALCULATION	87
A.1.1 RUN-PERIOD	87
A.1.2 WEATHER-DATA	87
A.1.3. BUILDING-LOCATION	88
A.1.4. BUILDING-SHADE:	88
A.1.5. FLOOR-PLAN	88
A.1.6 CONSTRUCTION LAYER DESCRIPTION	90
A.1.6.1 LAYER TYPE IDENTIFICATION	90
A.1.6.2 LAYER DESCRIPTION	90
A.1.7 WINDOW TYPE AND DESCRIPTION	93
A.1.8 SPACE DESCRIPTION	93
A.1.8.1 SPACE IDENTIFICATION	93
A.1.8.2 SPACE DESCRIPTION	95
A.1.9. TEST ROOMS OPERATION	98
A.2 INPUT FOR SYSTEM MODEL	99
Appendix B Uncertainty Analysis	101
B.1 Calibration Information	101
B.2 Corrected Data	103
B.3 Propagation of Error	105
Appendix C Hourly Averaged Experimental Data	107
C.1 Weather Data	107
C.2 Hourly averaged data	107
C.3 Air Handling Unit Data	108
C.4 Test Room Data	109

C.5 Exterior Illuminance Data	110
Appendix D Modelers Reports	111
References.....	115

List of Tables

Table 1.1 Participants.....	3
Table 1.2. Output Data.....	4
Table 2.1 Lighting and baseboard power for each test room.....	10
Table 2.2 Lighting and baseboard heating schedules for all test rooms	10
Table 2.3 Reference point illuminance values and light power for the “B” test rooms.	13
Table 2.4 Test room set-point temperatures and airflow rates.....	13
Table 2.5 Statistical comparison of weather parameters	15
Table 2.6 Statistical comparison of AHU-A parameters	18
Table 2.7 Statistical comparison of the daylighting illuminance in the “A” test rooms, Lux	22
Table 2.8 Statistical comparison of the room temperature in the “A” test rooms, °C	24
Table 2.9 Statistical comparison of the supply airflow rates in the “A” test rooms, m ³ /hr	26
Table 2.10 Statistical comparison of the reheat power in the “A” test rooms, W	28
Table 2.11 Statistical comparison of the thermal loads in the “A” test rooms, W	31
Table 2.12 Statistical comparison of AHU-B parameters	33
Table 2.13 Statistical comparison of lighting electrical power in the “B” test rooms, W	35
Table 2.14 Statistical comparison of the daylighting illuminance in the “B” test rooms, Lux	37
Table 2.15 Statistical comparison of the room temperature in the “B” test rooms, °C	39
Table 2.16 Statistical comparison of the supply airflow rates in the “B” test rooms, m ³ /hr	41
Table 2.17 Statistical comparison of the reheat power in the “B” test rooms, W	43
Table 2.18 Statistical comparison of the thermal loads in the “B” test rooms, W.....	45
Table 3.1 Lighting and baseboard power for each test room.....	50
Table 3.2 Lighting and baseboard heating schedules for all test rooms	50
Table 3.3 Reference point illuminance values and light power for the “B” test rooms.	53
Table 3.4 provides values for the temperature set points and airflow rates for the test rooms.....	53
Table 3.5 Statistical comparison of weather parameters.	55
Table 3.6 Statistical comparison of AHU-A parameters	57
Table 3.7 Statistical comparison of the daylighting illuminance in the “A” test rooms, Lux	61
Table 3.8 Statistical comparison of the room temperature in the “A” test rooms, °C	63
Table 3.9 Statistical comparison of the supply airflow rates in the “A” test rooms, m ³ /hr	65
Table 3.10 Statistical comparison of the reheat power in the “A” test rooms, W	67
Table 3.11 Statistical comparison of the room thermal loads in the “A” test rooms, W.....	69
Table 3.12 Statistical comparison of AHU-B parameters	71
Table 3.13 Statistical comparison of lighting electrical power in the “B” test rooms, W	73
Table 3.14 Statistical comparison of the daylighting illuminance in the “B” test rooms, Lux	75
Table 3.15 Statistical comparison of the room temperature in the “B” test rooms, °C	77
Table 3.16 Statistical comparison of the supply airflow rates in the “B” test rooms, m ³ /hr	79
Table 3.17 Statistical comparison of the reheat power in the “B” test rooms, W	81
Table 3.18 Statistical comparison of the room thermal loads in the “B” test rooms, W	83
Table 4.1 Lighting energy comparison for the daylighting test, in kWh.....	85
Table 4.2 Cooling energy comparison for the daylighting test, in kWh.....	85
Table A.1 Identification of construction layers used in the ERS building	90
Table A.2 Thickness and thermal properties used for construction layers	91
Table A.3 Window identification and its characteristics with size.....	94
Table A.4. Identification of plenum and conditioned space	94
Table A.5. Description of the space and details of its six surfaces.....	96

Table B.1 Summary of the fit for the temperature calibration.....	102
Table B.2: Analysis of variance for the temperature calibration.....	102
Table B.3: Parameter estimates for the temperature calibrations.....	102
Table B.4 Summary of the fit for the airflow rate correction.....	104
Table B.5 Analysis of variance for the airflow correction.....	104
Table B.6 Parameter estimates for the airflow correction.....	104
Table B.7 Statistical parameters for uncertainty bound calculations for zone airflow rates.....	105
Table B.8 Accuracy of ERS instrumentation.....	106
Table C.1 Fields modified in the TMY weather files.....	107
Table C.2 AHU System A and System B Nomenclature.....	109
Table C.3 Test rooms (East, South, West, Interior) nomenclature.....	110

List of Figures

Figure 1.1 An ERS test room used for daylighting tests.	3
Figure 2.1 Location of table and light sensor	11
Figure 2.2 Illuminance distribution in the east test rooms, Lux.	11
Figure 2.3 Reference-point illuminance levels as a function of lighting power.	12
Figure 2.5 Weather parameters	16
Figure 2.6 AHU-A parameters.....	19
Figure 2.8 Reference point illuminance values due to daylight in the “A” test rooms.....	23
Figure 2.9 Room temperature values for the “A” test rooms	25
Figure 2.10 Supply airflow rates to the “A” test rooms.....	27
Figure 2.12 Thermal loads for the “A” test rooms.....	32
Figure 2.13 AHU-B parameters.....	34
Figure 2.14 Lighting electrical power values for the “B” test rooms	36
Figure 2.15 Reference point illuminance values due to daylight in the “B” test rooms.....	38
Figure 2.16 Room temperature values for the “B” test rooms.....	40
Figure 2.17 Supply airflow rates to the “B” test rooms	42
Figure 2.18 Reheat power values for the “B” test rooms	44
Figure 3.1 De-stratification fan	48
Figure 3.2(a) Temperature sensors located near windows.....	49
Figure 3.2(b) Temperature sensors located near back wall	49
Figure 3.3 Location of table and light sensor	51
Figure 3.4 Reference-point illuminance levels as a function of lighting power.	52
Figure 3.5 Fan power as a function of volumetric flow rate.....	54
Figure 3.6 Weather parameters	56
Figure 3.7 AHU-A parameters.....	58
Figure 3.8 Lighting electrical power values for the “A” test rooms	60
Figure 3.9 Reference point illuminance values due to daylight in the “A” test rooms.....	62
Figure 3.10 Room temperature values for the “A” test rooms	64
Figure 3.11 Supply airflow rates to the “A” test rooms.....	66
Figure 3.12 Reheat power for the “A” test rooms	68
Figure 3.13 Thermal loads for the “A” test rooms.....	70
Figure 3.14 AHU-B parameters.....	72
Figure 3.15 Lighting electrical power values for the “B” test rooms	74
Figure 3.16 Reference point illuminance values due to daylight in the “B” test rooms.....	76
Figure 3.17 Room temperature values for the “B” test rooms.....	78
Figure 3.18 Supply airflow rates to the “B” test rooms	80
Figure 3.19 Reheat power values for the “B” test rooms	82
Figure 3.20 Thermal load values for the “B” test rooms	84
Figure A.1 A floor plan of the Energy Resource station	89
Figure A.2(a) Geometry presentation for plenum spaces	95
Figure A.2(b) Geometry presentation for conditioned spaces	95
Figure A.4 Zone level HVAC system.....	100
Figure B.1 Hart temperature versus RTD temperature with 95% uncertainty bounds.....	101
Figure B.2 East “A” test room airflow rate correction curve.	103
Figure C.1 Air handling unit schematic.....	108
Figure C.2 Test Room HVAC Schematic.....	110

PREFACE: INTRODUCTION TO THE INTERNATIONAL ENERGY AGENCY

BACKGROUND

The International Energy Agency (IEA) was established in 1974 as an autonomous agency within the framework of the Economic Cooperation and Development (OECD) to carry out a comprehensive program of energy cooperation among its 24 member countries and the Commission of the European Communities.

An important part of the Agency's program involves collaboration in the research, development, and demonstration of new energy technologies to reduce excessive reliance on imported oil, increase long-term energy security, and reduce greenhouse gas emissions. The IEA's R&D activities are headed by the Committee on Energy Research and Technology (CERT) and supported by a small Secretariat staff, headquartered in Paris. In addition, three Working Parties are charged with monitoring the various collaborative energy agreements, identifying new areas for cooperation, and advising the CERT on policy matters.

Collaborative programs in the various energy technology areas are conducted under Implementing Agreements, which are signed by contracting parties (government agencies or entities designated by them). There are currently 40 Implementing Agreements covering fossil fuel technologies, renewable energy technologies, efficient energy end-use technologies, nuclear fusion science and technology, and energy technology information centers.

SOLAR HEATING AND COOLING PROGRAM

The Solar Heating and Cooling Program was one of the first IEA Implementing Agreements to be established. Since 1977, its 21 members have been collaborating to advance active solar, passive solar, and photovoltaic technologies and their application in buildings.

The members are:

Australia	France	Norway
Austria	Germany	Portugal
Belgium	Italy	Spain
Canada	Japan	Sweden
Denmark	Mexico	Switzerland
European Commission	Netherlands	United Kingdom
Finland	New Zealand	United States

A total of 30 Tasks have been initiated, 21 of which have been completed. Each Task is managed by an Operating Agent from one of the participating countries. Overall control of the program rests with an Executive Committee comprised of one representative from each contracting party to the Implementing Agreement. In addition, a number of special ad hoc activities – working groups, conferences, and workshops – have been organized.

The Tasks of the IEA Solar Heating and Cooling Programme, both completed and current, are as follows:

Completed Tasks:

Task 1	Investigation of the Performance of Solar Heating and Cooling Systems
Task 2	Coordination of Solar Heating and Cooling R&D
Task 3	Performance Testing of Solar Collectors
Task 4	Development of an Insolation Handbook and Instrument Package
Task 5	Use of Existing Meteorological Information for Solar Energy Application
Task 6	Performance of Solar Systems Using Evacuated Collectors
Task 7	Central Solar Heating Plants with Seasonal Storage
Task 8	Passive and Hybrid Solar Low Energy Buildings
Task 9	Solar Radiation and Pyranometry Studies
Task 10	Solar Materials R&D
Task 11	Passive and Hybrid Solar Commercial Buildings
Task 12	Building Energy Analysis and Design Tools for Solar Applications
Task 13	Advanced Solar Low Energy Buildings
Task 14	Advanced Active Solar Energy Systems
Task 16	Photovoltaics in Buildings
Task 17	Measuring and Modeling Spectral Radiation
Task 18	Advanced Glazing and Associated Materials for Solar and Building Applications
Task 19	Solar Air Systems
Task 20	Solar Energy in Building Renovation
Task 21	Daylight in Buildings
Task 30	Solar Cities

Current Tasks and Working Groups:

Task 22	Building Energy Analysis Tools
Task 23	Optimization of Solar Energy Use in Large Buildings
Task 24	Solar Procurement
Task 25	Solar Assisted Cooling Systems for Air Conditioning of Buildings
Task 26	Solar Combisystems Working Group Materials in Solar Thermal Collectors
Task 27	Performance Assessment of Solar Building Envelope Components
Task 28	Solar Sustainable Housing
Task 29	Solar Crop Drying
Task 31	Daylight Buildings in the 21st Century

Task 22: Building Energy Analysis Tools

Goal and objectives of the task

The overall goal of Task 22 is to establish a sound technical basis or analyzing solar, low-energy buildings with available and emerging building energy analysis tools. This goal will be pursued by accomplishing the following objectives:

Assess the accuracy of available building energy analysis tools in predicting the performance of widely used solar and low-energy concepts;

Collect and document engineering models of widely used solar and low-energy concepts for use in the next generation building energy analysis tools; and

Assess and document the impact (value) of improved building analysis tools in analyzing solar, low-energy buildings, and widely disseminate research results tools, industry associations, and government agencies.

Scope of the task

This Task will investigate the availability and accuracy of building energy analysis tools and engineering models to evaluate the performance of solar and low-energy buildings. The scope of the Task is limited to whole building energy analysis tools, including emerging modular type tools, and to widely used solar and low-energy design concepts. Tool evaluation activities will include analytical, comparative, and empirical methods, with emphasis given to blind empirical validation using measured data from test rooms of full scale buildings. Documentation of engineering models will use existing standard reporting formats and procedures. The impact of improved building energy analysis will be assessed from a building owner perspective.

The audience for the results of the Task is building energy analysis tool developers and national building energy standards development organizations. However, tool users, such as architects, engineers, energy consultants, product manufacturers, and building owners and managers, are the ultimate beneficiaries of the research, and will be informed through targeted reports and articles.

Means

In order to accomplish the stated goal and objectives, the Participants will carry out research in the framework of four Subtasks:

- Subtask A: Tool Evaluation
- Subtask B: Model Documentation
- Subtask C: Comparative Evaluation
- Subtask D: Empirical Evaluation

Participants

The participants in the Task are: Australia, Canada, Finland, France, Germany, Spain, Sweden, Switzerland, United Kingdom, and United States. The United States serves as Operating Agent for this Task, with Michael J. Holtz of Architectural Energy Corporation providing Operating Agent services on behalf of the U.S. Department of Energy.

This report documents work carried out under Subtask D Empirical Validation.

Executive Summary

Under the auspices of Task 22 of the International Energy Agency's Solar Heating and Cooling Program, two daylighting tests were developed to evaluate the ability of whole-building energy analysis simulation programs to accurately model lighting, heating and cooling energy consumption in a commercial building.

Two tests were conducted at the Energy Resource Station to obtain data sets for use in model validation of daylighting-HVAC interactions. Each test contains five days of data collection. The data sets include measured values of system-level and room-level parameters as well as local weather data necessary to construct weather files for use in the simulations.

This report documents the experimental facility used for the empirical validation exercises, the specifications for each test, and the comparisons between simulation results and experimental results. The two simulation programs that were used for this validation exercise were DOE2.1E and TRNSYS.

Overall, the comparison of daylighting illuminance calculations to measured light levels showed deficiencies in the models under conditions of excessive daylight. For a daylighting controlled space, these deficiencies do not necessarily result in inaccuracies in the predicted reduction of lighting electrical power since in most cases the electric lights are operating at a minimum power level when the daylight levels are high. Results show that the models can predict the light power within 15% of the measured values for a daylight controlled space. Results from this work also show a reduction in cooling energy for the daylight controlled spaces as compared to the non-daylight controlled spaces.

A significant finding of this work showed that thermal stratification within a room affects the heating energy requirements to maintain the space temperature. Because many simulation programs do not account for spatial temperature variation within the space, differences will occur between model predictions and actual energy usage. Based on the results from the tests, an improvement in the agreement between the models and the experimental results of at least 150% was seen.

1 Introduction

1.1 Background and motivation for the work

This project is an extension of the work completed in IEA Task 22, Subtask A. The main goal of this project is to assess the accuracy of building energy analysis tools in predicting the performance of a realistic commercial building with real operating conditions and HVAC equipment. Specifically, this project addresses the accuracy of building energy software to model the interaction between HVAC systems and artificial lighting which is controlled by daylighting. The HVAC system is a variable air volume system utilizing terminal reheat.

Daylighting is the use of exterior sun light to provide light inside the building. Normally the light level on a work plane (desk or table) is maintained at a prescribed level by proper illumination from artificial lights within the space. When sufficient daylight is available, the amount of artificial light can be reduced and the light level on the work plan is maintained at the desired level. Typically a photo sensor measures the light level on the work plan and provides feedback to a dimming controller that adjusts the artificial lights. If sufficient light levels on the work plan can be achieved by day light alone, it is possible to turn off the artificial lights. Aside from the obvious electrical energy savings from reduced power to the lights, there is reduced cooling energy required by the HVAC system since the system no longer has to remove the heat energy created by the lights. However, during the heating season, reductions in the heat produced by the lights results in an increase in HVAC reheat energy.

Tests were conducted at the Energy Resource Station facility to obtain building HVAC system data as well as measured lighting power and light levels for two daylighting control schemes. Concurrent with the system data, local weather data were recorded. The data sets provide modelers with empirical results with which to compare the output from building energy simulation software.

The rationale for the Iowa ERS validation exercise work is as follows:

1. Completion of the Iowa ERS empirical validation study would address designer needs for greater confidence in software tools used to design and analyze passive solar buildings, because realistic commercial construction material and practices are considered.
2. To properly evaluate the amount of “conventional” energy displaced by passive solar design and active solar mechanical equipment, it must be shown that simulations are properly and accurately modeling “conventional” mechanical equipment.
3. The ERS exercises intends to create a suite of test cases for evaluating the capability of building energy analysis tools to model HVAC system and realistic commercial construction buildings.
4. These exercises complement the HVAC BESTEST and the IEA BESTEST work by adding empirical validation to the overall validation process.

1.2 Overview of the Energy Resource Station

The Energy Resource Station (ERS) building is an excellent test facility for conducting empirical validation because it is representative of commercial construction practices and operating conditions.

The ERS is part of the Iowa Energy Center, a non-profit research and education organization funded through and by utilities operating in Iowa. The research portion of the facility has two identical HVAC systems referred to as “A” and “B.” Each system serves four test rooms, three of which have exterior exposures (East, South, and West) and one which is interior. The eight test rooms are often referred to as “paired” in that they are positioned side by side with a particular orientation. The test rooms on the East side of the building are referred to as “East A” and “East B”. Similar pairings exist for the South and West exposures as well as the interior space. Each “A” test room is served by the “A” air handling unit system and each “B” test room is served by the “B” air handling unit system. Each pair of rooms is identical in construction, but differ in that their floor plans are mirror images of each other.

The rooms can be configured to test a variety of HVAC, control and architectural strategies. It is the only public facility in the United States with the ability to simultaneously test full-scale commercial building systems. Detailed data can be collected on any aspect of mechanical and electrical system behavior. With the ability to simultaneously collect detailed weather information, the ERS offers a unique opportunity to have a highly controlled experimental setting for data collection required for simulation tool validation.

A description of the ERS is provided in Appendix A. This description should be sufficient for a modeler to create an input file for energy simulation.

1.3 Overview of the testing conducted

Two tests were conducted in this facility to obtain data sets for use in model validation of daylighting-HVAC interactions. Each test contains five days of data collection. The data sets include measured values of system-level and room-level parameters as well as local weather data necessary to construct weather files for use in the simulations.

For these tests all of the windows in the test rooms were covered with flat sheets of white muslin fabric. The fabric prevented direct rays from the sun from entering the space, thus providing diffuse daylight to each test room. In the “B” test rooms, dimmable ballasts and daylighting controls were used to reduce the power to the fluorescent lights when sufficient daylight was available. The fluorescent lights in the “A” test rooms were non-dimmable. Lights in both the “A” and “B” test rooms were adjusted so that both sets of rooms produced nearly the same light level and used the same light power when the lamps were operated at full power. Figure 1.1 is a photograph of one of the test rooms.



Figure 1.1 An ERS test room used for daylighting tests.

The HVAC system was operated as a variable air volume system with hydronic reheat. The outdoor air dampers were closed and the system operated on 100% recirculated air. In order to increase the cooling load in each test room, two stages of electric baseboard heat were used. The baseboard heaters were scheduled to operate during the day and were off at night. The additional internal load provided greater dynamics to the HVAC system which was seen by increased airflow rates to the rooms.

During the first test, it was observed that a significant amount of vertical temperature stratification occurred when the rooms were in the heating mode. This was a result from using a relatively low minimum airflow rate setting on the VAV terminal units. During the second test, small fans were used to mix the room air and significantly reduce the vertical temperature stratification. During the second test, each test room had one fan that was hung from the ceiling. The fan pointed downwards drawing warm air from near the ceiling and blowing it towards the floor. Details of the air temperature de-stratification are discussed in Section 3.1

1.4 Overview of the simulation tools used in the study and participating organizations

Two organizations participated in the validation exercises. Each organization used a different computer program. Table 1.1 identifies the organization and the simulation tool used.

Table 1.1 Participants

Notation	Program	Implemented by.
DRESDEN	TRNSYS	University of Dresden Dresden, Germany
IOWA	DOE2.1E	Iowa State University Ames, Iowa

1.5 Analysis procedure

An output format was defined, so each participant supplied the same hourly output data. The data considered are given in Table 1.2.

Table 1.2. Output Data

GLOBAL REPORT	
Description	Units
Outside Air Dry Bulb	°C
Outside Air Wet Bulb	°C
Direct Normal Solar Radiation	W/m ²
Total Horizontal Solar Radiation	W/m ²
ZONE REPORT	
Description	Units
Load without ventilation.	W
Zone Temperature	°C
Supply Air flow	m ³ /h
Reheat Energy	W
Luminance level at the reference point	Lux
Lighting electrical power	W
SYSTEM REPORT	
Description	Units
Supply Air flow	m ³ /h
Outside Air flow	m ³ /h
Temp. of air entering cooling coil	°C
Temp. of air leaving cooling coil	°C
Temperature of return air	°C
Cooling coil energy input	W

Statistical parameters were used as the means for comparing simulation results to experimental results. In addition uncertainty analysis and propagation of error analysis of the experimental results were conducted in order to determine confidence limits for the experimental results. The statistical parameters calculated were divided into two general groups: standard numerical summary and comparative statistics.

1.5.1 Standard numerical summary

The standard numerical summaries are the parameters that describe results from an individual measurement or simulation program output. These parameters include: arithmetic mean, standard deviation, and maximum and minimum values. These parameters were calculated for the experimental results as well as the building simulation results.

The arithmetic mean was calculated using the relationship defined by Equation 1.1.

$$\bar{x} = \frac{1}{n} \sum_{i=1}^n x_i \quad (1.1)$$

where:

n is the number of samples.

x_i is the individual value.

The sample standard deviation was calculated using the relationship defined by Equation 1.2.

$$s = \sqrt{\frac{1}{n-1} \sum_{i=1}^n (x_i - \bar{x})^2} \quad (1.2)$$

The maximum value was calculated using the following relationship defined by Equation 1.3

$$x_{max} = \max(x_i) \quad (1.3)$$

while the minimum value was calculated using the relationship defined by Equation 1.4.

$$x_{min} = \min(x_i). \quad (1.4)$$

1.5.2 Comparative statistics

Comparative statistics are used as a measure of the agreement between the output from the simulation programs to results obtained from ERS data. These quantities included: average difference, maximum and minimum differences, average absolute difference, and root mean squared difference.

The average difference is defined by Equation 1.5. This quantity provides relevant summary information about how well the results from the simulation programs compare with the empirical results.

$$\bar{D} = \frac{1}{n} \sum_{i=1}^n (E_i - P_i) \quad (1.5)$$

where:

E_i is the measured experimental value at an instant in time.

P_i is the predicted value for the building simulations, which corresponds to the measured value.

The maximum difference is defined by Equation 1.6. This quantity indicates the magnitude of the greatest error that was found between the experimental value and the simulation result.

$$D_{max} = \max |E_i - P_i| \quad (1.6)$$

The minimum difference is defined by Equation 1.7. This quantity indicates the magnitude of the smallest error that was found between the experimental value and the simulations results.

$$D_{\min} = \min|E_i - P_i| \quad (1.7)$$

The absolute average difference is the absolute value of the difference between the measured parameter at a given instance in time and value predicted by the building for that same instant in time normalized over the entire test. This quantity reflects how well the building simulation predicts hour-by-hour results compared to the empirical results. This quantity was calculated using the relationship defined by Equation 1.8.

$$|\overline{D}| = \frac{1}{n} \sum_{i=1}^n |E_i - P_i| \quad (1.8)$$

A root mean squared comparison is another valuable quantity when comparing the predicted results with the empirical results. This is a more conventional comparison that also accounts for differences without regard to positive or negative signs. This method also reflects how well the building simulation predicted hour-by-hour results compared with the experiment. The quantity was calculated using the relationship defined by Equation 1.9.

$$D_{rms} = \sqrt{\frac{1}{n} \sum_{i=1}^n (E_i - P_i)^2} \quad (1.9)$$

The error for the simulations was calculated in two different ways to quantify how the building simulations performed on an hour-by-hour analysis and over the duration of the experiments. Both parameters are important for the validation process. In the building design phase, where a simulation might be used to quantify energy savings by implementing or removing a hypothetical control scheme, it would be advantageous knowing that the building simulation does a good job predicting the annual energy usage. For other applications, it may be advantageous to accurately predict parameters on an hour-by-hour basis. The summary error, defined by Equation 1.10, is useful for comparing summary quantities.

$$SE = \frac{\sum_{i=1}^n (E_i - P_i)}{\sum_{i=1}^n E_i} \times 100\% \quad (1.10)$$

The instantaneous error, defined by Equation 1.11, is useful in comparing the experiment data with the predicted values at a given instant in time.

$$IE = \frac{\sum_{i=1}^n |E_i - P_i|}{\sum_{i=1}^n E_i} \times 100\% \quad (1.11)$$

1.5.3 Experimental Uncertainty

The experimental uncertainty was calculated for each parameter measured at the ERS or calculated using measured values. For the temperature measurements, calibration information

was used to estimate 95% uncertainty bands from a linear regression analysis. Ninety-five percent uncertainty bands were also calculated from corrected room airflow rates for Daylight Test 2. The uncertainty associated with the measured values of the so-called gold standard for the airflow and temperature regression analyses and other parameters without extensive calibration information were estimated from manufacturers' product information and current literature. Some measurements contained error estimated using statistical analysis as well as some specified error from the manufacturer. For the manufacturer error, a 95% uncertainty interval was estimated by assuming a uniform distribution. The Pythagorean methodology was used to estimate the total experimental error. The total experimental error calculated in Equation 1.12. is the value recommended by BIPM/ISO *Guide* to account for all the errors in the experiment for a 95% uncertainty bound (Gleser, 1998).

$$\sigma = \sqrt{u^2 + \sum \left(\frac{1.96d^2}{3} \right)} \quad (1.12)$$

where

u is a 95% uncertainty band calculated using regression analysis.

d are all errors not found using statistical analyses (i.e. published manufacturer error).

Information regarding the linear analysis for the temperatures and the zone airflow rates for Daylight Case II are described in Appendix B.

Several parameters were not measured directly at the ERS, but were calculated from measured quantities. Therefore, the experimental uncertainty was a function of the parameters required to make this calculation. To estimate the 95% uncertainty limits, uncertainty analysis or propagation of error equation was used. The methods used to perform the calculations are contained in Appendix B.

2 Daylighting Test 1

2.1 Description of the exercise.

This section contains information regarding the operating parameters and conditions used for Daylighting Test 1 conducted at the Energy Resource Station. The test was conducted over an five-day period from April 19 to April 23, 2002

Internal heat loads for the test rooms was produced from electric baseboard heaters. These were scheduled on during a portion of the day and off the remainder of the time. The windows of the test rooms were covered with flat sheets of white muslin fabric. This fabric provided diffuse daylight in the space and prevented direct sunlight for entering the space.

The “B” test rooms were used for the daylighting-HVAC interaction study. Dimmable ballasts in the “B” test rooms allowed for reduction in electric lighting power when sufficient daylight was available in the space. The control scheme permitted the lights to be completely turned off if the light level set point could be achieved from daylighting. The “A” test room lights were operated at full power with no capability of dimming. Ballasts in both the “A” and “B” test rooms were adjusted so that all test rooms produced nearly the same light level and used the same light power when the lamps were operated at full power. The lights in both rooms were operated on a time of day schedule. Light were turned on approximately one hour before sunrise and turned off approximately one hour after sunset.

Thermostats in the test rooms were programmed for a constant heating set-point temperature and a constant cooling set-point temperature. For non-test room spaces in the ERS that are adjacent to the test rooms, the zone thermostats were programmed with the same set-point temperatures as the test rooms. This reduced the thermal interaction between the test rooms and the remainder of the building.

The “A” and “B” systems were operated as variable air volume with hydronic terminal reheat at the zone level. The outdoor air dampers were closed and the systems operated on 100% recirculated air. The systems were run 24 hours per day and chilled water was available for mechanical cooling throughout the test period.

2.1.1 Run period and general weather conditions

This item is used to specify the initial and final dates of the desired simulation period and also the general conditions and location of the ERS facility. The TMY weather file that accompanies this report has ERS weather station information only for the dates of the tests.

- Test dates: April 19, 2002 through April 23, 2002.
- Weather data for the ERS is organized into TMY format. The weather file is called “IEA2002.TMY”.
- Building location
 - Latitude: 41.71 °N
 - Longitude: 93.61 °W
 - Altitude: 285.9 m (938 ft)
 - Time-zone: 6, Central time zone in U.S. Daylight-saving: YES

2.1.2 Test rooms operation and control parameters

This item describes the operation and control of the test rooms that apply to this test.

2.1.2.1 Internal loads and general room conditions

The only internal heating loads used during this test are from ceiling mounted fluorescent lights and baseboard electric heaters. These internal loads were scheduled “ON” for only certain hours during the day. The baseboard heaters have two stages of heat, and for this test, both stages of baseboard heat were used. Due to variations in the installed equipment, the baseboard power is not identical for each unit. Furthermore, slight variations also exist for the lighting power. Table 2.1 provides power values for the lights and baseboard heaters for each test room. For the “B” test rooms, the minimum dimmable light power is shown.

Table 2.2 provides the schedule for the operation of the lights and the first stage of baseboard heat used in this test. The time represents the beginning of each hour where 1 represents 1 AM and 24 represents midnight.

2.1.2.2 Daylighting controls specifications

The dimmable ballasts in each exterior “B” test room were controlled based on light-level measurements made at a single reference point in the room. Each test room had a table with a sensor on it located near the room center. The sensor pointed upwards and measured illuminance coming from all directions within a hemispherical field of view. Light incident on the sensor was the sum of daylight into the space and artificial light from the ceiling mounted lamps. The “A” test rooms had identical table and sensor locations. The lights in the “A” test rooms were not dimmed, but operated at maximum output during the day. Figure 2.1 illustrates the table and sensor location for the test rooms. Figure 2.2 illustrates the illuminance distribution within the East “A” and “B” test rooms from the fluorescent lights. The illuminance measurements were made at table-height. The other test rooms had similar illuminance distributions.

The lighting control sequence was based on an illuminance set-point level of 646.8 lux (60 foot-candles) measured at the reference point. As the amount of daylight in the space increased, the power output from the ballasts to the lights decreased in order to maintain the illuminance set point. The minimum power output from the dimmable ballasts was approximately 24% of the maximum ballast power output. (Refer to Table 2.1 for actual values.) If the ballasts power output was at the minimum value and the daylight levels in the space continued to increase such that the illuminance at the reference point exceeded 645.8 lux (60 foot-candles), then the room lights were turned off. The lights were turned back on when the illuminance at the reference point dropped below 538.2 lux (50 foot-candles).

Table 2.1 Lighting and baseboard power for each test room.

Room	Stage 1 W	Stage 2 W	Maximum Lights, W	Minimum Lights, W
East A	900	880	358.5	NA
East B	875	845	359.5	89.1
South A	885	875	359.0	NA
South B	870	875	367.5	89.4
West A	855	845	361.5	NA
West B	855	885	364.0	85.8
Interior A	865	880	354.3	NA
Interior B	915	900	360.0	NA

Table 2.2 Lighting and baseboard heating schedules for all test rooms

Hour	Lights	Stage 1&2 Baseboard	Hour	Lights	Stage 1&2 Baseboard
1	OFF	OFF	13	ON	ON
2	OFF	OFF	14	ON	ON
3	OFF	OFF	15	ON	ON
4	OFF	OFF	16	ON	ON
5	ON	OFF	17	ON	OFF
6	ON	OFF	18	ON	OFF
7	ON	OFF	19	ON	OFF
8	ON	ON	20	ON	OFF
9	ON	ON	21	OFF	OFF
10	ON	ON	22	OFF	OFF
11	ON	ON	23	OFF	OFF
12	ON	ON	24	OFF	OFF

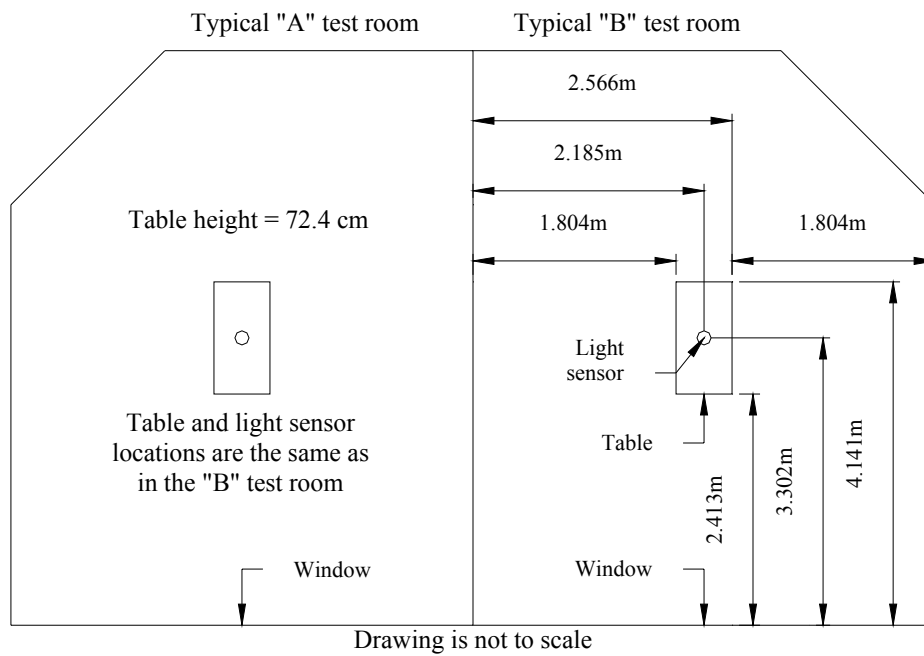


Figure 2.1 Location of table and light sensor

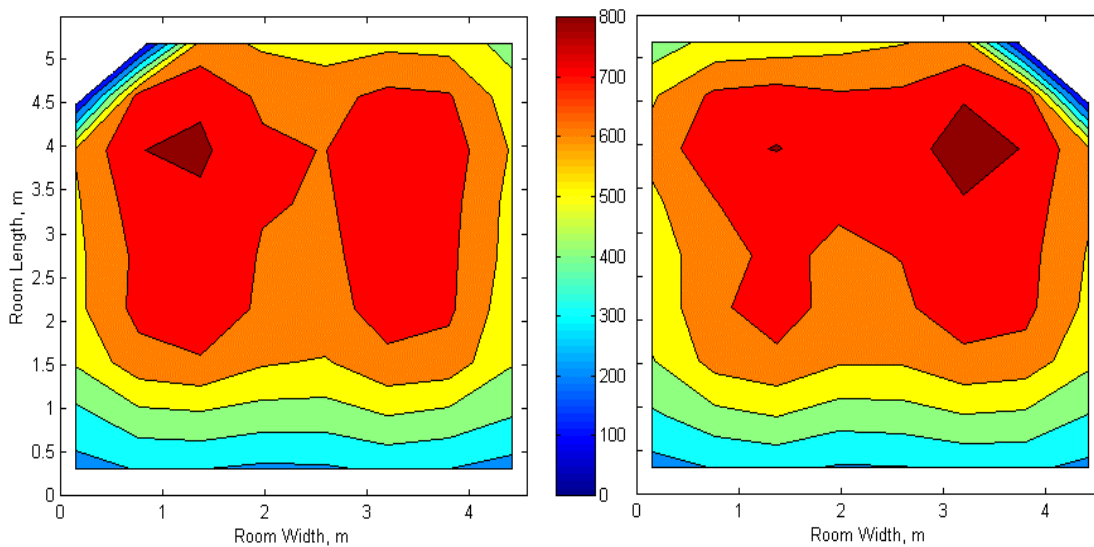


Figure 2.2 Illuminance distribution in the east test rooms, Lux.

Because the lighting control is based on total (artificial light plus daylight) illuminance at the reference point, it is important for the modeler to know the relationship between lighting power and the illuminance at the reference point due to artificial lights alone. Figure 2.2 is a plot of the illuminance at the reference point as a function of power to the room lights. The graph includes data for each of the three exterior “B” test rooms. Values used to create Figure 2.3 are provided in Table 2.3.

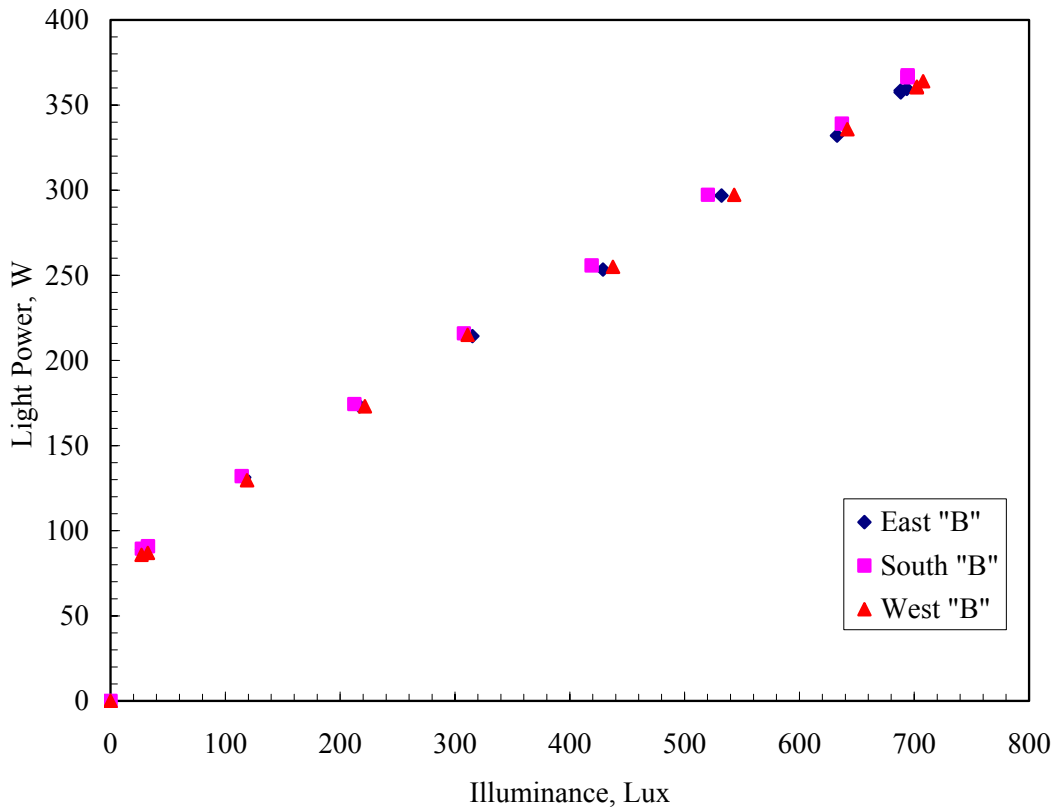


Figure 2.3 Reference-point illuminance levels as a function of lighting power.

2.1.2.3 Room-level HVAC controls specifications

Space temperature conditions were maintained by utilizing variable airflow rates (VAV) for space cooling and hydronic reheat for space heating. The cooling and heating set-point temperatures were the same for all test rooms and their values remained fixed throughout the test.

In heating mode the terminal unit operates at a prescribed minimum airflow rate, and the two-way hot water control valve modulates in response to the zone heating needs. In cooling mode, the two-way hot water control valve is closed, and the terminal unit modulates the primary supply airflow rate in response to the zone cooling needs. In addition to a minimum airflow rate,

Table 2.3 Reference point illuminance values and light power for the “B” test rooms.

East “B” Test Room		South “B” Test Room		West “B” Test Room	
Light Power W	Illuminance Lux	Light Power W	Illuminance Lux	Light Power W	Illuminance Lux
0.0	0.000	0.0	0.000	0.0	0.000
89.1	27.437	89.4	27.222	85.8	27.017
90.3	31.764	90.9	32.668	86.9	32.421
131.3	116.465	132.0	114.366	129.6	118.909
173.1	216.957	174.4	212.415	173.1	221.500
214.3	315.178	215.9	307.815	215.0	310.980
253.4	428.877	255.8	419.125	255.0	437.617
296.8	532.146	297.3	520.370	297.3	543.243
332.0	632.713	339.0	637.094	335.8	641.798
357.5	688.222	366.3	694.272	360.5	702.344
359.5	693.604	367.5	694.272	364.0	707.726
358.5	688.222	366.5	694.272	360.8	702.344

each unit has a maximum airflow rate. The values of these airflow rates depend on whether the room is an exterior room or an interior room. Table 2.4 provides values for the temperature set points and airflow rates for the test rooms.

Table 2.4 Test room set-point temperatures and airflow rates

Test room Location	Heating set-point Temperature, °C	Cooling set-point Temperature, °C	Minimum airflow rate m ³ /hr	Maximum airflow rate m ³ /hr
Interior	22.2	22.8	340	934
Exterior	22.2	22.8	340	1,699

2.1.3 System-level HVAC operation and control

This item describes the operation and control of the air handling systems that apply to this test. The air handling units for both the “A” and “B” systems were operated in the same manner throughout this test.

2.1.3.1 Air handling unit controls specifications

The system controls were specified as follows:

Heating schedule: always available

Cooling schedule: always available

Cooling control supply air temperature set point after the fan: 15.6 °C (60 °F)

Preheat: NOT available

Humidity control: NOT available

Economizer: disabled

Outside air control: disabled (0 % outside air)

2.1.3.2 System air specifications

The system airflow rates were specified as follows:

Supply air flow rate: maximum 6,031 m³/hr (3,550 cfm)

Return air path: plenum

Minimum outside air flow: none

Outside air control: none

Duct air loss: none

Duct heat gain: negligible

2.1.3.3 System fans specifications

The air-handling unit fans are specified as follows:

Supply air static pressure: 348.4 Pa (1.4 inch H₂O)

Fan schedule: always on

Supply fan power versus supply flow rate (See Figure 2.4)

Supply fan control: 348.4 Pa (1.4 inch H₂O)

Return fan control differential: 340 m³/h (200 cfm) offset

Motor placement: In-air flow

Fan placement: Draw-through

Figure 2.4 shows the relationship between supply fan power and supply airflow rate. A quadratic regression analysis of the data is shown on the graph.

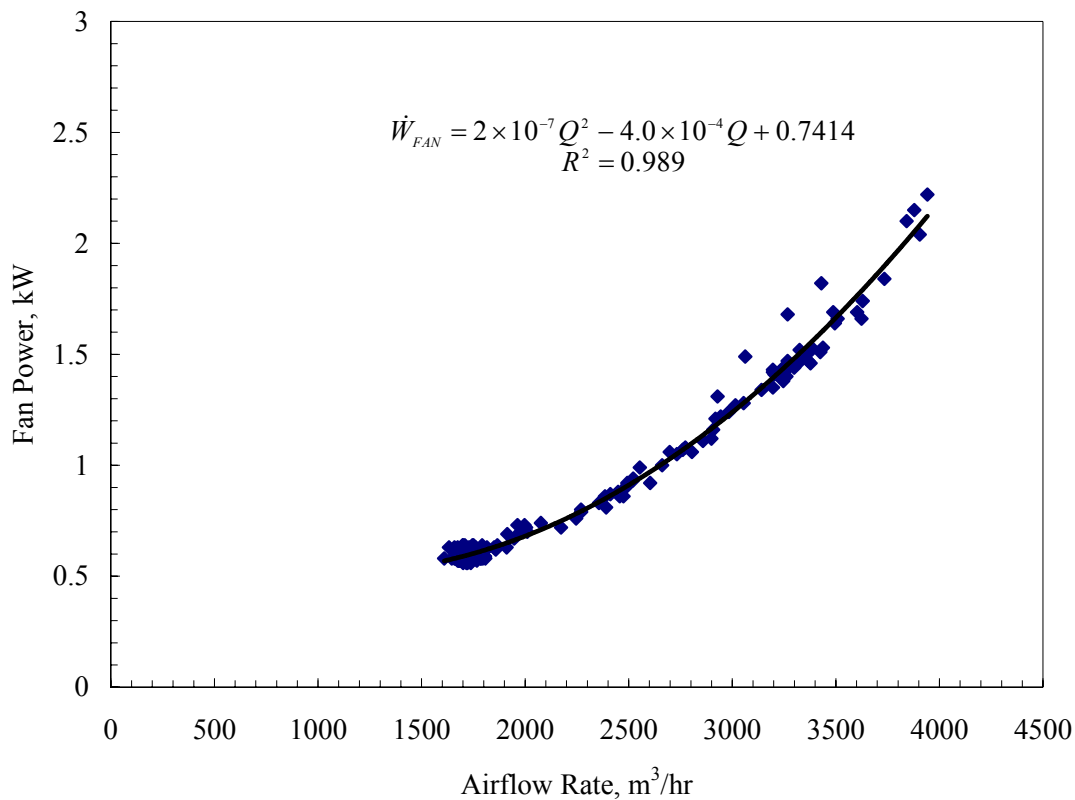


Figure 2.4 Fan power as a function of volumetric airflow rate

2.2 Comparison between experimental results and simulation results

In this section the results from the computer simulations are compared with the values obtained from the experiments run at the ERS. The comparisons are made both graphically and statistically. The statistical parameters used were defined in Section 1.5. In general comparisons will be made using the average difference (experimental result minus model prediction) and the 95% uncertainty bounds based on experimental error. An indication that the model is in agreement with the experiment is when the average difference lies within this interval.

Before comparing the results for any system or zone level parameters, the weather information used by each model must be validated. Weather data collected at the ERS were converted to TMY format and provided to each modeler. Comparison of the key weather parameters is a test to assure each program's weather processor is correctly interpreting the provided weather information.

2.2.1 Weather data

The key weather parameters are dry-bulb and wet-bulb temperatures, direct normal solar irradiation, and total horizontal solar irradiation. Table 2.5 gives the statistical comparison of the temperatures and solar fluxes, respectively. Figure 2.5 illustrates the weather parameters during the 5-day test period. The agreement between the ERS data and the models is acceptable, and indicates that the models are accurately processing the ERS weather data.

Table 2.5 Statistical comparison of weather parameters

Statistical Parameter	Dry-bulb temperature, °C			Wet-bulb temperature, °C			Direct normal irradiation, W/m ²			Total horizontal irradiation, W/m ²		
	ERS	DOE2.1E	TRNSYS	ERS	DOE2.1E	TRNSYS	ERS	DOE2.1E	TRNSYS	ERS	DOE2.1E	TRNSYS
\bar{x}	9.2	9.2	9.2	6.8	6.8	6.8	137.8	138.3	138.3	172.7	174.1	174.1
σ												
s	5.0	5.0	5.0	3.7	3.7	3.7	280.6	281.8	281.8	256.6	258.4	258.4
x_{\max}	22.8	22.8	22.8	16.7	16.7	16.7	922.6	926.8	926.8	889.0	892.2	892.2
x_{\min}	2.2	2.2	2.2	1.7	1.7	1.7	0.0	0.0	0.0	0.0	0.0	0.0
\bar{D}		0.0	0.0		0.0	0.0		-0.5	-0.5		-1.4	-1.4
D_{\max}		0.0	0.0		0.0	0.0		5.9	5.9		41.0	41.0
D_{\min}		0.0	0.0		0.0	0.0		0.0	0.0		0.0	0.0
$ D $		0.0	0.0		0.0	0.0		0.8	0.8		1.6	1.6
D_{rms}		0.0	0.0		0.0	0.0		1.6	1.6		6.1	6.1
SE		0.0	0.0		0.0	0.0		-0.4	-0.4		-0.8	-0.8
IE		0.0	0.0		0.0	0.0		0.6	0.6		0.9	0.9

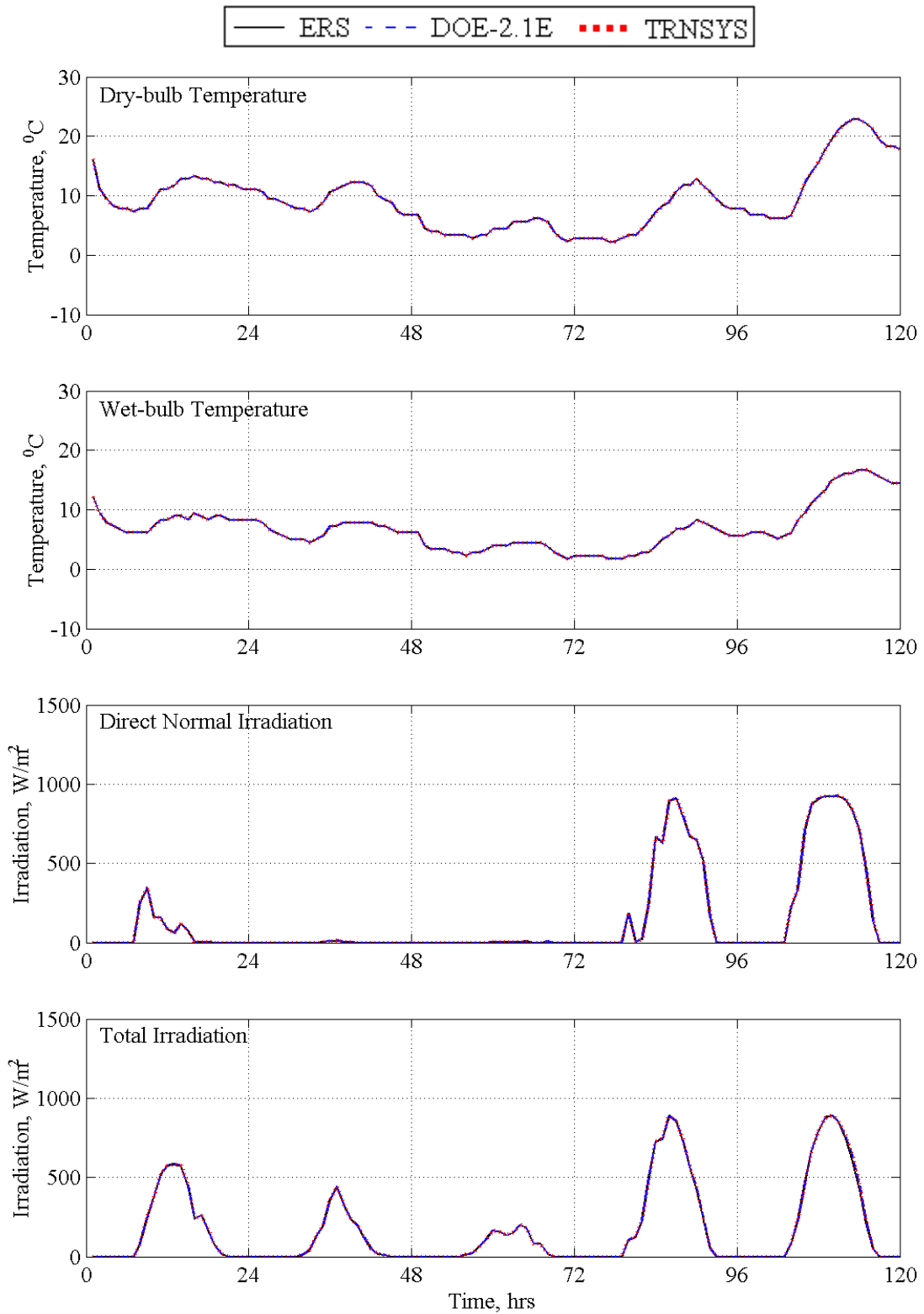


Figure 2.5 Weather parameters

2.2.2 Comparison with non-daylight controlled “A” test rooms

As described in Section 2.1, the “A” test rooms did not use daylight controls. Modelers simulated this condition, and in this section the results from the models are compared to the experimental values.

2.2.2.1 System level results for the “A” system

Air handling unit “A” supplies air to the “A” test rooms. As was shown Table 1.2, the parameters generally used for system-level comparison are the supply airflow rate, the outside airflow rate, the temperature of air entering cooling coil, the temperature of air leaving cooling coil, the temperature of return air, and the cooling coil heat transfer rate. However, for this test, the outside airflow rate was specified to equal zero; therefore, the air temperature entering the cooling coil equals the return air temperature. Thus in the comparisons that follow, the outdoor airflow rate and inlet air temperature to the cooling coil are omitted.

The cooling coil heat transfer rate was calculated using Equation 2.1. While this equation only accounts for the sensible cooling load, this is acceptable since there were no latent loads in the test rooms and no outdoor air was used for the system.

$$CHTR = \frac{Qp}{RT_{LAT}} c_p (T_{LAT} - T_{EAT}) \quad (2.1)$$

where

Q is the system airflow rate

p is the ambient pressure

R is the gas constant for air

T_{LAT} is the air temperature at the coil inlet

c_p is the constant specific heat of air

T_{EAT} is the air temperature at the coil exit

Table 2.6 provides a statistical summary of the air handling unit parameters, while Figure 2.6 shows the graphical results for the five days of the test. The TRNSYS model over predicts the supply airflow rates during most of the test days.

Table 2.6 Statistical comparison of AHU-A parameters

Statistical Parameter	Supply airflow rate, m ³ /hr			Return air temperature, °C			Leaving coil air temperature, °C			Cooling coil heat transfer rate, kW		
	ERS	DOE2.1E	TRNSYS	ERS	DOE2.1E	TRNSYS	ERS	DOE2.1E	TRNSYS	ERS	DOE2.1E	TRNSYS
\bar{x}	1911.1	1944.0	2293.8	23.8	23.3	22.6	14.0	13.5	14.1	6.0	6.2	6.1
σ	31.6			0.2			0.2			0.8		
s	732.3	866.2	1221.0	0.5	0.3	0.3	0.1	0.6	0.0	2.4	2.4	3.5
x_{\max}	3773.0	4252.0	4618.0	24.8	24.0	23.0	14.3	14.8	14.1	11.8	12.5	12.8
x_{\min}	1356.0	1359.0	1360.0	22.4	22.7	22.3	13.6	13.0	14.1	3.9	4.4	3.5
\bar{D}		-33.0	-382.7		0.5	1.2		0.5	-0.1		-0.2	-0.1
D_{\max}		716.0	1677.0		1.9	2.2		1.2	0.5		2.0	3.7
D_{\min}		0.0	0.0		0.0	0.0		0.0	0.0		0.0	0.1
$ D $		132.3	447.7		0.8	1.3		0.8	0.1		0.5	1.2
D_{rms}		197.5	692.0		0.9	1.4		0.8	0.2		0.6	1.4
SE		-1.7	-16.7		2.1	5.5		3.5	-0.9		-3.7	-2.2
IE		6.8	19.5		3.2	5.6		5.6	1.0		7.6	20.2

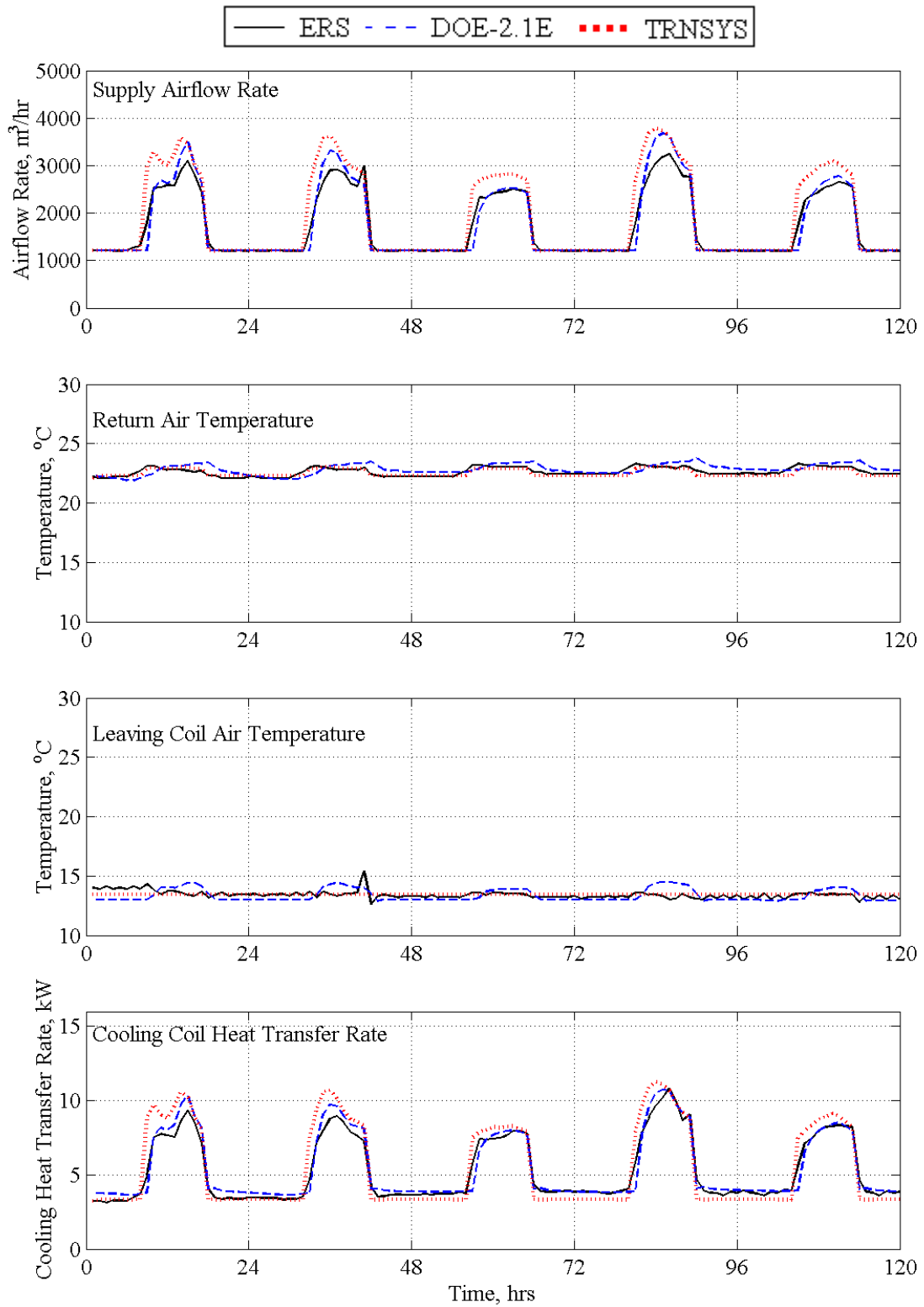


Figure 2.6 AHU-A parameters

2.2.2.2 Zone level results for the “A” test rooms

In this section, comparisons are made for the zone-level parameters. As was shown in Table 1.2, the zone-level parameters used for comparison are: the lighting electrical power, the luminance level at the reference point, the zone temperature, the supply airflow rate, the reheat energy, and the thermal load (without ventilation).

2.2.2.2.1 Lighting electrical power

Figure 2.7 shows the graphical results of the lighting electrical power. Because daylighting controls were not used for the “A” test rooms, the lighting electrical power remains constant while the lights are scheduled on and zero when the lights are scheduled off. Because this parameter is an input, it is expected that each model will produce the same results unless an input error has occurred. The plots show 100% agreement between the experiment and the models. A statistical comparison is not necessary for this parameter.

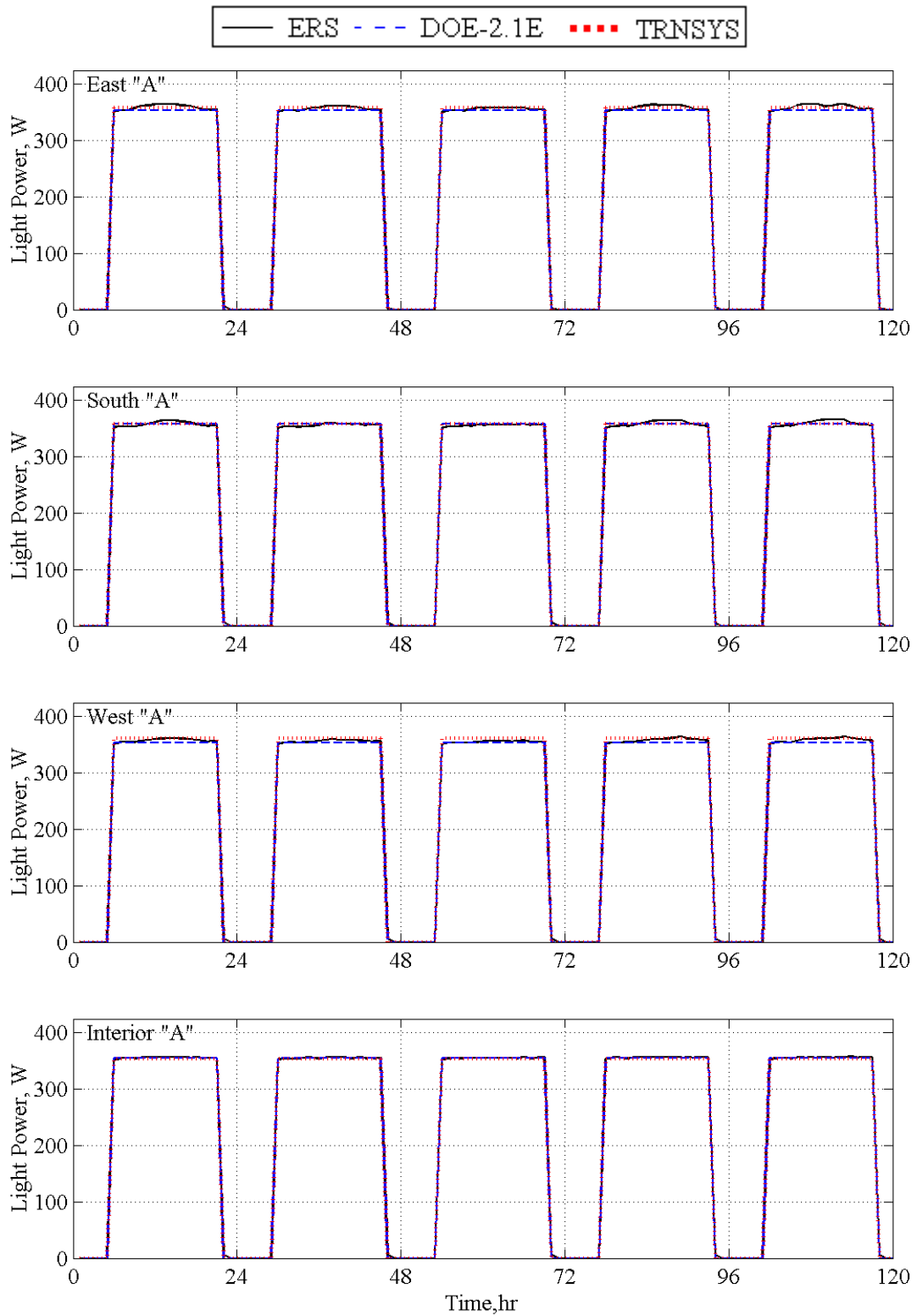


Figure 2.7 Lighting electrical power values for the "A" test rooms

2.2.2.2.2 Reference point illuminance

Figure 2.8 shows the graphical results of the illuminance values at the reference point. It is important to note that the values shown in the plots are illuminance values from daylight only since each model only accounts for daylight illuminance in the space. Light level measurements made during the experiment were modified to account for the illuminance from the overhead fluorescent lights. Because the interior test rooms have no exterior windows, the illuminance due to daylight is zero. Table 2.7 provides a statistical summary of the daylighting illuminance comparison for the “A” test rooms. When high levels of daylight enter the space, both models significantly under predict the light level at the reference point. For lower daylighting levels, both models more accurately predict the illuminance.

Table 2.7 Statistical comparison of the daylighting illuminance in the “A” test rooms, Lux

Statistical Parameter	East "A"			South "A"			West "A"		
	ERS	DOE2.1E	TRNSYS	ERS	DOE2.1E	TRNSYS	ERS	DOE2.1E	TRNSYS
\bar{x}	265.9	205.9	244.2	279.7	267.8	276.8	283.6	230.5	248.3
σ	39.4			41.3			40.3		
s	482.2	342.2	382.7	413.1	361.3	421.2	571.7	420.7	406.7
x_{\max}	2641.0	1526.4	1874.4	1604.0	1205.2	1618.8	2940.0	2015.0	1720.6
x_{\min}	0.0	0.0	-2.7	0.0	0.0	0.0	0.0	0.0	-9.6
\bar{D}		60.0	21.7		12.0	2.9		53.1	35.3
D_{\max}		1114.6	1328.8		462.5	368.7		925.0	1310.7
D_{\min}		0.0	0.0		0.0	0.0		0.0	0.0
$ D $		82.3	72.6		69.3	42.1		82.1	110.1
D_{rms}		198.1	177.5		126.8	81.6		190.5	266.5
SE		29.1	8.9		4.5	1.1		23.0	14.2
IE		40.0	29.7		25.9	15.2		35.6	44.3

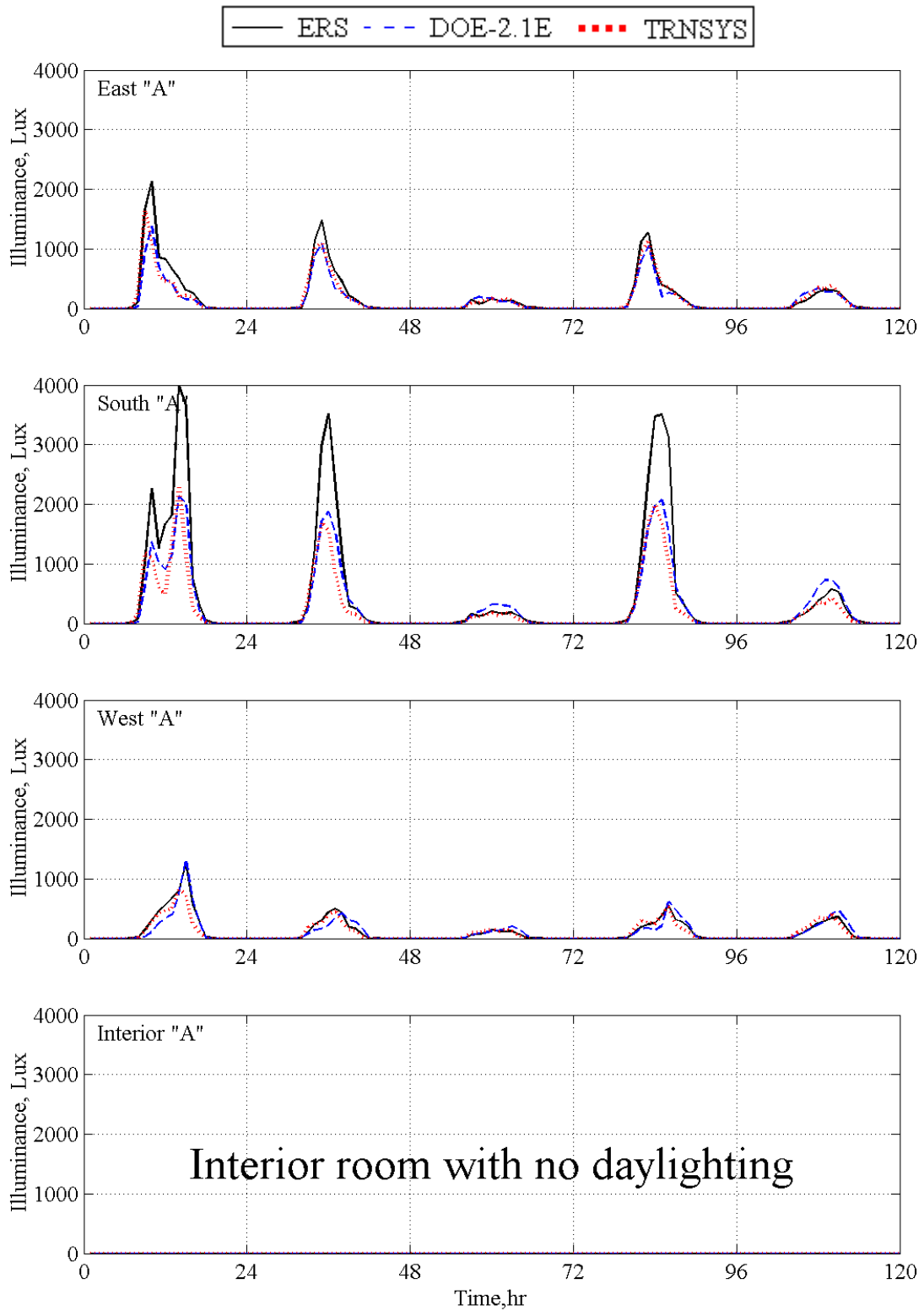


Figure 2.8 Reference point illuminance values due to daylight in the “A” test rooms

2.2.2.2.3 Zone temperatures

Figure 2.9 illustrates the zone temperatures for the “A” test rooms. The thermostat schedule called for a fixed heating set-point temperature of 22.2 °C and a fixed cooling set-point temperature of 22.8 °C. Table 2.8 provides a statistical summary of the room temperature comparison. Both models accurately predict the zone temperatures except for the Interior “A” test room. After the test was run it was discovered that the hydronic heating valve on the reheat coil for the Interior “A” test room did not close completely, thus causing the room temperature to deviate from the specified test conditions. This is clearly seen in Figure 2.8.

Table 2.8 Statistical comparison of the room temperature in the “A” test rooms, °C

Statistical Parameter	East "A"			South "A"			West "A"			Interior "A"		
	ERS	DOE2.1E	TRNSYS	ERS	DOE2.1E	TRNSYS	ERS	DOE2.1E	TRNSYS	ERS	DOE2.1E	TRNSYS
\bar{x}	22.4	22.4	22.4	22.4	22.4	22.4	22.4	22.4	22.4	23.1	22.4	22.4
σ	0.2			0.2			0.2			0.2		
s	0.5	0.4	0.3	0.5	0.4	0.3	0.5	0.4	0.3	0.8	0.4	0.3
x_{\max}	24.0	23.0	22.8	23.0	23.0	22.8	23.0	23.0	22.8	24.0	23.0	22.8
x_{\min}	22.0	22.0	22.2	22.0	22.0	22.2	22.0	22.0	22.2	22.0	22.0	22.2
\bar{D}		0.0	0.0		0.0	-0.1		0.0	0.0		0.7	0.7
D_{\max}		1.2	1.2		0.9	0.8		0.7	0.7		1.2	1.2
D_{\min}		0.0	0.2		0.0	0.2		0.0	0.2		0.0	0.2
$ D $		0.2	0.2		0.2	0.2		0.2	0.2		0.8	0.8
D_{rms}		0.2	0.3		0.2	0.2		0.2	0.2		0.9	0.9
SE		0.0	-0.1		-0.2	-0.3		0.1	-0.1		3.1	3.2
IE		0.8	1.0		0.7	1.0		0.7	0.9		3.6	3.6

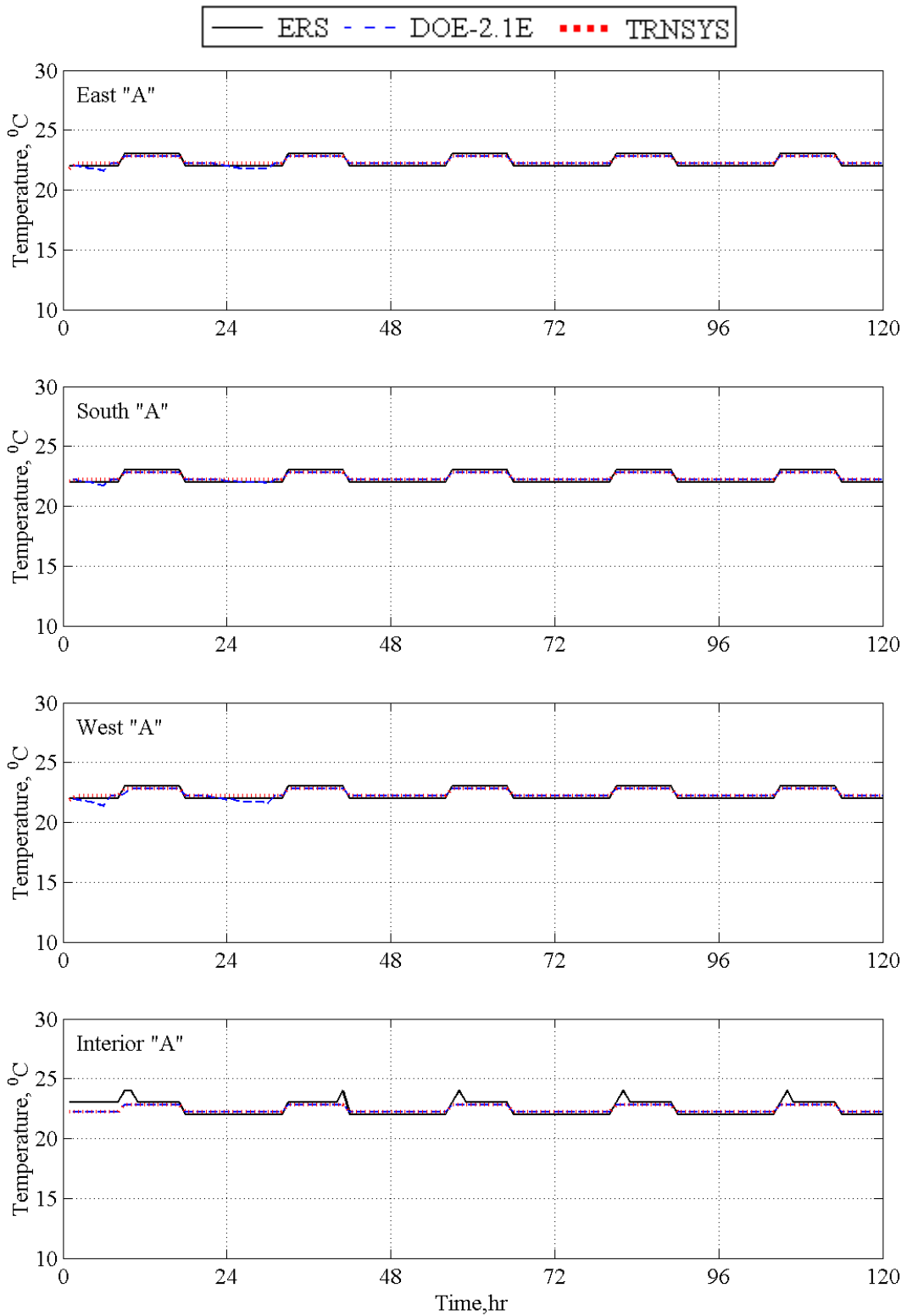


Figure 2.9 Room temperature values for the “A” test rooms

2.2.2.2.4 Zone airflow rates

Figure 2.10 illustrates the zone airflow rates for the “A” test rooms. For this test, the specified minimum supply airflow rates varied slightly from room to room (refer to Table 2.4). Table 2.9 provides a statistical summary of the room supply airflow rate comparison. The solar heat gains were the greatest on the last two days of this test (see Figure 2.4). On these days both models compared well with each other and the experimentally measured airflow rates. The days with very little solar heat gain, the TRNSYS model over predicted the cooling airflow rates. It is possible the amount of internal heat gain may not be correct for the TRNSYS model.

Table 2.9 Statistical comparison of the supply airflow rates in the “A” test rooms, m³/hr

Statistical Parameter	East "A"			South "A"			West "A"			Interior "A"		
	ERS	DOE2.1E	TRNSYS	ERS	DOE2.1E	TRNSYS	ERS	DOE2.1E	TRNSYS	ERS	DOE2.1E	TRNSYS
\bar{x}	510.8	479.3	600.9	460.7	493.7	591.4	465.8	485.3	573.2	473.8	486.4	528.4
σ	14.8			14.2			14.9			14.4		
s	258.7	220.2	357.8	215.4	249.9	348.0	195.4	231.6	304.8	132.7	210.6	243.8
x_{\max}	1335.0	1208.0	1588.0	1130.0	1190.0	1413.0	1254.0	1464.0	1521.0	652.0	862.0	855.0
x_{\min}	338.0	340.0	340.0	337.0	340.0	340.0	339.0	340.0	340.0	339.0	340.0	340.0
\bar{D}		31.5	-90.1		-33.1	-130.7		-19.5	-107.4		-12.6	-54.5
D_{\max}		453.0	587.0		304.0	523.0		210.0	446.0		270.0	218.0
D_{\min}		0.0	0.0		0.0	0.0		0.0	0.0		0.0	0.0
$ D $		35.9	99.3		39.5	137.2		27.8	114.3		78.5	98.5
D_{rms}		79.4	166.5		74.3	225.0		52.8	184.9		109.6	132.8
SE		6.6	-15.0		-6.7	-22.1		-4.0	-18.7		-2.6	-10.3
IE		7.5	16.5		8.0	23.2		5.7	19.9		16.1	18.6

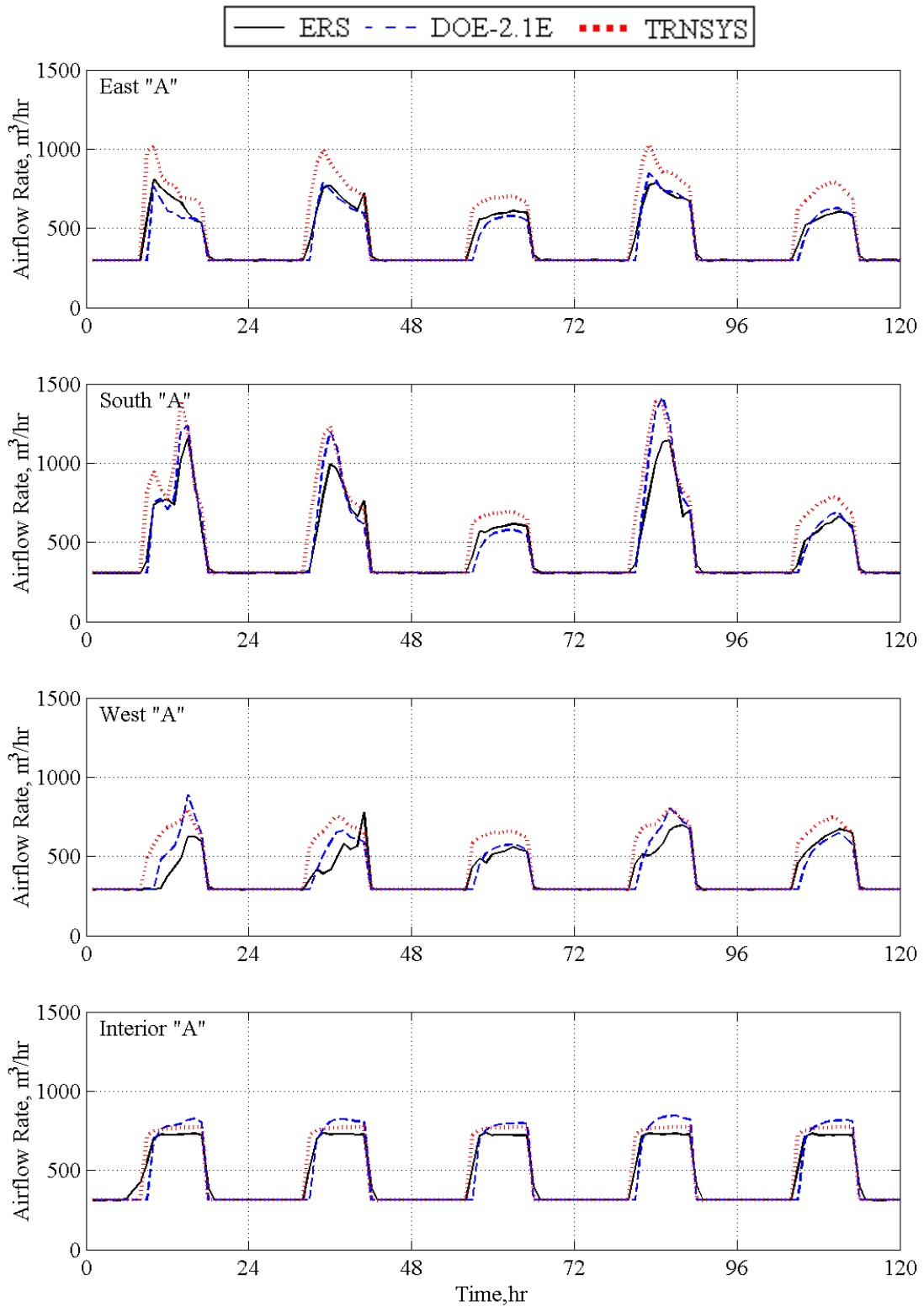


Figure 2.10 Supply airflow rates to the “A” test rooms

2.2.2.2.5 Zone reheat power

Figure 2.11 illustrates the zone reheat power for the “A” test rooms. Table 2.10 provides a statistical summary of the zone reheat power comparison. Zone reheat power comparisons show both models under predict the measured reheat power. As mentioned in the introduction, there was considerable vertical temperature stratification in the test rooms during this test. It is assumed that a significant amount of warm supply air was flowing back into the return air path in the test rooms. The models do not account for room air stratification; therefore, they would predict less reheat power to the space than was experimentally observed.

The reheat power was calculated using Equation 2.2.

$$RP = \frac{Qp}{RT_{IAT}} c_p (T_{EAT} - T_{IAT}) \quad (2.2)$$

where

- Q is the zone airflow rate
- p is the ambient pressure
- R is the gas constant for air
- T_{IAT} is the air temperature at the coil inlet
- c_p is the constant specific heat of air
- T_{EAT} is the air temperature at the coil exit

Table 2.10 Statistical comparison of the reheat power in the “A” test rooms, W

Statistical Parameter	East "A"			South "A"			West "A"			Interior "A"		
	ERS	DOE2.1E	TRNSYS	ERS	DOE2.1E	TRNSYS	ERS	DOE2.1E	TRNSYS	ERS	DOE2.1E	TRNSYS
\bar{x}	1145.5	608.3	453.0	1133.2	611.9	460.0	1115.4	593.6	454.8	876.4	374.8	366.5
σ	217.9			200.2			202.2			187.4		
S	1080.4	552.9	422.4	988.9	555.0	418.0	1007.6	566.8	427.3	678.0	344.9	319.3
x_{max}	3137.0	1375.0	1084.0	2771.0	1375.0	1073.0	2711.0	1373.0	1090.0	1800.0	833.0	765.0
x_{min}	0.0	0.0	0.0	0.0	0.0	0.0	0.0	0.0	0.0	70.0	0.0	0.0
\bar{D}		537.2	692.5		521.3	673.2		521.8	660.6		501.6	509.9
D_{max}		1835.0	2089.0		1464.0	1724.0		1409.0	1653.0		1362.0	1385.0
D_{min}		0.0	0.0		0.0	0.0		0.0	0.0		70.0	18.0
D		544.2	704.1		521.3	677.8		523.1	664.9		501.6	521.8
D_{rms}		777.1	972.0		691.8	894.4		697.5	893.1		646.1	674.1
SE		88.3	152.8		85.2	146.4		87.9	145.3		133.8	139.1
IE		89.5	155.4		85.2	147.4		88.1	146.2		133.8	142.4

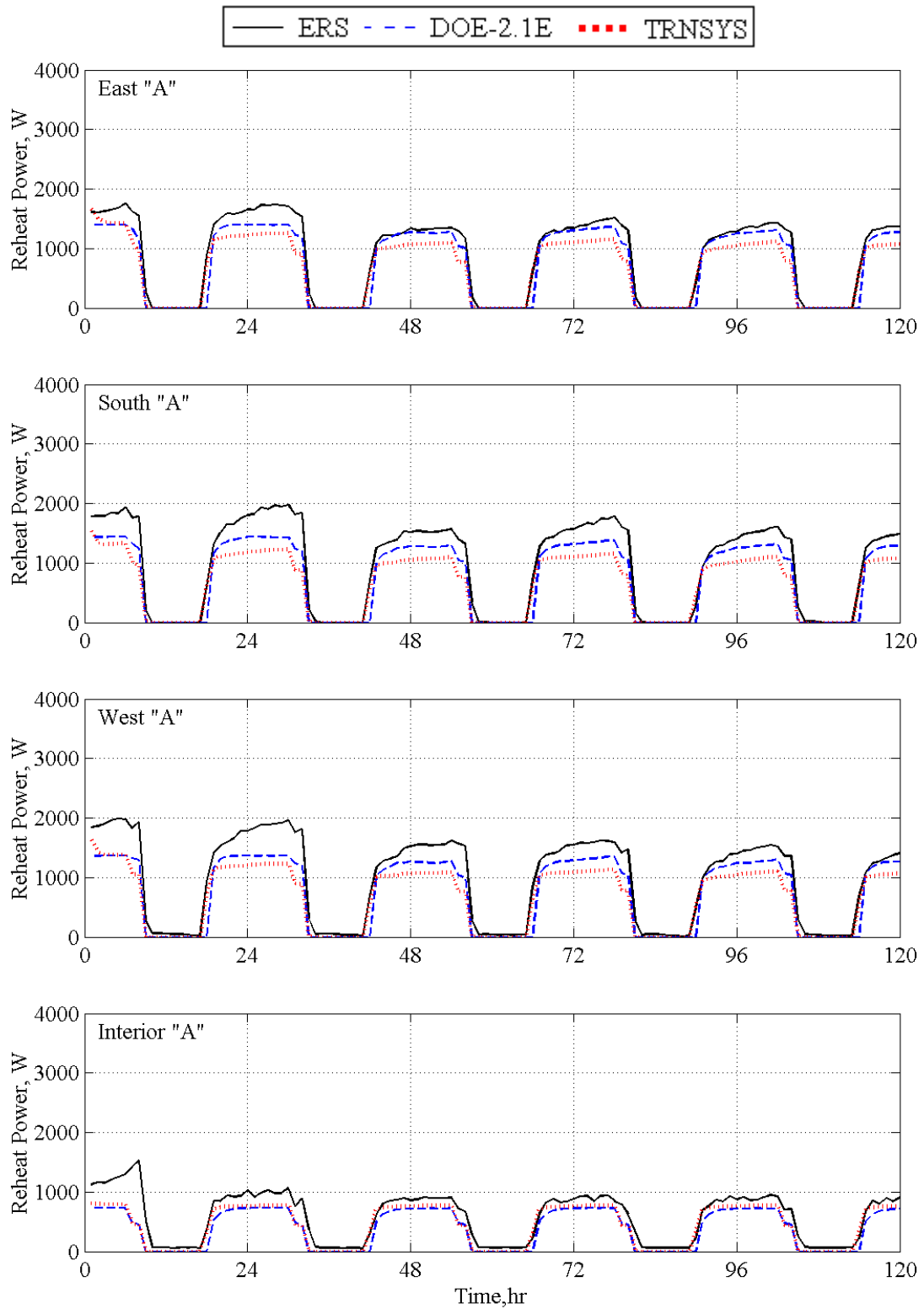


Figure 2.11 Reheat power for the "A" test rooms

2.2.2.2.6 Zone thermal load

Figure 2.12 illustrates the thermal load for each of the “A” test rooms. Positive values indicate cooling loads while negative values show heating loads. Table 2.11 provides a statistical summary of the room thermal load comparison. The table is divided into heating and cooling loads, and for simplicity, heating loads are given as positive values. The thermal stratification in the rooms accounts for the large experimental uncertainty values.

Thermal loads were calculated using Equation 2.3.

$$TL = \frac{Qp}{RT_{DAT}} c_p (T_{ZAT} - T_{DAT}) \quad (2.3)$$

where

Q is the zone airflow rate

p is the ambient pressure

R is the gas constant for air

T_{DAT} is the discharge air temperature to the zone

c_p is the constant specific heat of air

T_{ZAT} is the zone air temperature

Table 2.11 Statistical comparison of the thermal loads in the “A” test rooms, W

Statistical Parameter	East "A"			South "A"			West "A"			Interior "A"		
	ERS	DOE2.IE	TRNSYS	ERS	DOE2.IE	TRNSYS	ERS	DOE2.IE	TRNSYS	ERS	DOE2.IE	TRNSYS
Room Cooling Loads, W												
\bar{x}	1312.4	639.8	933.2	1035.6	654.5	920.8	1096.4	656.6	901.8	1175.4	753.8	816.8
σ	629.3			549.4			567.1			671.7		
S	1712.2	816.8	1114.9	1407.2	848.2	1115.3	1363.9	804.7	1039.0	1318.2	803.2	881.3
x_{max}	6284.0	2635.0	3548.0	4735.0	2489.4	3213.0	5470.0	3033.6	3501.0	2977.0	1831.4	1967.0
x_{min}	0.0	0.0	0.0	0.0	0.0	0.0	0.0	0.0	0.0	0.0	0.0	0.0
\bar{D}		672.6	379.2		381.1	114.8		439.8	194.6		421.5	358.6
D_{max}		3699.4	2816.0		2255.9	1543.0		2589.4	2147.0		1339.5	1517.0
D_{min}		0.0	0.0		0.0	0.0		0.0	0.0		0.0	0.0
$ D $		685.7	464.8		394.9	296.5		449.9	303.1		494.1	445.5
D_{rms}		1159.5	801.3		738.6	512.8		744.2	528.4		693.4	628.2
SE		105.1	40.6		58.2	12.5		67.0	21.6		55.9	43.9
IE		107.2	49.8		60.3	32.2		68.5	33.6		65.5	54.5
Room Heating Loads, W												
\bar{x}	490.8	219.5	98.8	420.0	222.6	90.6	427.3	223.5	89.9	36.6	18.6	20.2
σ	796.5			794.5			769.0			519.8		
S	588.5	247.1	146.6	487.2	243.9	137.1	486.9	246.8	138.0	64.7	29.7	29.1
x_{max}	1908.0	660.8	422.0	1517.0	660.7	397.0	1452.0	682.2	405.0	254.0	71.9	71.0
x_{min}	0.0	0.0	0.0	0.0	0.0	0.0	0.0	0.0	0.0	0.0	0.0	0.0
\bar{D}		271.3	392.0		197.4	329.4		203.8	337.4		18.0	16.4
D_{max}		1287.3	1523.0		893.4	1144.0		831.3	1100.0		188.3	191.0
D_{min}		0.0	0.0		0.0	0.0		0.0	0.0		0.0	0.0
$ D $		284.3	392.7		204.8	329.5		212.5	337.9		24.7	26.4
D_{rms}		458.6	607.0		332.3	498.7		333.8	506.3		48.3	49.6
SE		123.6	397.0		88.7	363.5		91.2	375.4		96.6	81.2
IE		129.5	397.7		92.0	363.6		95.1	375.9		132.6	130.4

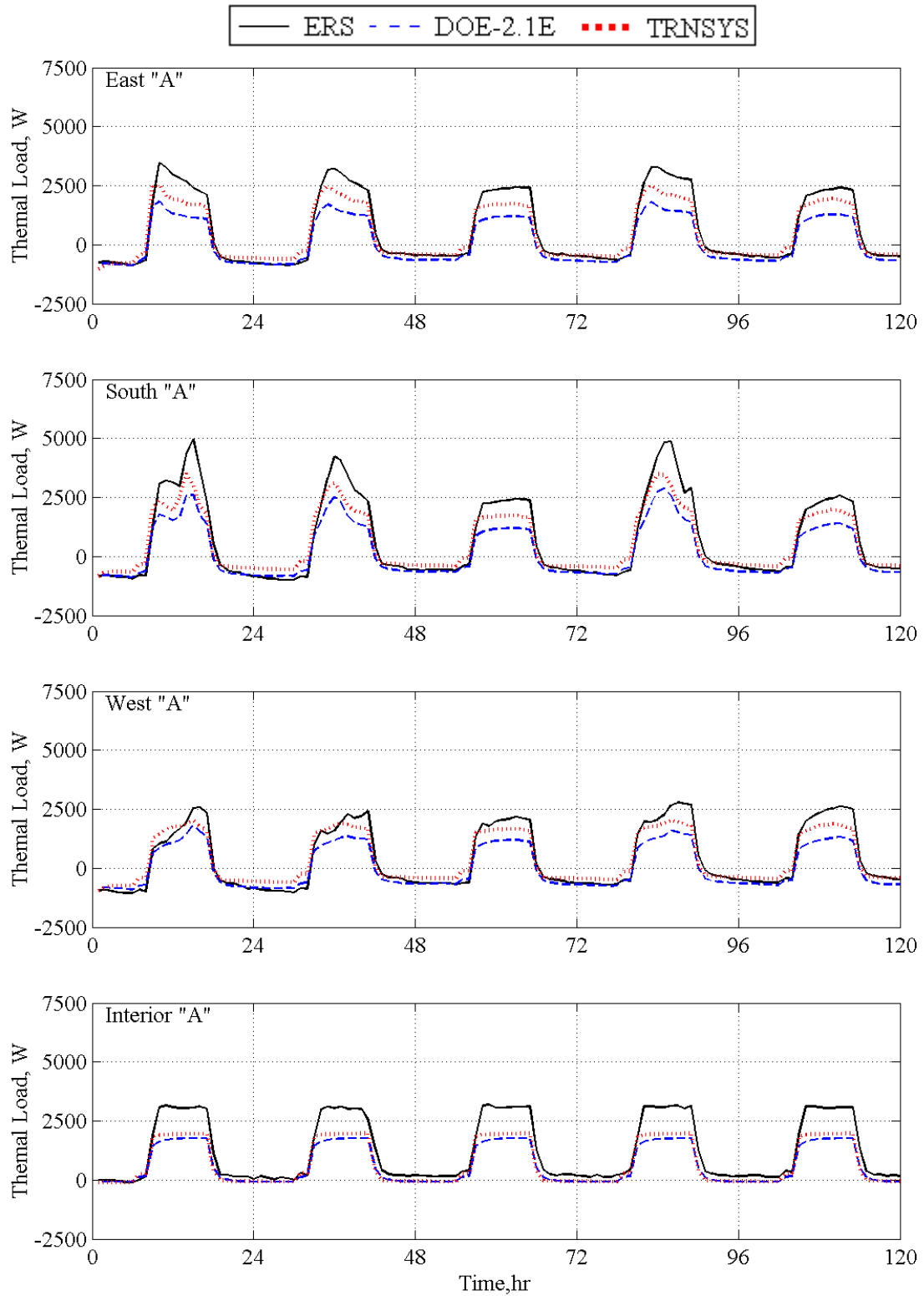


Figure 2.12 Thermal loads for the "A" test rooms

2.2.3 Comparison with daylight controlled “B” test rooms

As discussed in Section 1.3 the “B” test rooms used daylight controls. Modelers simulated this condition, and in this section the results from the models are compared to the experimental values.

2.2.3.1 System level results for the “B” system

Air handling unit “B” supplies air to the “B” test rooms. As was shown Table 1.2, the parameters generally used for system-level comparison are the supply airflow rate, the outside airflow rate, the temperature of air entering cooling coil, the temperature of air leaving cooling coil, the temperature of return air, and the cooling coil heat transfer rate. However, for this test, the outside airflow rate was specified to equal zero; therefore, the air temperature entering the cooling coil equals the return air temperature. Table 2.12 provides a statistical summary of the air handling unit parameter comparison. As in the case for the “A” system, TRNSYS is over predicting the system airflow rates. The remaining AHU parameters for the “B” system are reasonably well matched with the experimental results.

Table 2.12 Statistical comparison of AHU-B parameters

Statistical Parameter	Supply airflow rate, m ³ /hr			Return air temperature, °C			Leaving coil air temperature, °C			Cooling coil heat transfer rate, kW		
	ERS	DOE2.1E	TRNSYS	ERS	DOE2.1E	TRNSYS	ERS	DOE2.1E	TRNSYS	ERS	DOE2.1E	TRNSYS
\bar{x}	1816.1	1847.7	2196.7	23.6	23.3	22.7	13.9	13.5	14.1	5.6	6.0	5.8
σ	30.0			0.2			0.2			0.8		
s	647.5	731.6	1090.9	0.6	0.3	0.3	0.1	0.5	0.0	2.0	2.1	3.1
x_{\max}	3728.0	3875.0	4316.0	24.6	24.0	23.2	14.1	14.6	14.1	11.4	11.5	11.9
x_{\min}	1355.0	1359.0	1360.0	21.8	22.7	22.4	13.6	13.0	14.1	3.8	4.4	3.4
\bar{D}		-31.6	-380.6		0.3	0.9		0.4	-0.2		-0.4	-0.3
D_{\max}		625.0	1688.0		2.1	1.9		1.0	0.5		1.5	4.0
D_{\min}		0.0	0.0		0.0	0.0		0.0	0.0		0.0	0.3
$ D $		99.6	426.0		0.7	1.0		0.7	0.2		0.5	1.2
D_{rms}		165.4	678.5		0.9	1.1		0.7	0.3		0.6	1.4
SE		-1.7	-17.3		1.2	4.1		3.0	-1.7		-7.2	-4.4
IE		5.4	19.4		2.9	4.4		4.9	1.7		8.3	20.7

Figure 2.13 shows the graphical results of the AHU-B system parameters during the five days of the test.

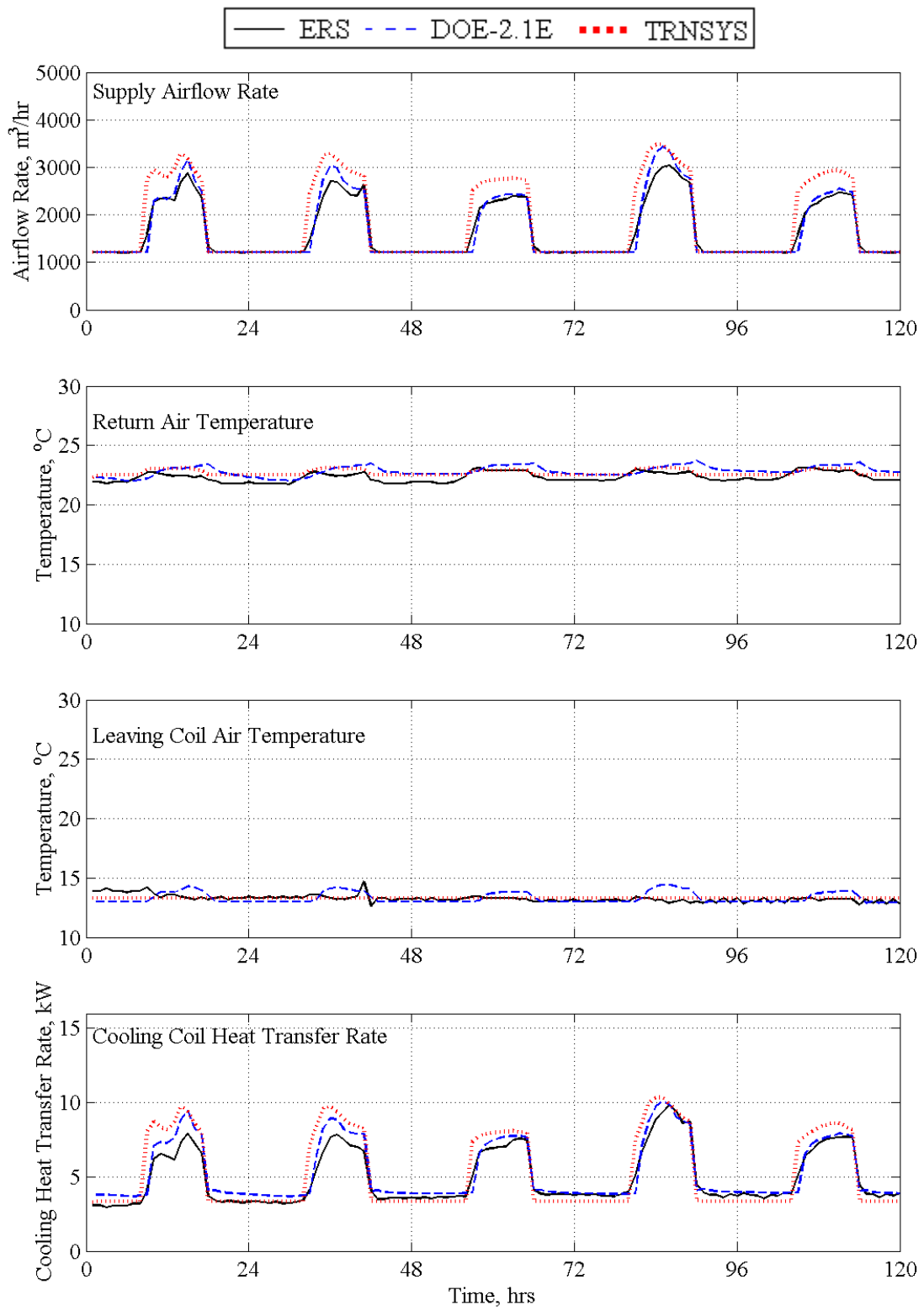


Figure 2.13 AHU-B parameters

2.2.3.2 Zone level results for the “B” test rooms

In this section, comparisons are made for the zone-level parameters. As was shown in Table 1.2, the zone-level parameters used for comparison are: the lighting electrical power, the luminance level at the reference point, the zone temperature, the supply airflow rate, the reheat power, and the thermal load (without ventilation).

2.2.3.2.1 Lighting electrical power

Because daylighting controls were used for the “B” test rooms, the lighting electrical power was reduced as the amount of available daylight entered the space. The control algorithm allowed for the lights to be turned off if sufficient daylight was available. Figure 2.14 shows the graphical results of the lighting electrical power. Because there was no daylight available for the interior test room, the interior room lights remain at 100% power while they are scheduled on. Table 2.13 provides a statistical summary of the lighting electrical power comparison. While none of the models predict the light levels within the error bounds, the graphical results show reasonable agreement. Simulation errors are within 10% for both models for the East and West test rooms; however, on the third and fifth day of the test discrepancies are seen for the South test room for the DOE2 model.

Table 2.13 Statistical comparison of lighting electrical power in the “B” test rooms, W

Statistical Parameter	East “B”			South “B”			West “B”			Interior “B”		
	ERS	DOE2.1E	TRNSYS	ERS	DOE2.1E	TRNSYS	ERS	DOE2.1E	TRNSYS	ERS	DOE2.1E	TRNSYS
\bar{x}	147.7	152.8	140.2	141.0	122.3	136.1	152.5	151.4	140.3	239.8	238.7	240.0
σ	0.3			0.3			0.4			0.4		
s	139.6	146.0	142.1	142.6	139.4	145.3	138.7	142.6	142.4	169.8	169.5	170.4
x_{max}	333.0	341.1	337.0	334.0	329.6	337.0	333.0	339.3	337.0	361.0	358.0	360.0
x_{min}	0.0	0.0	0.0	0.0	0.0	0.0	0.0	0.0	0.0	0.0	0.0	0.0
\bar{D}		-5.2	7.5		18.7	4.9		1.1	12.2		1.2	-0.2
D_{max}		221.0	132.0		212.0	152.0		195.0	207.0		6.0	6.0
D_{min}		0.0	0.0		0.0	0.0		0.0	0.0		0.0	0.0
$ D $		19.0	12.4		18.8	9.8		18.4	22.0		1.3	1.0
D_{rms}		37.3	25.5		42.1	22.9		34.7	47.8		2.0	1.8
SE		-3.4	5.3		15.3	3.6		0.7	8.7		0.5	-0.1
IE		12.5	8.8		15.4	7.2		12.2	15.7		0.6	0.4

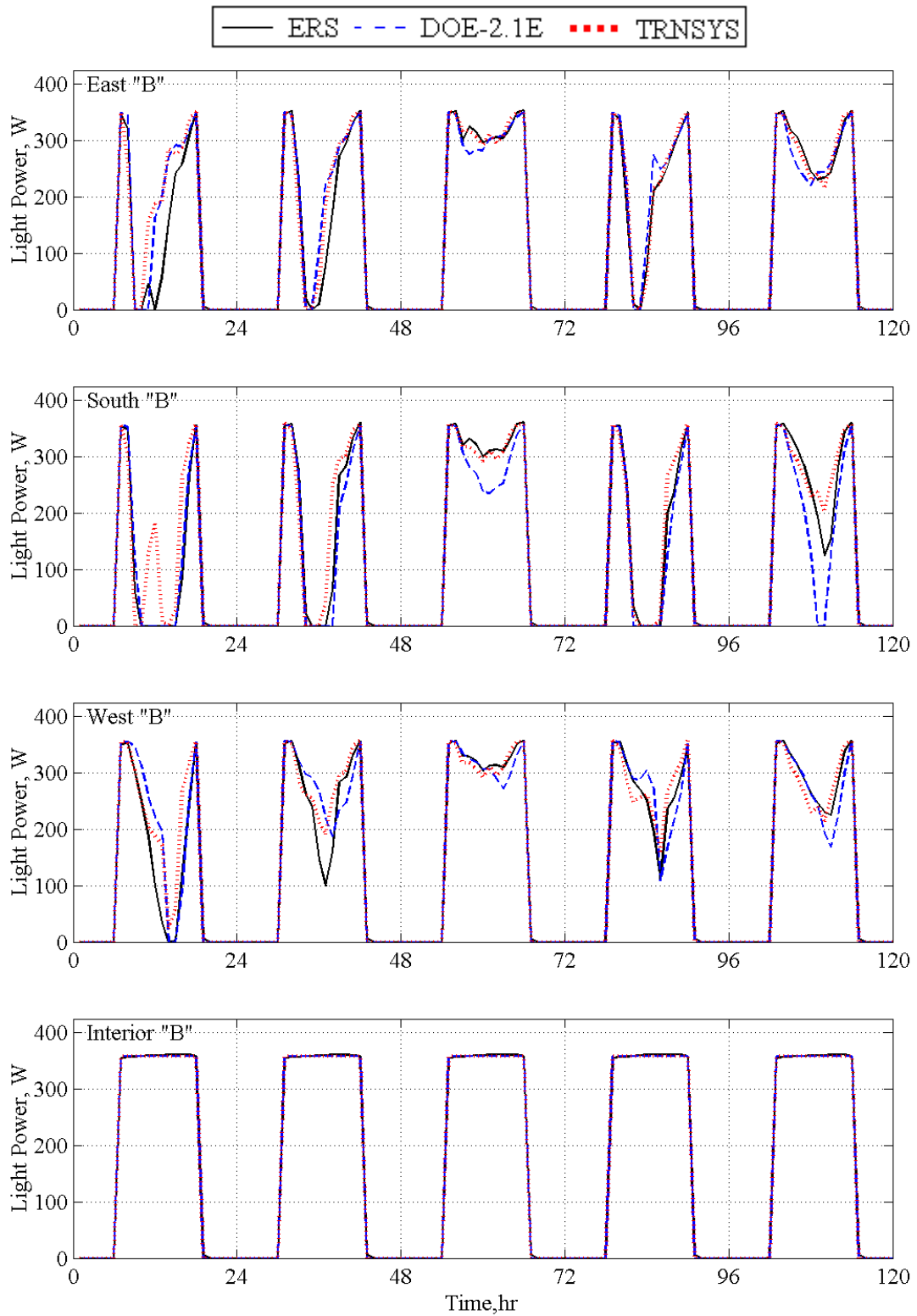


Figure 2.14 Lighting electrical power values for the "B" test rooms

2.2.3.2.2 Reference point illuminance

Figure 2.15 shows the graphical results of the illuminance values at the reference point. It is important to note that the values shown in the plots are illuminance values from daylight only since each model only accounts for daylight illuminance in the space. Light level measurements made during the experiment were modified to account for the illuminance from the overhead fluorescent lights. Because the interior test rooms have no exterior windows, the illuminance due to daylight is zero. Table 2.14 provides a statistical summary of the daylighting illuminance comparison. The results for the “B” test rooms similar to the “A” test rooms. Even though the illuminance values from the models contain errors at high daylight conditions, the predicted light power is unaffected. The daylighting level at the reference point exceeded the light-level set point for both the experiment and the models, thus the lights were turned off in both cases.

Table 2.14 Statistical comparison of the daylighting illuminance in the “B” test rooms, Lux

Statistical Parameter	East "B"			South "B"			West "B"		
	ERS	DOE2.1E	TRNSYS	ERS	DOE2.1E	TRNSYS	ERS	DOE2.1E	TRNSYS
\bar{x}	279.2	206.1	249.0	248.0	252.7	275.7	275.7	232.8	255.4
σ	28.1			27.4			28.7		
s	498.7	342.6	384.4	384.0	340.8	415.1	550.4	425.0	409.5
x_{\max}	2692.0	1528.9	1877.1	1483.0	1137.0	1604.3	2833.0	2035.1	1730.2
x_{\min}	0.0	0.0	0.0	0.0	0.0	0.0	0.0	0.0	0.0
\bar{D}		73.1	30.2		-4.8	-27.8		42.9	20.3
D_{\max}		1181.3	1399.1		409.1	385.2		797.9	1194.1
D_{\min}		0.0	0.0		0.0	0.0		0.0	0.0
$ D $		92.7	67.8		65.4	45.6		77.3	106.1
D_{rms}		214.2	186.1		119.0	88.0		168.1	249.5
SE		35.5	12.1		-1.9	-10.1		18.5	8.0
IE		45.0	27.2		25.9	16.5		33.2	41.6

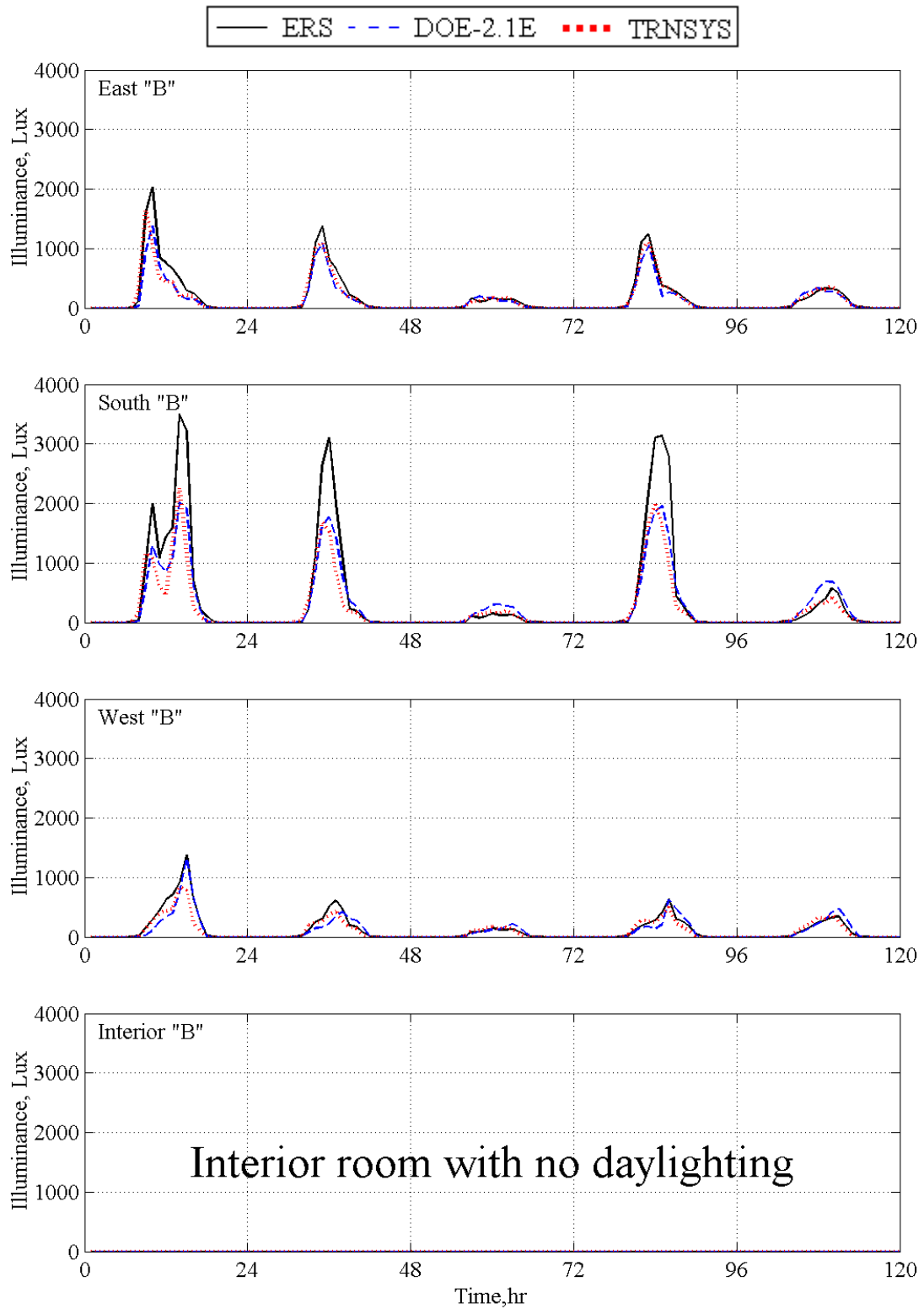


Figure 2.15 Reference point illuminance values due to daylight in the “B” test rooms

2.2.3.2.3 Zone temperatures

Figure 2.16 illustrates the zone temperatures for the “B” test rooms. The thermostat schedule called for a fixed heating set-point temperature of 22.2 °C and a fixed cooling set-point temperature of 22.8 °C. Table 2.15 provides a statistical summary of the room temperature. The results show that the all rooms are under temperature control and that the models predict the zone temperatures.

Table 2.15 Statistical comparison of the room temperature in the “B” test rooms, °C

Statistical Parameter	East "B"			South "B"			West "B"			Interior "B"		
	ERS	DOE2.1E	TRNSYS	ERS	DOE2.1E	TRNSYS	ERS	DOE2.1E	TRNSYS	ERS	DOE2.1E	TRNSYS
\bar{x}	22.4	22.4	22.4	22.4	22.4	22.4	22.4	22.4	22.4	22.4	22.4	22.4
σ	0.2			0.2			0.2			0.2		
s	0.5	0.3	0.3	0.5	0.3	0.3	0.5	0.3	0.3	0.5	0.4	0.3
x_{\max}	23.0	23.0	22.8	23.0	23.0	22.8	23.0	23.0	22.8	23.0	23.0	22.8
x_{\min}	22.0	22.0	22.2	22.0	22.0	22.2	22.0	22.0	22.2	22.0	22.0	22.1
\bar{D}		0.0	-0.1		0.0	-0.1		0.0	0.0		-0.1	0.0
D_{\max}		0.3	0.2		0.8	0.8		0.7	0.8		0.3	0.2
D_{\min}		0.0	0.2		0.0	0.2		0.0	0.2		0.0	0.1
$ D $		0.2	0.2		0.2	0.2		0.2	0.2		0.2	0.2
D_{rms}		0.2	0.2		0.2	0.2		0.2	0.3		0.2	0.2
SE		-0.1	-0.2		-0.2	-0.3		0.1	-0.1		-0.3	-0.2
IE		0.7	0.9		0.7	1.0		0.7	1.0		0.7	0.9

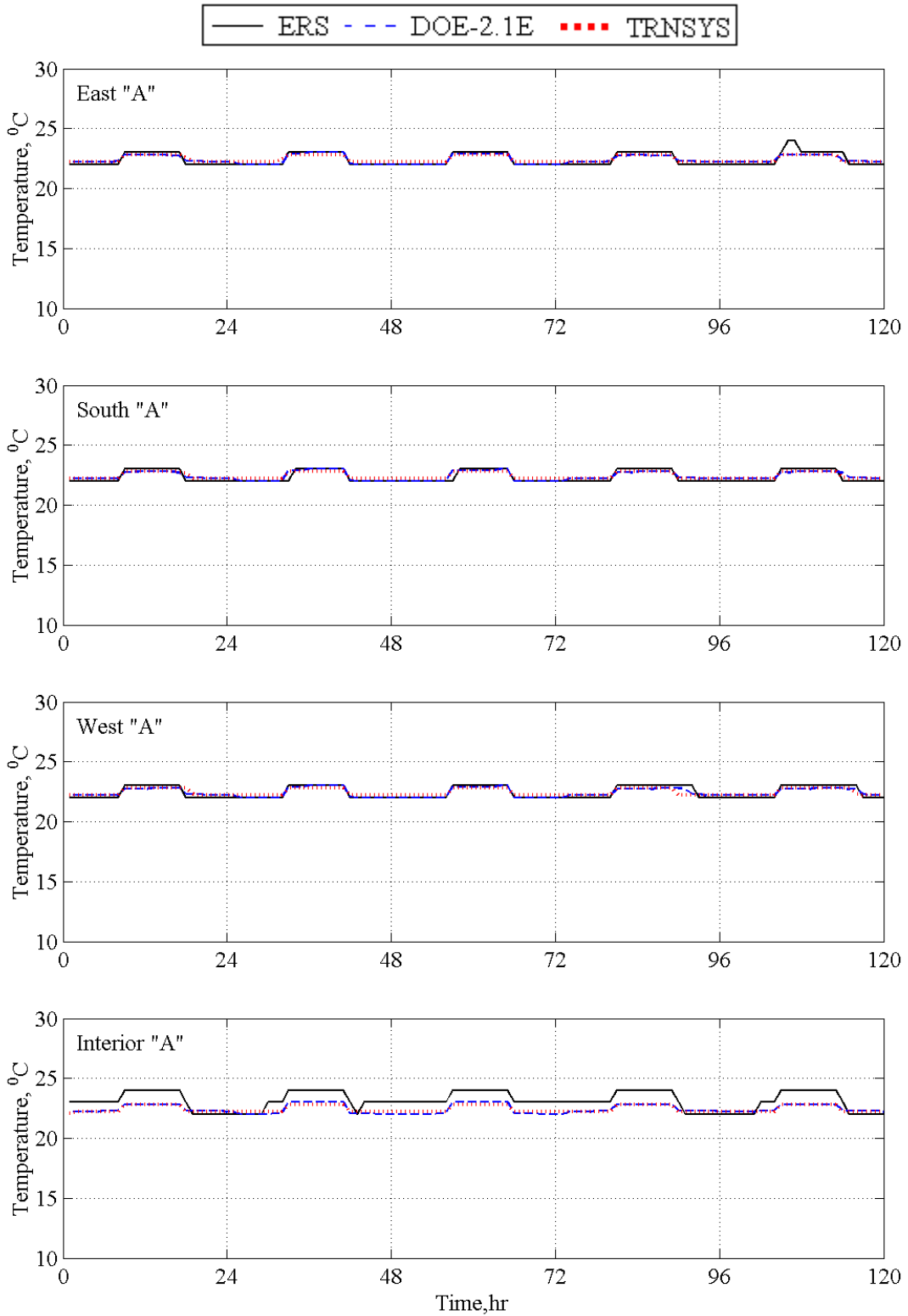


Figure 2.16 Room temperature values for the “B” test rooms

2.2.3.2.4 Zone airflow rates

Figure 2.17 illustrates the zone airflow rates for the “B” test rooms. For this test, the specified minimum supply airflow rates varied slightly from room to room (refer to Table 3.4). Table 2.16 provides a statistical summary of the room supply airflow rate comparison. The results show that for DOE2 the values are nearly within the error bounds. As with the “A” test room results, the TRNSYS model is over predicting the airflow rates.

Table 2.16 Statistical comparison of the supply airflow rates in the “B” test rooms, m³/hr

Statistical Parameter	East "B"			South "B"			West "B"			Interior "B"		
	ERS	DOE2.1E	TRNSYS	ERS	DOE2.1E	TRNSYS	ERS	DOE2.1E	TRNSYS	ERS	DOE2.1E	TRNSYS
\bar{x}	456.9	451.5	549.0	435.9	455.4	549.9	451.4	455.7	560.6	471.8	485.7	537.2
σ	14.8			14.2			14.9			14.4		
s	196.0	178.8	284.2	191.9	192.5	288.3	188.3	187.2	287.5	168.7	209.2	255.3
x_{\max}	1246.0	1056.0	1354.0	1101.0	1031.0	1247.0	1287.0	1301.0	1459.0	728.0	858.0	880.0
x_{\min}	335.0	340.0	340.0	338.0	340.0	340.0	339.0	340.0	340.0	339.0	340.0	340.0
\bar{D}		5.5	-92.1		-19.5	-114.0		-4.3	-109.2		-13.9	-65.3
D_{\max}		333.0	544.0		221.0	419.0		329.0	452.0		221.0	349.0
D_{\min}		0.0	0.0		0.0	0.0		0.0	0.0		0.0	0.0
$ D $		30.7	97.9		35.7	119.4		32.0	135.6		36.5	73.6
D_{rms}		61.0	165.7		67.0	201.4		69.4	212.3		62.4	119.1
SE		1.2	-16.8		-4.3	-20.7		-0.9	-19.5		-2.9	-12.2
IE		6.8	17.8		7.8	21.7		7.0	24.2		7.5	13.7

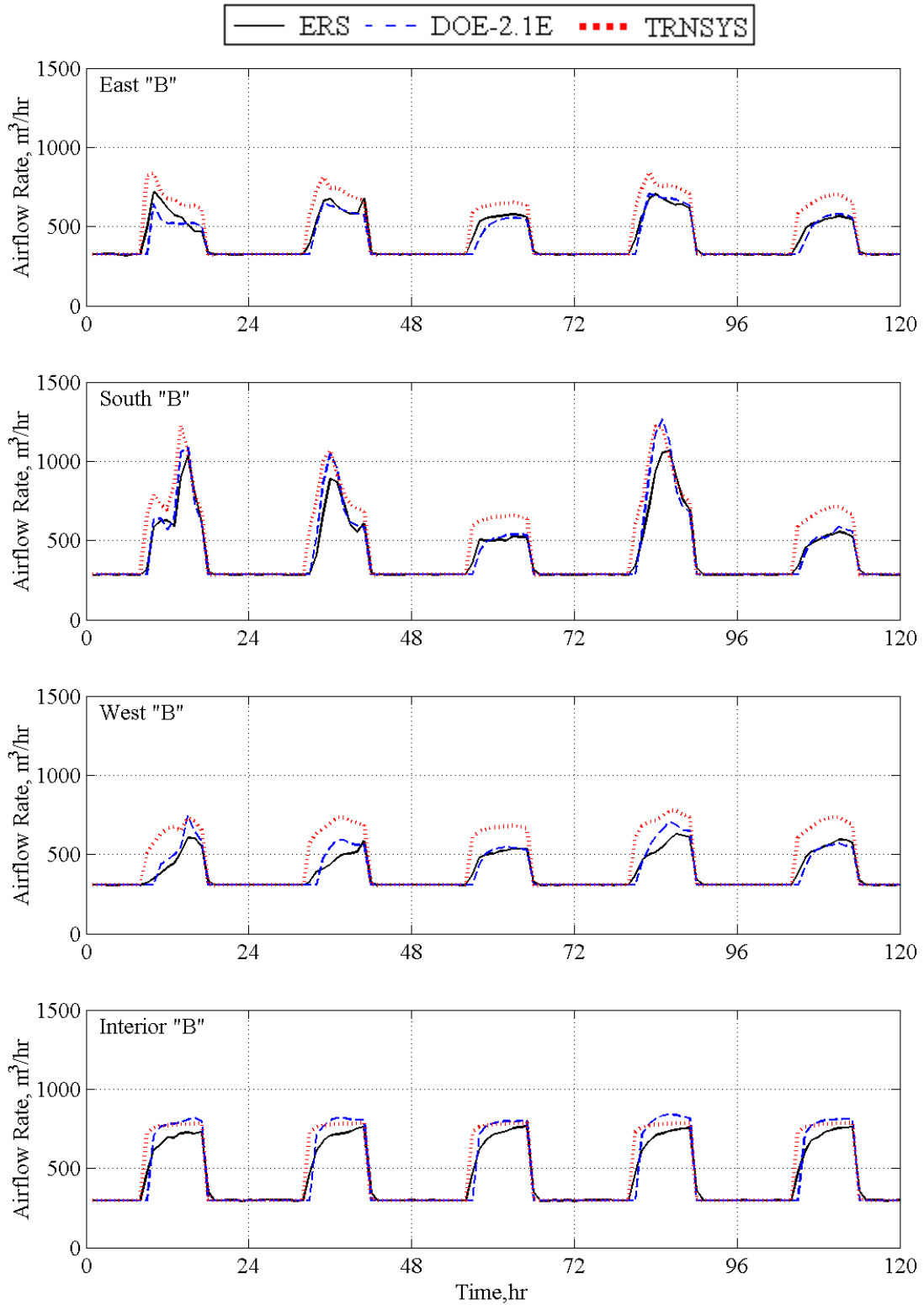


Figure 2.17 Supply airflow rates to the "B" test rooms

2.2.3.2.5 Zone reheat power

Figure 2.18 illustrates the zone reheat power for the “B” test rooms. The reheat power was calculated using Equation 2.2 (Section 2.2.2.2.5). Table 2.17 provides a statistical summary of the zone reheat power comparison. The results here are similar to those of the “A” test rooms. Room temperature stratification is the primary cause of the discrepancies

Table 2.17 Statistical comparison of the reheat power in the “B” test rooms, W

Statistical Parameter	East "B"			South "B"			West "B"			Interior "B"		
	ERS	DOE2.1E	TRNSYS	ERS	DOE2.1E	TRNSYS	ERS	DOE2.1E	TRNSYS	ERS	DOE2.1E	TRNSYS
\bar{x}	1210.6	618.2	480.4	1267.1	627.4	478.4	1118.5	604.5	445.2	782.1	379.0	360.8
σ	201.8			200.2			197.4			184.2		
s	1072.9	554.0	422.9	1068.3	556.7	421.2	1015.8	567.6	414.3	562.0	346.5	317.3
x_{max}	3286.0	1375.0	1087.0	2969.0	1376.0	1082.0	2909.0	1374.0	1056.0	1439.0	839.0	761.0
x_{min}	0.0	0.0	0.0	0.0	0.0	0.0	0.0	0.0	0.0	60.0	0.0	0.0
\bar{D}		592.4	730.2		639.6	788.7		514.0	673.4		403.1	421.3
D_{max}		1991.0	2263.0		1659.0	1910.0		1601.0	1876.0		844.0	866.0
D_{min}		0.0	0.0		0.0	0.0		0.0	0.0		60.0	60.0
$ D $		599.9	741.0		644.2	794.5		517.4	675.3		403.1	422.3
D_{rms}		807.0	992.2		832.5	1031.8		707.7	915.3		475.4	509.2
SE		95.8	152.0		101.9	164.9		85.0	151.3		106.4	116.7
IE		97.0	154.3		102.7	166.1		85.6	151.7		106.4	117.0

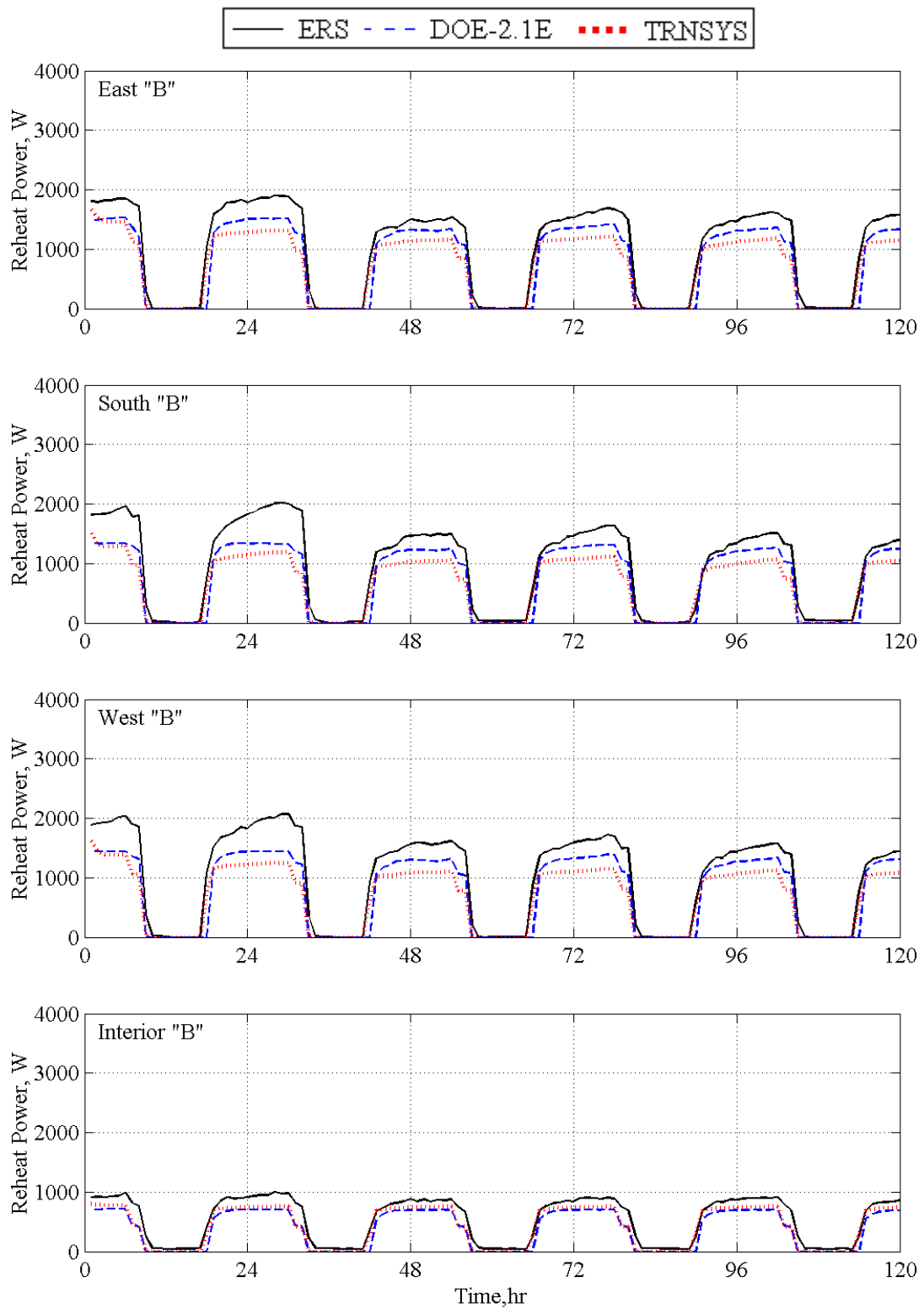


Figure 2.18 Reheat power values for the “B” test rooms

2.2.3.2.6 Zone thermal load

Figure 2.19 illustrates the thermal load for each of the “B” test rooms. The zone thermal load was calculated using Equation 2.3 (Section 2.2.2.2.6). Table 2.18 provides a statistical summary of the room thermal load comparison. The table is divided into heating and cooling loads, and for simplicity, heating loads are given as positive values. The thermal stratification in the rooms accounts for the large experimental uncertainty values.

Table 2.18 Statistical comparison of the thermal loads in the “B” test rooms, W

Statistical Parameter	East "B"			South "B"			West "B"			Interior "B"		
	ERS	DOE2.1E	TRNSYS	ERS	DOE2.1E	TRNSYS	ERS	DOE2.1E	TRNSYS	ERS	DOE2.1E	TRNSYS
Room Cooling Loads, W												
\bar{x}	1064.6	567.9	823.3	928.0	561.6	818.0	1010.1	590.0	824.5	1201.0	766.7	841.6
σ	539.9			485.6			537.8			715.5		
S	1405.5	733.4	992.9	1302.8	738.7	996.0	1318.7	725.1	958.5	1401.2	825.5	905.1
x_{max}	5701.0	2323.9	3116.0	4705.0	2178.9	2854.0	5695.0	2732.7	3200.0	3237.0	1860.5	2026.0
x_{min}	0.0	0.0	0.0	0.0	0.0	0.0	0.0	0.0	0.0	0.0	0.0	0.0
\bar{D}		496.7	241.3		366.4	109.9		420.2	185.6		434.3	359.5
D_{max}		3377.1	2585.0		2537.2	1873.0		2962.3	2840.0		1377.7	1219.0
D_{min}		0.0	0.0		0.0	0.0		0.0	0.0		0.0	0.0
$ D $		505.3	328.8		375.1	312.6		432.5	289.0		486.0	452.8
D_{rms}		887.8	610.3		753.9	550.8		787.0	641.0		748.8	666.0
SE		87.5	29.3		65.2	13.4		71.2	22.5		56.6	42.7
IE		89.0	39.9		66.8	38.2		73.3	35.1		63.4	53.8
Room Heating Loads, W												
\bar{x}	457.9	222.9	95.9	507.6	231.3	94.1	438.3	229.9	92.5	20.6	20.2	18.6
σ	771.4			794.5			769.0			411.4		
S	537.6	247.2	140.7	558.2	243.9	138.6	525.3	246.4	138.8	39.0	30.5	26.9
x_{max}	1936.0	660.8	402.0	1676.0	660.7	401.0	1677.0	682.2	407.0	142.0	72.1	68.0
x_{min}	0.0	0.0	0.0	0.0	0.0	0.0	0.0	0.0	0.0	0.0	0.0	0.0
\bar{D}		234.9	362.0		276.2	413.5		208.4	345.8		0.5	2.0
D_{max}		1312.7	1599.0		1055.4	1298.0		1054.1	1293.0		70.0	77.0
D_{min}		0.0	0.0		0.0	0.0		0.0	0.0		0.0	0.0
$ D $		244.4	362.0		280.5	413.5		219.3	345.8		9.3	10.7
D_{rms}		394.6	555.0		432.4	607.5		373.3	538.0		19.6	21.9
SE		105.4	377.5		119.4	439.3		90.6	373.8		2.4	11.0
IE		109.6	377.5		121.3	439.3		95.4	373.8		45.9	57.4

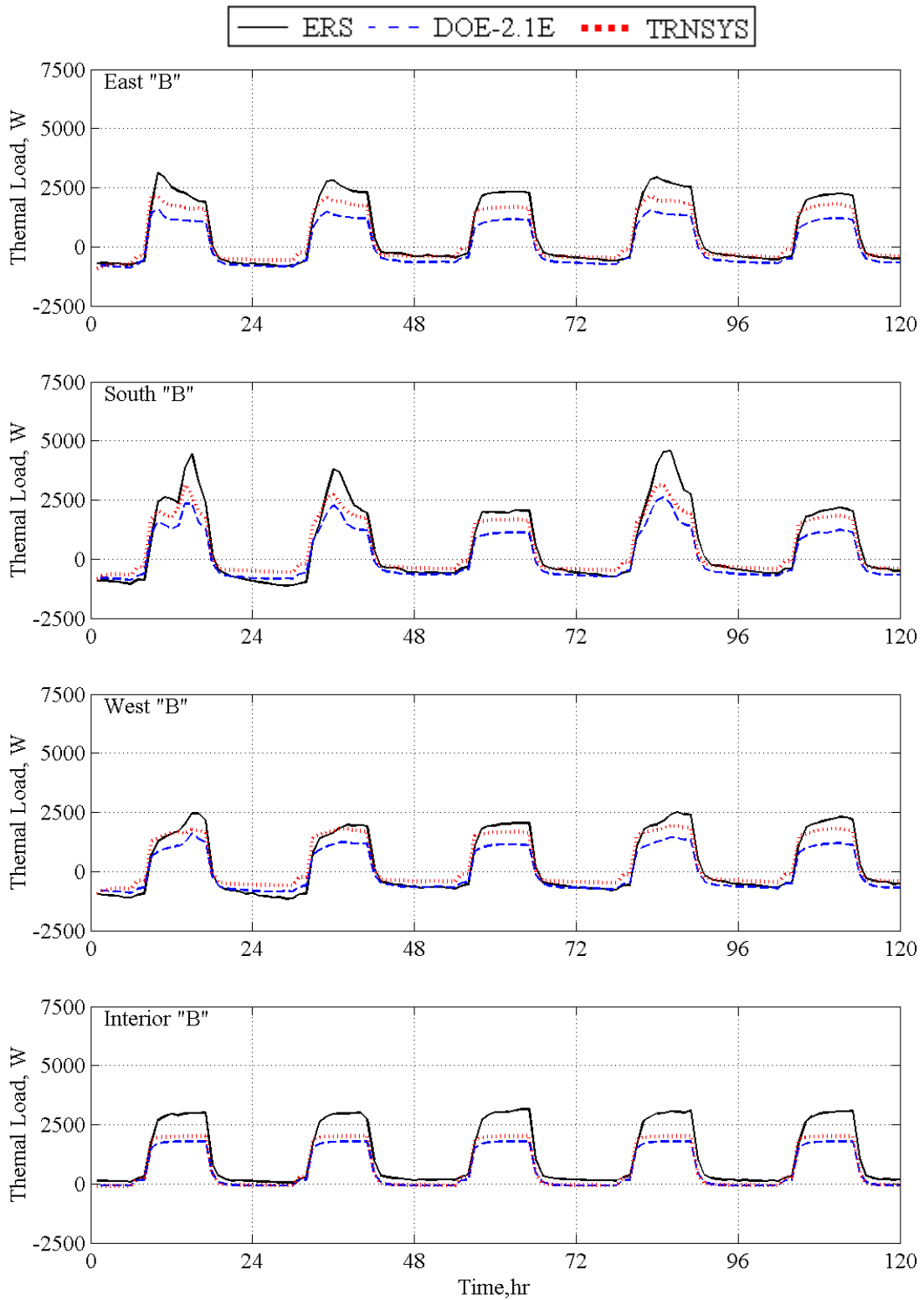


Figure 2.19 Thermal load values for the “B” test rooms

3 Daylighting Test 2

3.1 Description of the exercise

This section contains information regarding the operating parameters and conditions used for Daylighting Test 2 conducted at the Energy Resource Station. The test was conducted over a five-day period from January 29 to February 2, 2003.

Internal heat loads for the test rooms were produced from electric baseboard heaters. These were scheduled on during a portion of the day and off the remainder of the time. The windows of the test rooms were covered with flat sheets of white muslin fabric. This fabric provided diffuse daylight in the space and prevented direct sunlight for entering the space.

The “B” test rooms were used for the daylighting-HVAC interaction study. Dimmable ballasts in the “B” test rooms allowed for reduction in electric lighting power when sufficient daylight was available in the space. The control scheme permitted the lights to be completely turned off if the light level set point could be achieved from daylighting. The “A” test room lights were operated at full power with no capability of dimming. Ballasts in both the “A” and “B” test rooms were adjusted so that all test rooms produced nearly the same light level and used the same light power when the lamps were operated at full power. The lights in both rooms were operated on a time of day schedule. Lights were turned on approximately one hour before sunrise and turned off approximately one hour after sunset.

Thermostats in the test rooms were programmed for a constant heating set-point temperature and a constant cooling set-point temperature. For non-test room spaces in the ERS that are adjacent to the test rooms, the zone thermostats were programmed with the same set-point temperatures as the test rooms. This reduced the thermal interaction between the test rooms and the remainder of the building.

For this test, room air temperature stratification was reduced significantly by increasing the room air mixing through the use of a small electric fan. The fan used was a low power propeller type fan commonly used to provide an increase in the air motion within a room. For this test, each test room had a small fan suspended from the ceiling (see Figure 3.1). The fan drew warm air from near the ceiling and blew it towards the floor. The fans ran continuously throughout the test.

In order to quantify the reduction in room air temperature stratification, temperature measurements were made in the East “A” test room with the fan running and with the fan off. Two tripods were equipped with RTD temperature sensors mounted at heights of 30.5, 91.4, 152, and 213 centimeters above the floor. One tripod was located near the windows and the other located near the back wall. The thermostat heating set-point temperature was 22.2 °C. Figures 3.2 (a, b) show the air temperature values measured before and after the fan was turned on. Clearly the decrease in room air temperature stratification is seen.

The “A” and “B” systems were operated as variable air volume with hydronic terminal reheat at the zone level. The outdoor air dampers were closed and the systems operated on 100%

recirculated air. The systems were run 24 hours per day and chilled water was available for mechanical cooling throughout the test period.



Figure 3.1 Destratification fan

3.1.1 Run period and general weather conditions

This item is used to specify the initial and final dates of the desired simulation period and also the general conditions and location of the ERS facility. The TMY weather file that accompanies this report has ERS weather station information only for the dates of the tests.

- Test dates: January 29, 2003 through February 2, 2003.
- Weather data for the ERS is organized into TMY format. The weather file is called “IEA2003.TMY”.
- Building location
 - Latitude: 41.71 °N
 - Longitude: 93.61 °W
 - Altitude: 285.9 m (938 ft)
 - Time-zone: 6, Central time zone in U.S.
 - Daylight-saving: NO

3.1.2 Test rooms operation and control parameters

This item describes the operation and control of the test rooms that apply to this test.

3.1.2.1 Internal loads and general room conditions

The only internal heating loads used during this test are from ceiling mounted fluorescent lights and baseboard electric heaters. These internal loads were scheduled “ON” for only certain hours during the day. The baseboard heaters have two stages of heat, and for this test, both stages of baseboard heat were used. Due to variations in the installed equipment, the baseboard power is not identical for each unit. Furthermore, slight variations also exist for the lighting power. Table 3.1 provides power values for the lights and baseboard heaters for each test room. For the “B” test rooms, the minimum dimmable light power is shown.

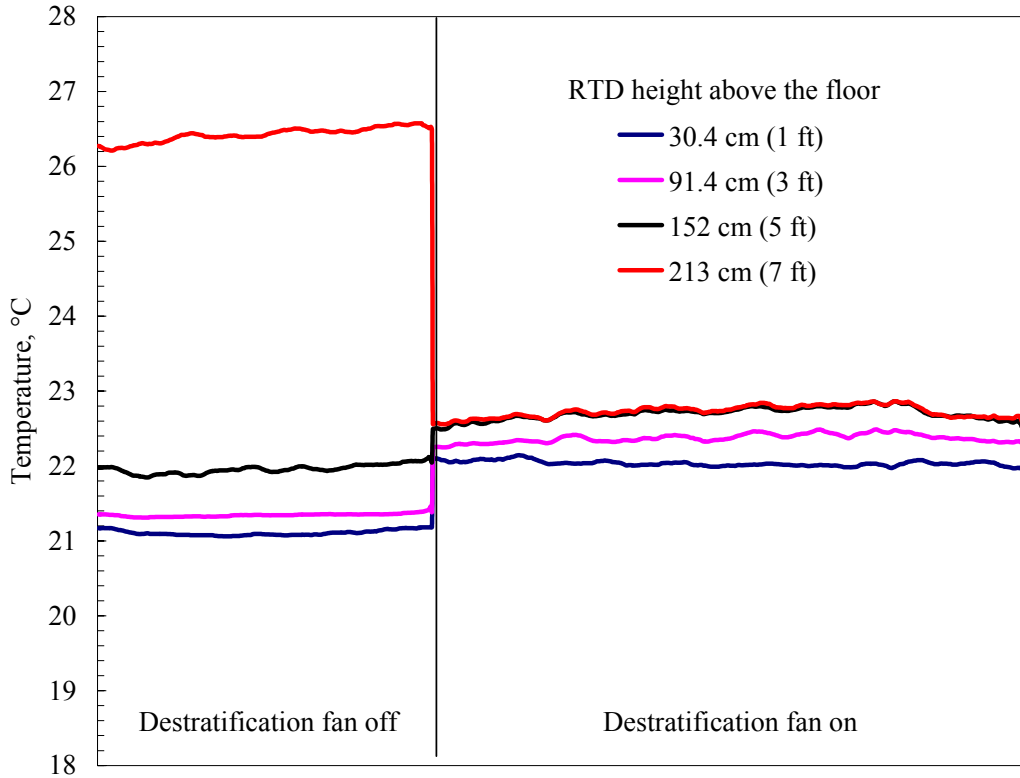


Figure 3.2(a) Temperature sensors located near windows

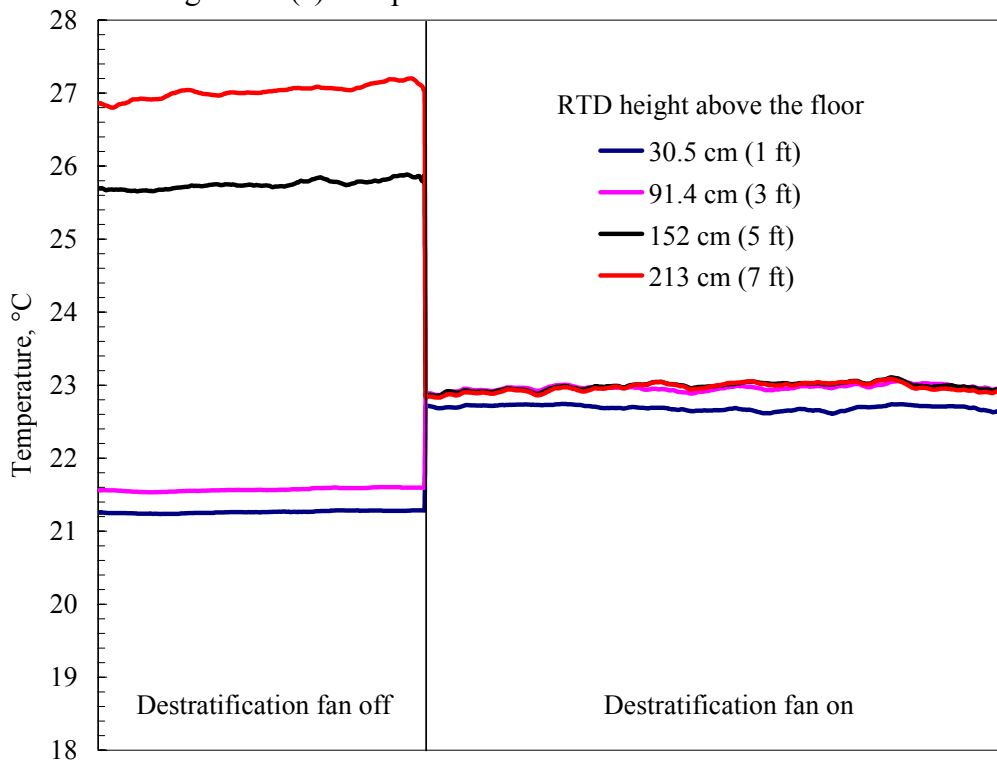


Figure 3.2(b) Temperature sensors located near back wall

Table 3.1 Lighting and baseboard power for each test room.

Room	Stage 2 W	Stage 2 W	Maximum Lights, W	Minimum Lights, W
East A	900	880	353.5	
East B	875	845	350.5	91.8
South A	885	875	358.5	
South B	870	875	359.0	91.8
West A	855	845	353.0	
West B	855	885	356.8	89.0
Interior A	865	880	355.8	
Interior B	915	900	358.0	

Table 3.2 provides the schedule for the operation of the lights and the first stage of baseboard heat used in this test. The time represents the beginning of each hour where 1 represents 1 AM and 24 represents midnight.

3.1.2.2 Daylighting controls specifications

The dimmable ballasts in each exterior “B” test room were controlled based on light-level measurements made at a single reference point in the room. Each test room had a table with a sensor on it located near the room center. The sensor pointed upwards and measured illuminance coming from all directions within a hemispherical field of view. Light incident on the sensor was the sum of daylight into the space and artificial light from the ceiling mounted lamps. The “A” test rooms had identical table and sensor locations. The lights in the “A” test rooms were not dimmed, but run at maximum output during the day. Figure 3.3 illustrates the table and sensor location for the test rooms.

Table 3.2 Lighting and baseboard heating schedules for all test rooms

Hour	Lights	Stage 1&2 Baseboard	Hour	Lights	Stage 1&2 Baseboard
1	OFF	OFF	13	ON	ON
2	OFF	OFF	14	ON	ON
3	OFF	OFF	15	ON	ON
4	OFF	OFF	16	ON	ON
5	ON	OFF	17	ON	OFF
6	ON	OFF	18	OFF	OFF
7	ON	OFF	19	OFF	OFF
8	ON	ON	20	OFF	OFF
9	ON	ON	21	OFF	OFF
10	ON	ON	22	OFF	OFF
11	ON	ON	23	OFF	OFF
12	ON	ON	24	OFF	OFF

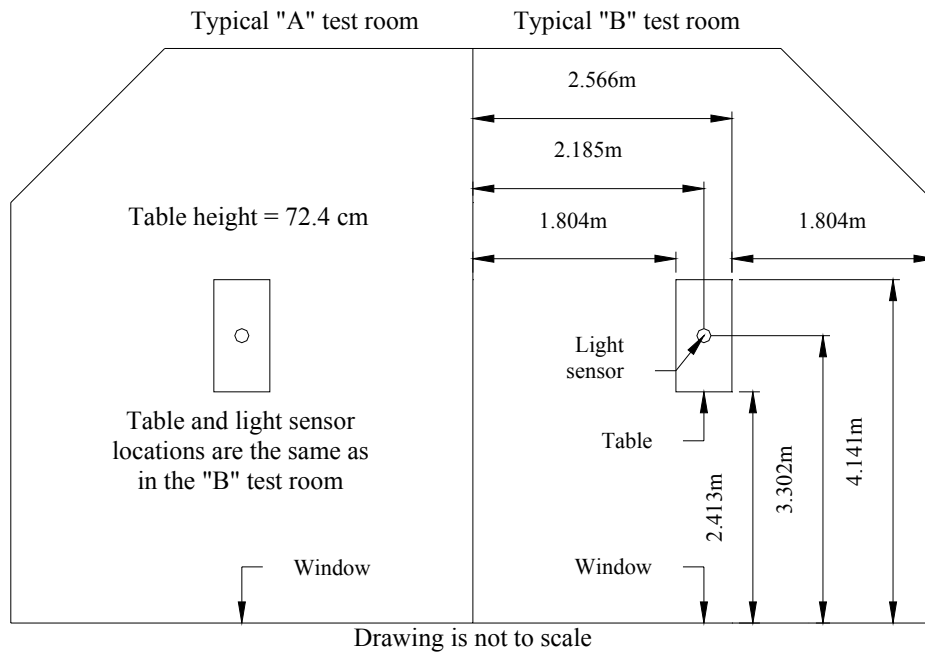


Figure 3.3 Location of table and light sensor

The lighting control sequence was based on an illuminance set-point level of 699.7 lux (65 foot-candles) measured at the reference point. As the amount of daylight in the space increased, the power output from the ballasts to the lights decreased in order to maintain the illuminance set point. The minimum power output from the dimmable ballasts was approximately 26% of the maximum ballast power output. (Refer to Table 3.3 for actual values.) If the ballasts power output was at the minimum value and the daylight levels in the space continued to increase such that the illuminance at the reference point exceeded 699.7 lux (65 foot-candles), then the room lights were turned off. The lights were turned back on when the illuminance at the reference point dropped below 592.0 lux (55 foot-candles).

Because the lighting control is based on total (artificial light plus daylight) illuminance at the reference point, it is important for the modeler to know the relationship between lighting power and the illuminance at the reference point due to artificial lights alone. Figure 3.4 is a plot of the illuminance at the reference point as a function of power to the room lights. The graph includes data for each of the three exterior "B test rooms.

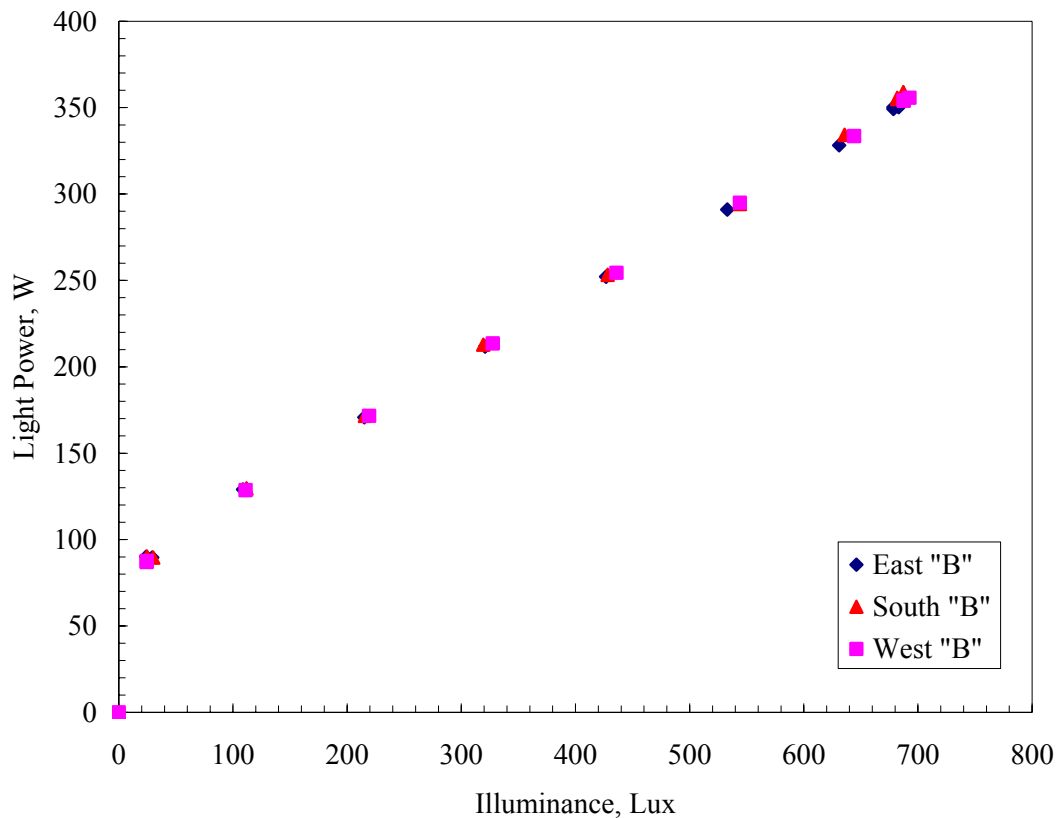


Figure 3.4 Reference-point illuminance levels as a function of lighting power.

3.1.2.3 Room-level HVAC controls specifications

Space temperature conditions were maintained by utilizing variable airflow rates (VAV) for space cooling and hydronic reheat for space heating. The cooling and heating set-point temperatures were the same for all test rooms and their values remained fixed throughout the test.

In heating mode the terminal unit operates at a prescribed minimum airflow rate, and the two-way hot water control valve modulates in response to the zone heating needs. In cooling mode, the two-way hot water control valve is closed, and the terminal unit modulates the primary supply airflow rate in response to the zone cooling needs. In addition to a minimum airflow rate, each unit has a maximum airflow rate. The values of these airflow rates depend on whether the room is an exterior room or an interior room. Table 3.4 provides temperature airflow set points for the test rooms.

Table 3.3 Reference point illuminance values and light power for the “B” test rooms.

East “B” Test Room		South “B” Test Room		West “B” Test Room	
Light Power W	Illuminance Lux	Light Power W	Illuminance Lux	Light Power W	Illuminance Lux
0.0	0.000	0.0	0.000	0.0	0.000
90.1	24.0	90.3	24.7	87.6	24.5
89.6	29.3	89.6	30.2	87.0	24.5
129.0	108.8	129.6	111.9	128.6	111.1
170.8	214.9	171.6	215.6	171.6	219.3
211.8	320.9	212.9	319.2	213.5	327.6
252.1	426.8	253.3	428.2	254.4	435.9
291.0	532.9	294.3	544.1	295.0	544.1
328.3	631.0	334.3	635.7	333.5	644.1
350.3	678.5	355.8	681.8	355.8	692.6
349.3	678.5	355.0	681.8	354.0	687.6

Table 3.4 provides values for the temperature set points and airflow rates for the test rooms.

Test room location	Heating set-point temperature, °C	Cooling set-point temperature, °C	Minimum airflow rate m ³ /hr	Maximum airflow rate m ³ /hr
East “A”	22.2	22.8	298	1,699
East “B”	22.2	22.8	323	1,699
South “A”	22.2	22.8	306	1,699
South “B”	22.2	22.8	283	1,699
West “A”	22.2	22.8	291	1,699
West “B”	22.2	22.8	307	1,699
Interior “A”	22.2	22.8	310	934
Interior “B”	22.2	22.8	298	934

3.1.3 System-level HVAC operation and control

This item describes the operation and control of the air handling systems that apply to this test. The air handling units for both the “A” and “B” systems were operated in the same manner throughout this test.

3.1.3.1 Air handling unit controls specifications

The system controls were specified as follows:

Heating schedule: always available

Cooling schedule: always available

Cooling control supply air temperature set point after the fan: 15.6 °C (60 °F)

Preheat: NOT available

Humidity control: NOT available

Economizer: disabled

Outside air control: disabled (0 % outside air)

3.1.3.2 System air specifications

The system airflow rates were specified as follows:
Supply air flow rate: maximum 6,031 m³/hr (3,550 cfm)
Return air path: plenum
Minimum outside air flow: none
Outside air control: none
Duct heat gain: 0.83 °C (1.5°F)

3.1.3.3 System fans specifications

The air-handling unit fans are specified as follows:
Supply air static pressure: 547.4 Pa (2.2 inch H₂O)
Fan schedule: always on
Supply fan power versus supply flow rate: shown in Figure 3.1
Supply fan control: 547.4 Pa (2.2 inch H₂O)
Return fan control differential: 340 m³/h (200 cfm) offset
Motor placement: In-air flow
Fan placement: Draw-through

Figure 3.5 shows the relationship between supply fan power and supply airflow rate. A quadratic regression analysis of the data is shown on the graph.

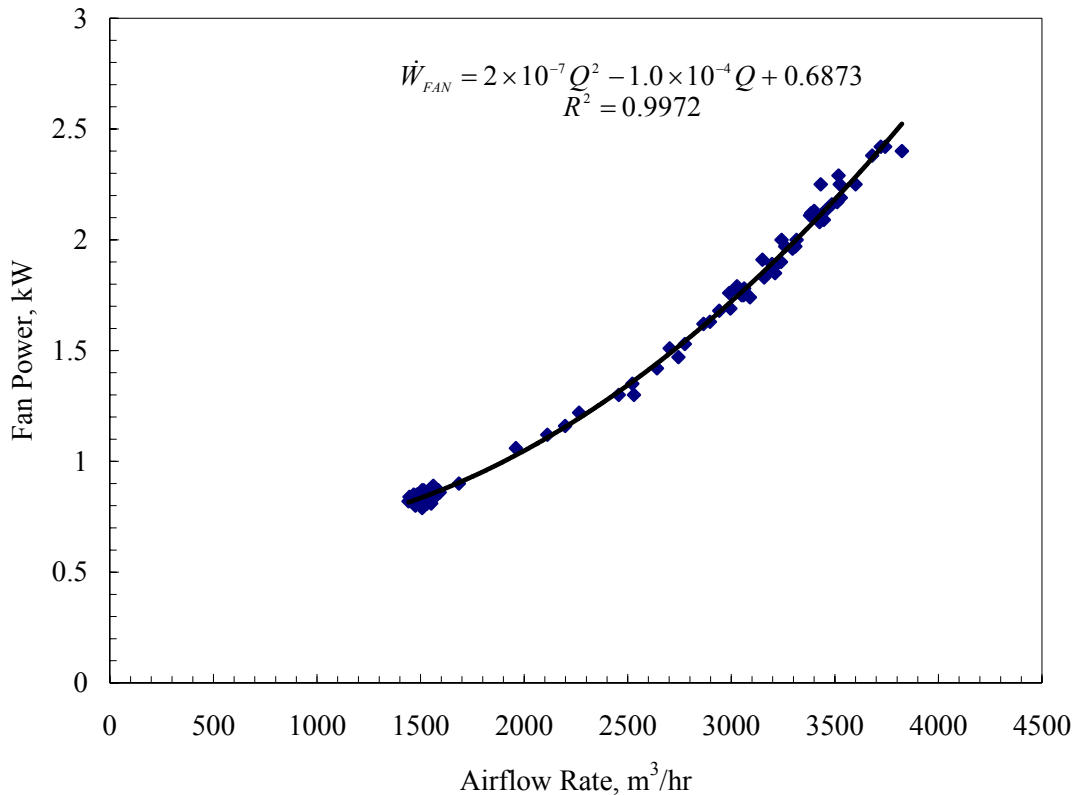


Figure 3.5 Fan power as a function of volumetric flow rate

3.2 Comparison between experimental results and simulation results

In this section the results from the computer simulations are compared with the values obtained from the experiments run at the ERS. The comparisons are made both graphically and statistically. The statistical parameters used were defined in Section 1.5.

Before comparing the results for any system or zone level parameters, the weather information used by each model must be validated. Weather data collected at the ERS were converted to TMY format and provided to each modeler. Comparison of the key weather parameters is a test to assure each program's weather processor is correctly interpreting the provided weather information.

3.2.1 Weather data

The key weather parameters are dry-bulb and wet-bulb temperatures, direct normal solar irradiation, and total horizontal solar irradiation. Table 3.5 gives the statistical comparison of the temperatures and solar fluxes, respectively. Figure 3.6 illustrates the weather parameters during the 5-day test period. The agreement between the ERS data and the models is acceptable.

Table 3.5 Statistical comparison of weather parameters.

Statistical Parameter	Dry-bulb temperature, °C			Wet-bulb temperature, °C			Direct normal irradiation, W/m ²			Total horizontal irradiation, W/m ²		
	ERS	DOE2.1E	TRNSYS	ERS	DOE2.1E	TRNSYS	ERS	DOE2.1E	TRNSYS	ERS	DOE2.1E	TRNSYS
\bar{x}	0.1	0.1	0.1	-1.1	-1.1	-1.1	62.8	68.1	68.1	73.1	73.3	73.3
σ												
s	4.6	4.6	4.6	4.4	4.4	4.4	175.6	187.2	187.2	127.7	127.6	127.6
x_{\max}	9.6	9.4	9.4	6.0	6.1	6.1	797.0	794.4	794.4	508.0	498.1	498.1
x_{\min}	-10.4	-10.6	-10.6	-11.4	-11.7	-11.7	0.0	0.0	0.0	0.0	0.0	0.0
\bar{D}		0.0	0.0		-0.1	-0.1		-5.3	-5.3		-0.2	-0.2
D_{\max}		0.4	0.4		0.5	0.5		140.4	140.4		39.5	39.5
D_{\min}		0.0	0.0		0.0	0.0		0.0	0.0		0.0	0.0
$ D $		0.2	0.2		0.2	0.2		10.8	10.8		3.7	3.7
D_{rms}		0.2	0.2		0.2	0.2		29.3	29.3		8.5	8.5
SE		-10.9	-10.9		4.8	4.8		-7.7	-7.7		-0.2	-0.2
IE		133.6	133.6		-14.5	-14.5		15.9	15.9		5.0	5.0

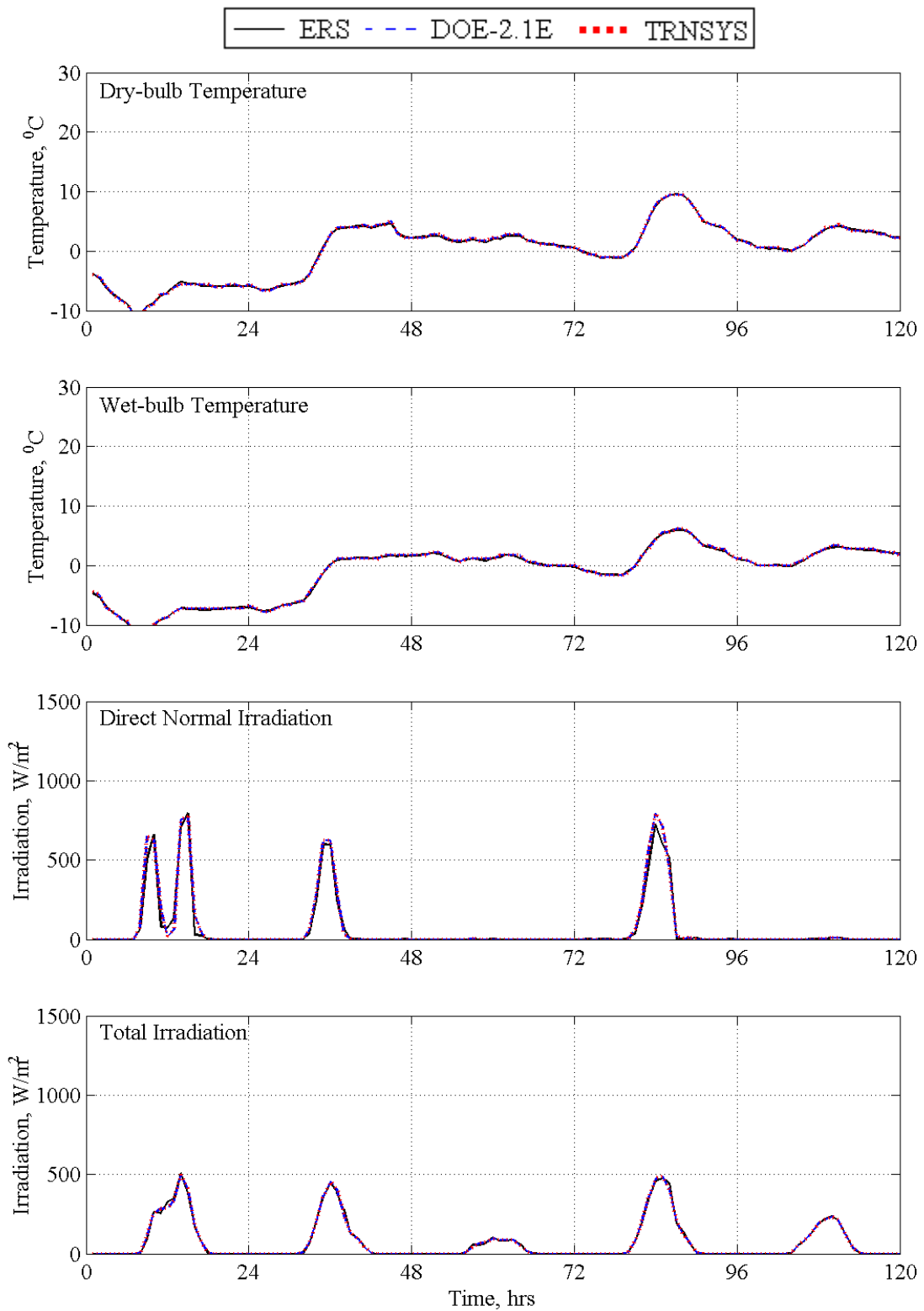


Figure 3.6 Weather parameters

3.2.2 Comparison with non-daylight controlled “A” test rooms

As described in Section 3.1, the “A” test rooms did not use daylight controls. Modelers simulated this condition, and in this section the results from the models are compared to the experimental values.

3.2.2.1 System level results for the “A” system

Air handling unit “A” supplies air to the “A” test rooms. As was shown Table 1.2, the parameters generally used for system-level comparison are the supply airflow rate, the outside airflow rate, the temperature of air entering cooling coil, the temperature of air leaving cooling coil, the temperature of return air, and the cooling coil energy. However, for this test, the outside airflow rate was specified to equal zero; therefore, the air temperature entering the cooling coil equals the return air temperature. Thus in the comparisons that follow, the outdoor airflow rate and inlet air temperature to the cooling coil are omitted.

Table 3.6 provides a statistical summary of the air handling unit parameters, while Figure 3.7 shows the graphical results for the five days of the test. The cooling coil load was calculated using Equation 2.1 (Section 2.2.2.1). The overall results show a good comparison between the models and the experimental results. However, the TRNSYS model over predicts the airflow rates for all days.

Table 3.6 Statistical comparison of AHU-A parameters

Statistical Parameter	Supply airflow rate, m ³ /hr			Return air temperature, °C			Leaving coil air temperature, °C			Cooling coil heat transfer rate, kW		
	ERS	DOE2.1E	TRNSYS	ERS	DOE2.1E	TRNSYS	ERS	DOE2.1E	TRNSYS	ERS	DOE2.1E	TRNSYS
\bar{x}	1716.9	1730.0	1898.7	22.6	22.8	22.5	13.4	13.3	13.4	5.3	5.4	5.5
σ	76.3			0.2			0.2			1.2		
s	687.0	784.1	922.0	0.4	0.4	0.3	0.3	0.5	0.0	2.2	2.3	2.8
x_{\max}	3246.0	3679.0	3791.0	23.3	23.8	23.0	15.4	14.5	13.4	10.8	10.7	11.2
x_{\min}	1201.0	1204.0	1205.0	22.1	21.9	22.1	12.6	12.9	13.4	3.1	3.6	3.3
\bar{D}		-13.1	-181.8		-0.2	0.1		0.1	0.0		-0.1	-0.2
D_{\max}		592.0	1208.0		1.1	0.7		1.5	2.0		2.0	3.9
D_{\min}		0.0	0.0		0.0	0.0		0.0	0.0		0.0	0.0
$ D $		92.1	201.0		0.4	0.2		0.5	0.2		0.3	0.7
D_{rms}		180.8	349.7		0.4	0.2		0.6	0.3		0.5	0.9
SE		-0.8	-9.6		-1.0	0.3		0.5	0.1		-2.7	-3.2
IE		5.3	10.6		1.7	0.7		3.5	1.6		6.4	12.3

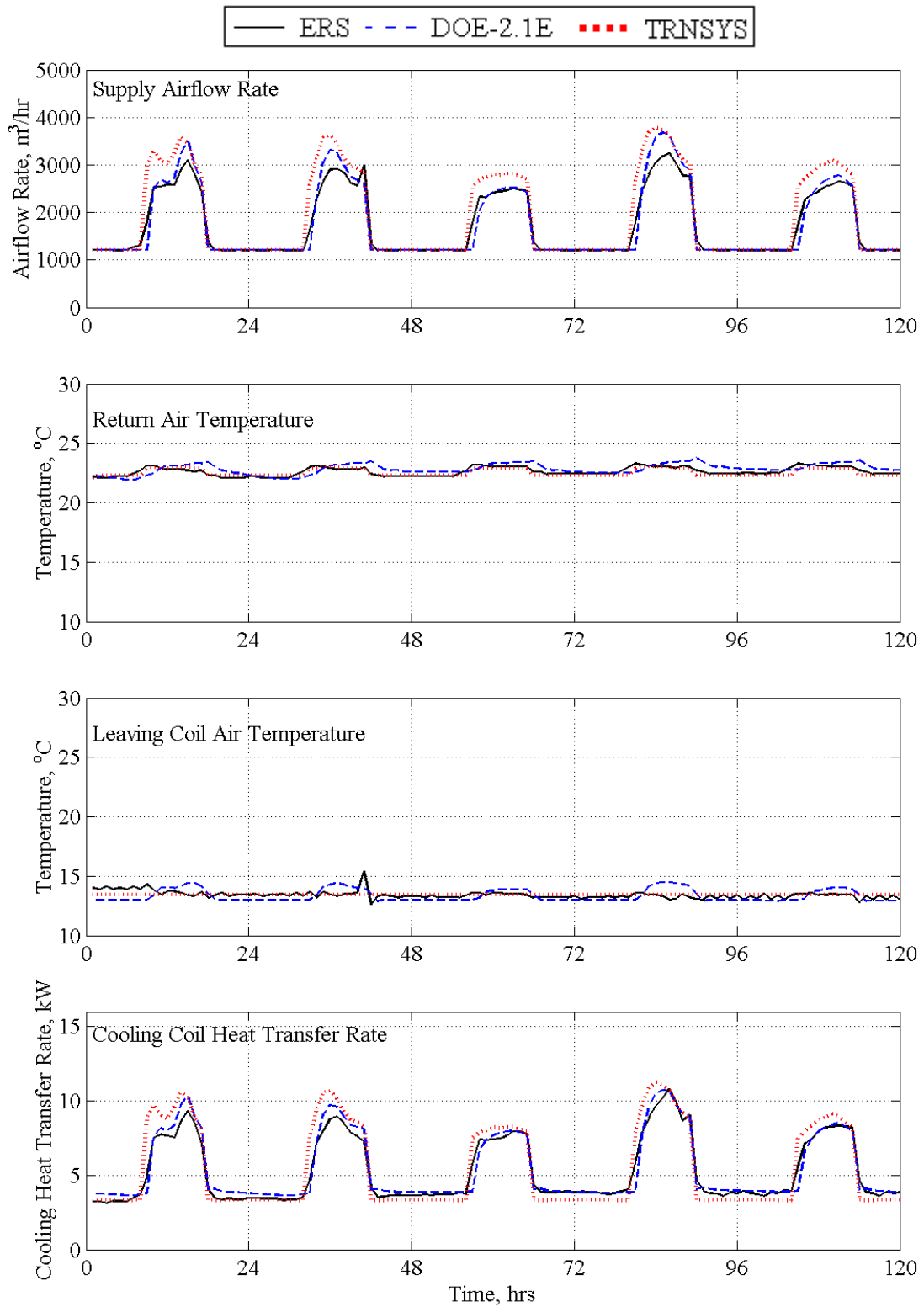


Figure 3.7 AHU-A parameters

3.2.2.2 Zone level results for the “A” test rooms

In this section, comparisons are made for the zone-level parameters. As was shown in Table 1.2, the zone-level parameters used for comparison are: the lighting electrical power, the luminance level at the reference point, the zone temperature, the supply airflow rate, the reheat energy, and the thermal load (without ventilation).

3.2.2.2.1 Lighting electrical power

Figure 3.8 shows the graphical results of the lighting electrical power. Because daylighting controls were not used for the “A” test rooms, the lighting electrical power remains constant while the lights are scheduled on and zero when the lights are scheduled off. Because this parameter is an input, it is expected that each model will produce the same results unless an input error has occurred. The plots show 100% agreement between the experiment and the models. A statistical comparison is not necessary for this parameter.

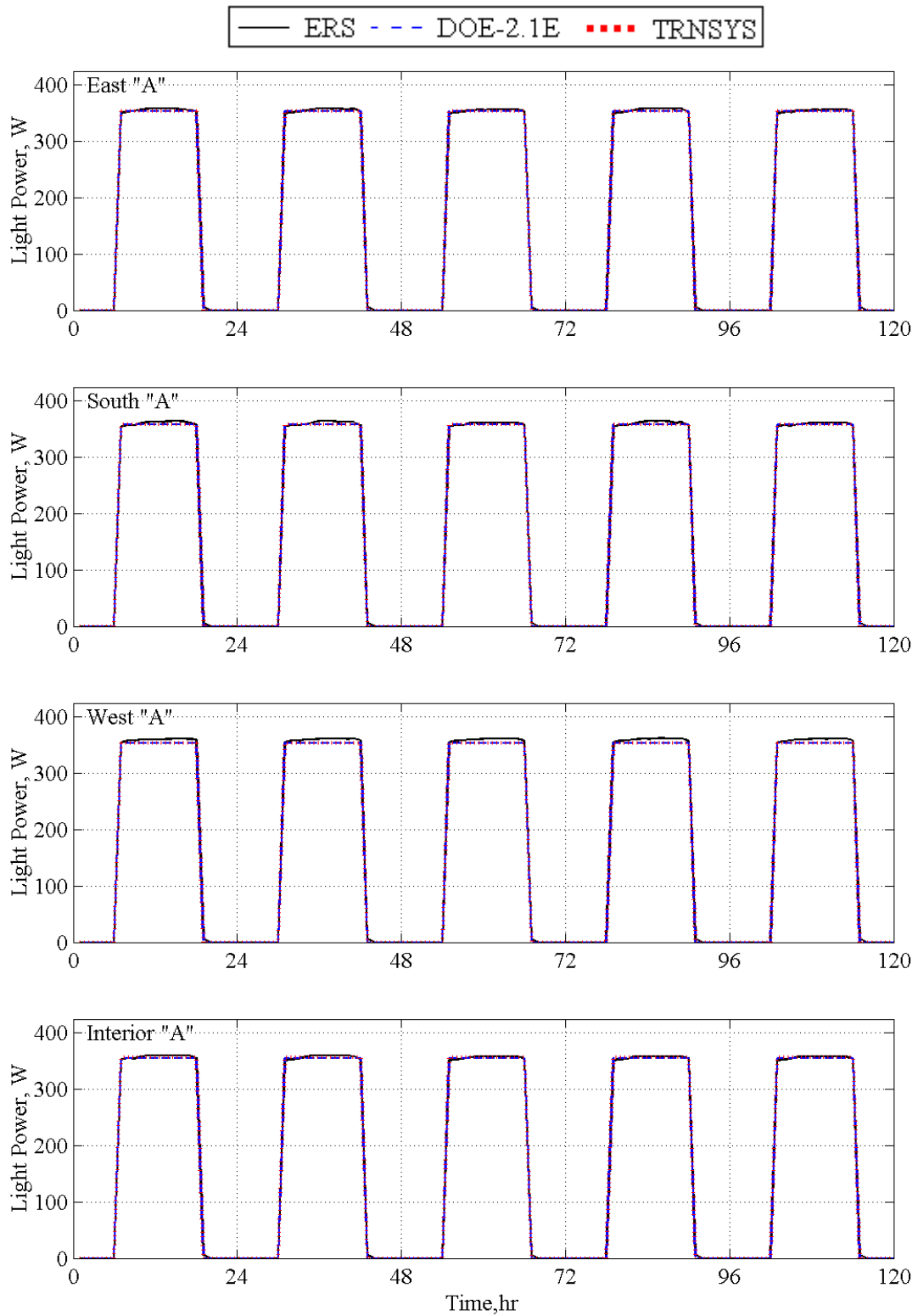


Figure 3.8 Lighting electrical power values for the "A" test rooms

3.2.2.2.2 Reference point illuminance

Figure 3.9 shows the graphical results of the illuminance values at the reference point. It is important to note that the values shown in the plots are illuminance values from daylight only since each model only accounts for daylight illuminance in the space. Light level measurements made during the experiment were modified to account for the illuminance from the overhead fluorescent lights. Because the interior test rooms have no exterior windows, the illuminance due to daylight is zero. Table 3.7 provides a statistical summary of the daylighting illuminance comparison for the “A” test rooms. The results show that both models are under predicting the illuminance in the space due to daylight on bright sunny days. These are similar results to those of Daylighting Test 1.

Table 3.7 Statistical comparison of the daylighting illuminance in the “A” test rooms, Lux

Statistical Parameter	East "A"			South "A"			West "A"		
	ERS	DOE2.1E	TRNSYS	ERS	DOE2.1E	TRNSYS	ERS	DOE2.1E	TRNSYS
\bar{x}	180.2	128.4	140.6	416.6	278.4	220.8	110.8	100.1	93.2
σ	5.6			8.2			3.8		
s	362.7	253.3	284.2	902.8	526.5	464.8	196.7	189.5	160.3
x_{\max}	2150.0	1379.5	1652.0	4004.0	2130.5	2285.5	1263.0	1314.5	822.7
x_{\min}	-2.0	0.0	0.0	11.0	0.0	0.0	-7.0	0.0	-1.4
\bar{D}		51.7	29.7		138.1	184.8		10.7	13.3
D_{\max}		770.5	1056.4		1873.5	2528.6		277.0	531.1
D_{\min}		1.0	0.0		4.6	0.0		0.2	0.0
$ D $		60.8	43.3		168.6	191.4		34.7	27.3
D_{rms}		135.8	125.8		423.8	520.4		66.4	70.2
SE		40.3	21.1		49.6	83.7		10.7	14.2
IE		47.3	30.8		60.5	86.7		34.7	29.3

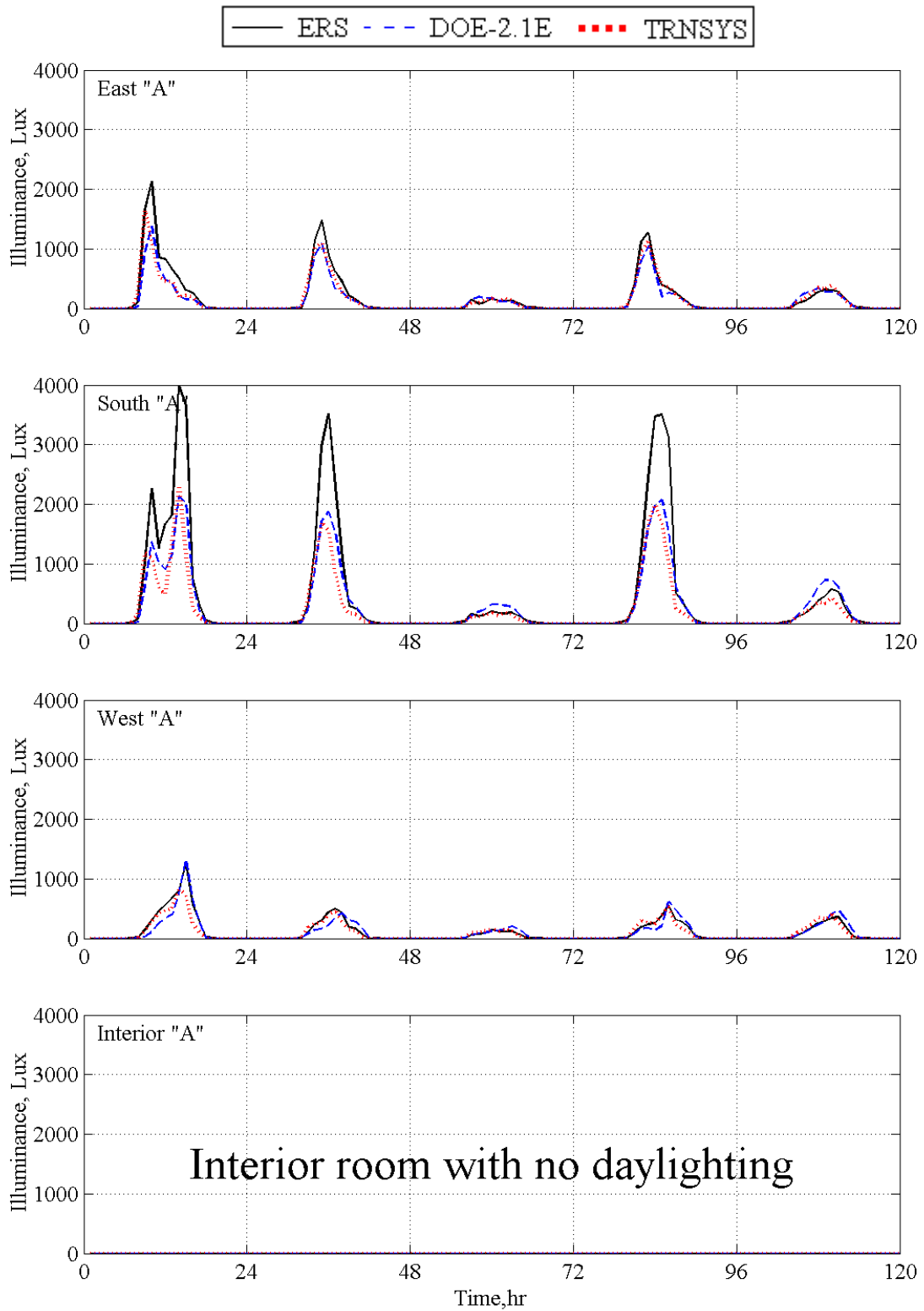


Figure 3.9 Reference point illuminance values due to daylight in the “A” test rooms

3.2.2.2.3 Zone temperatures

Figure 3.10 illustrates the zone temperatures for the “A” test rooms. The thermostat schedule called for a fixed heating set-point temperature of 22.2 °C and a fixed cooling set-point temperature of 22.8 °C. Table 3.8 provides a statistical summary of the room temperature comparison. These results show that the models are predicting the zone temperatures and that the “A” test rooms remained under temperature control through out the test. This is important given the heating valve problem discussed in Daylighting Test 1 which caused the Interior “A” test room to go out of control.

Table 3.8 Statistical comparison of the room temperature in the “A” test rooms, °C

Statistical Parameter	East "A"			South "A"			West "A"			Interior "A"		
	ERS	DOE2.1E	TRNSYS	ERS	DOE2.1E	TRNSYS	ERS	DOE2.1E	TRNSYS	ERS	DOE2.1E	TRNSYS
\bar{x}	22.4	22.4	22.4	22.4	22.4	22.4	22.4	22.4	22.4	22.5	22.4	22.4
σ	0.2			0.2			0.2			0.2		
s	0.5	0.3	0.3	0.5	0.3	0.3	0.5	0.4	0.3	0.6	0.3	0.3
x_{\max}	23.0	22.8	22.8	23.0	22.8	22.8	23.0	22.8	22.8	24.0	22.8	22.8
x_{\min}	22.0	21.6	22.0	22.0	21.7	22.1	22.0	21.4	22.1	22.0	22.2	22.2
\bar{D}		0.0	0.0		0.0	0.0		0.0	0.0		0.1	0.1
D_{\max}		0.4	0.2		0.3	0.2		0.6	0.2		1.2	1.2
D_{\min}		0.0	0.0		0.0	0.1		0.0	0.1		0.2	0.2
$ D $		0.2	0.2		0.2	0.2		0.2	0.2		0.3	0.3
D_{rms}		0.2	0.2		0.2	0.2		0.2	0.2		0.4	0.4
SE		0.0	-0.2		-0.1	-0.2		0.0	-0.2		0.3	0.3
IE		0.9	0.9		0.8	0.9		0.9	0.9		1.3	1.3

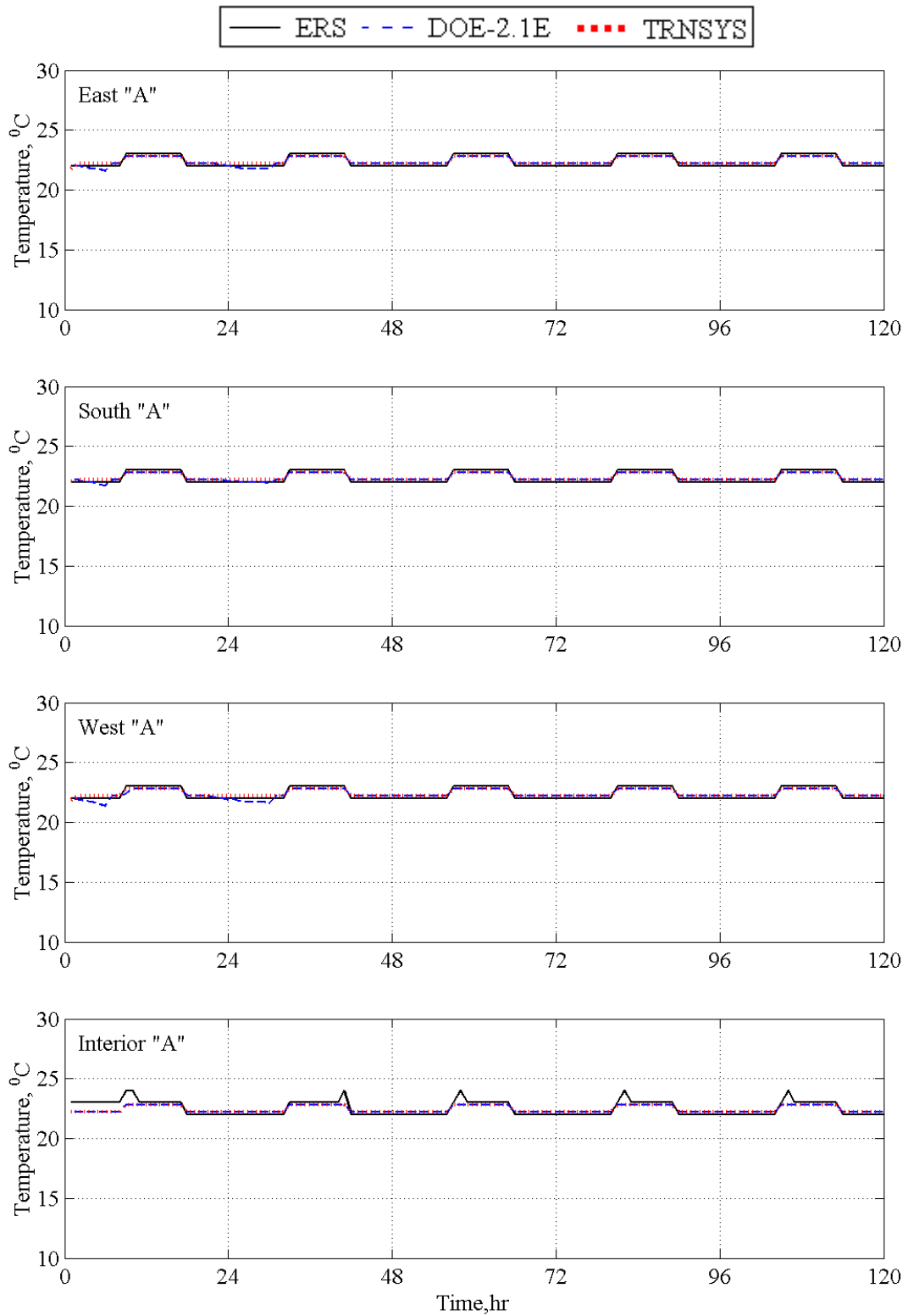


Figure 3.10 Room temperature values for the “A” test rooms

3.2.2.2.4 Zone airflow rates

Figure 3.11 illustrates the zone airflow rates for the “A” test rooms. For this test, the specified minimum supply airflow rates varied slightly from room to room (refer to Table 3.4). Table 3.9 provides a statistical summary of the room supply airflow rate comparison. The results show that the DOE2 results for the exterior test rooms are within the error bounds. TRNSYS is over predicting the airflow rates for all test rooms.

Table 3.9 Statistical comparison of the supply airflow rates in the “A” test rooms, m³/hr

Statistical Parameter	East "A"			South "A"			West "A"			Interior "A"		
	ERS	DOE2.1E	TRNSYS	ERS	DOE2.1E	TRNSYS	ERS	DOE2.1E	TRNSYS	ERS	DOE2.1E	TRNSYS
\bar{x}	421.1	407.4	475.0	452.7	462.0	510.0	380.9	391.7	433.8	462.2	469.6	480.0
σ	20.2			41.7			32.3			51.4		
s	168.8	163.7	238.8	226.0	266.3	296.9	134.3	156.5	189.0	191.6	228.0	220.1
x_{\max}	806.0	847.0	1029.0	1157.0	1412.0	1393.0	780.0	890.0	803.0	738.0	845.0	775.0
x_{\min}	294.0	298.0	298.0	304.0	306.0	306.0	290.0	291.0	291.0	310.0	310.0	310.0
\bar{D}		13.7	-53.8		-9.3	-57.2		-10.9	-53.0		-7.4	-17.8
D_{\max}		260.0	427.0		322.0	420.0		266.0	347.0		238.0	212.0
D_{\min}		0.0	0.0		0.0	0.0		0.0	0.0		0.0	0.0
$ D $		20.5	56.7		30.6	61.6		31.4	56.7		37.3	27.9
D_{rms}		43.9	101.7		66.5	122.2		63.7	103.6		65.1	52.6
SE		3.4	-11.3		-2.0	-11.2		-2.8	-12.2		-1.6	-3.7
IE		5.0	11.9		6.6	12.1		8.0	13.1		7.9	5.8

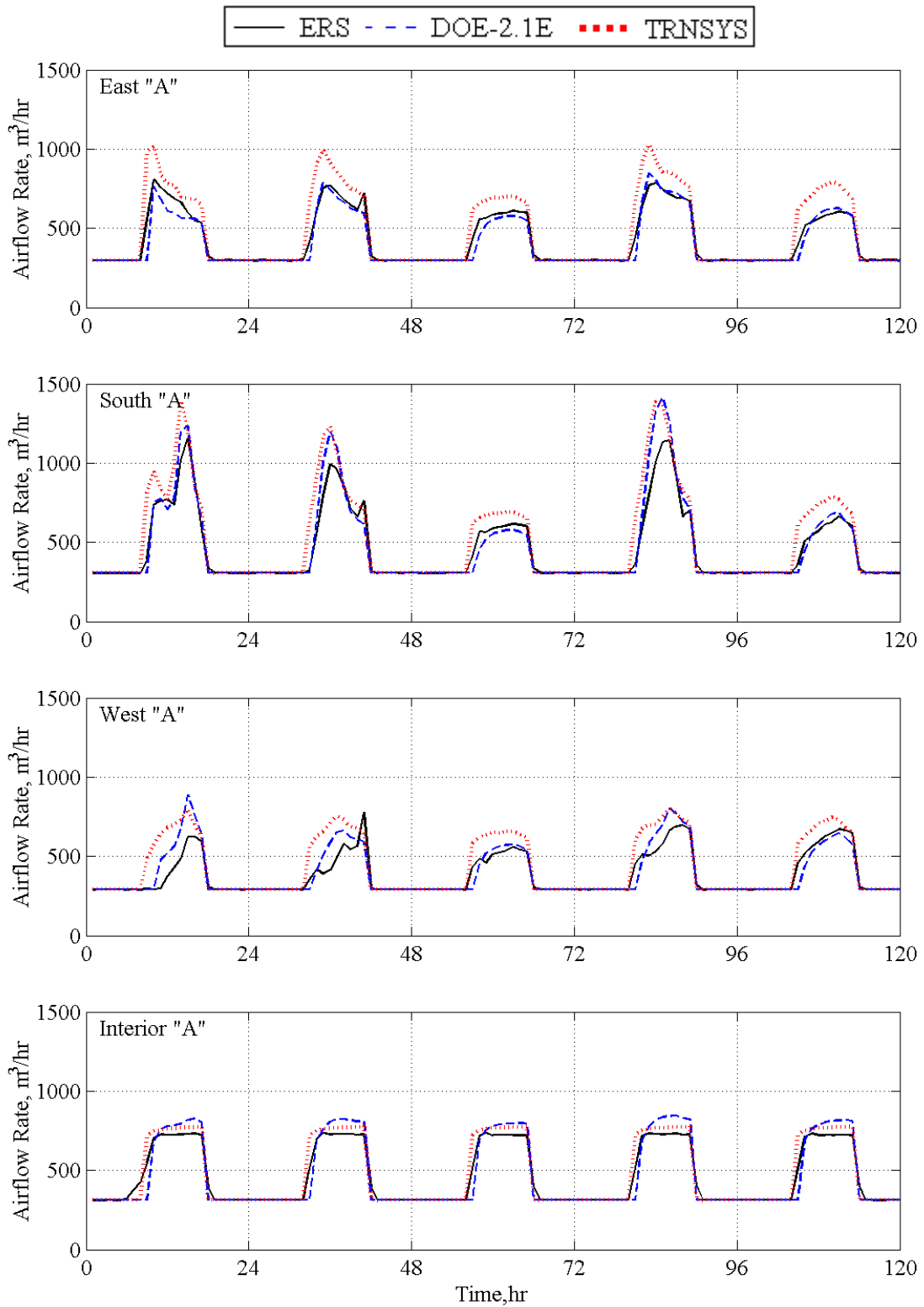


Figure 3.11 Supply airflow rates to the "A" test rooms

3.2.2.2.5 Zone reheat power

Figure 3.12 illustrates the zone reheat power for the “A” test rooms. The zone reheat power as calculated using Equation 2.2 (Section 2.2.2.2.5). Table 3.10 provides a statistical summary of the zone reheat power comparison. The results show that both models under predict the reheat power; however, the results are considerably better than for Daylighting Test 1. This is due to the reduction in vertical temperature stratification in the test rooms.

Table 3.10 Statistical comparison of the reheat power in the “A” test rooms, W

Statistical Parameter	East "A"			South "A"			West "A"			Interior "A"		
	ERS	DOE2.1E	TRNSYS	ERS	DOE2.1E	TRNSYS	ERS	DOE2.1E	TRNSYS	ERS	DOE2.1E	TRNSYS
\bar{x}	857.5	734.7	665.7	950.4	742.7	649.1	959.8	727.7	660.0	576.8	386.4	431.6
σ	249.8			420.9			344.5			329.4		
s	682.2	629.7	542.1	762.8	637.3	525.7	738.2	623.0	535.0	418.0	336.7	355.4
x_{\max}	1752.0	1402.0	1660.0	1975.0	1440.0	1528.0	1986.0	1370.0	1624.0	1534.0	736.0	811.0
x_{\min}	0.0	0.0	0.0	0.0	0.0	0.0	10.0	0.0	0.0	48.0	0.0	0.0
\bar{D}		122.8	191.9		207.8	301.3		232.1	299.9		190.4	145.2
D_{\max}		884.0	689.0		711.0	961.0		927.0	920.0		1078.0	1082.0
D_{\min}		0.0	0.0		0.0	0.0		10.0	10.0		48.0	11.0
$ D $		123.4	194.3		208.2	303.7		232.1	300.0		190.4	154.1
D_{rms}		199.6	264.8		282.0	405.4		312.7	387.4		246.1	219.3
SE		16.7	28.8		28.0	46.4		31.9	45.4		49.3	33.7
IE		16.8	29.2		28.0	46.8		31.9	45.5		49.3	35.7

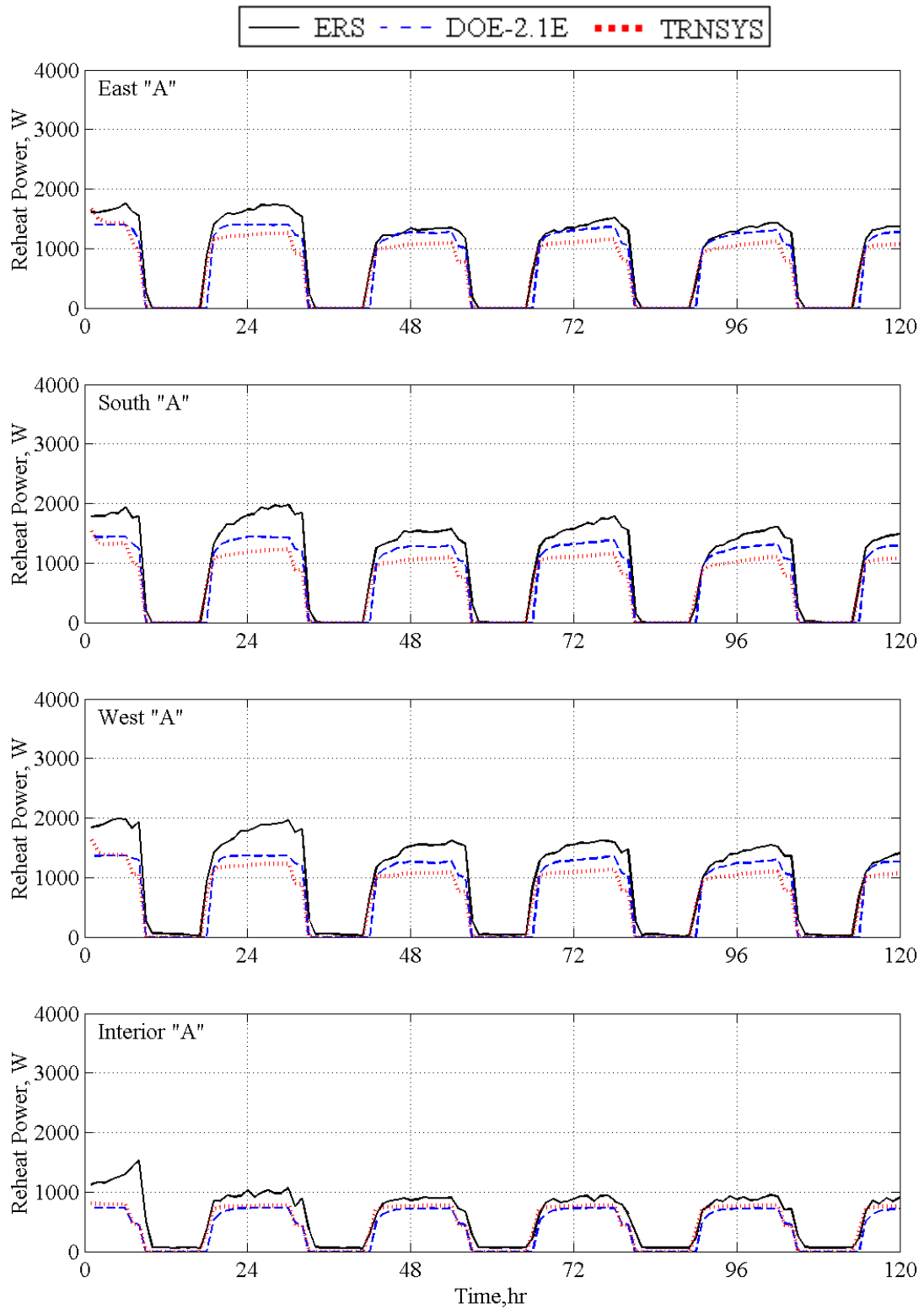


Figure 3.12 Reheat power for the "A" test rooms

3.2.2.2.6 Zone thermal load

Figure 3.13 illustrates the thermal load for each of the “A” test rooms. The zone thermal load was calculated using Equation 2.3 (Section 2.2.2.2.6). Table 3.11 provides a statistical summary of the room thermal load comparison. The table is divided into heating and cooling loads, and for simplicity, heating loads are given as positive values. The results show that overall the models are predicting the heating loads and under predicting the cooling loads. The uncertainty in the thermal load calculations makes it difficult for quantitative comparisons.

Table 3.11 Statistical comparison of the room thermal loads in the “A” test rooms, W

Statistical Parameter	East "A"			South "A"			West "A"			Interior "A"		
	ERS	DOE2.1E	TRNSYS	ERS	DOE2.1E	TRNSYS	ERS	DOE2.1E	TRNSYS	ERS	DOE2.1E	TRNSYS
Room Cooling Loads, W												
\bar{x}	951.4	481.9	716.4	1062.0	583.4	805.2	769.6	445.0	642.0	1261.4	677.5	765.4
σ	283.3			340.0			273.0			559.3		
s	1239.3	639.6	937.7	1459.8	825.6	1088.8	1020.0	593.7	833.1	1343.4	807.1	917.4
x_{max}	3472.0	1831.6	2543.0	4961.0	2883.4	3499.0	2789.0	1842.1	2038.0	3196.0	1768.7	1968.0
x_{min}	0.0	0.0	0.0	0.0	0.0	0.0	0.0	0.0	0.0	0.0	0.0	0.0
\bar{D}		469.5	235.0		478.6	256.8		324.6	127.6		583.8	495.9
D_{max}		1751.1	1174.0		2365.6	1959.0		1342.7	881.0		1522.9	1259.0
D_{min}		0.0	0.0		0.0	0.0		0.0	0.0		0.0	0.0
$ D $		469.5	264.8		478.6	305.1		324.6	174.9		585.9	505.1
D_{rms}		774.8	438.0		813.7	539.5		553.7	315.0		804.3	689.2
SE		97.4	32.8		82.0	31.9		73.0	19.9		86.2	64.8
IE		97.4	37.0		82.0	37.9		73.0	27.2		86.5	66.0
Room Heating Loads, W												
\bar{x}	312.5	394.1	263.8	354.6	388.9	229.3	367.4	398.1	255.0	2.4	27.0	29.3
σ	380.7			389.2			391.6			18.1		
s	299.0	336.5	257.8	340.9	334.3	223.9	357.4	340.0	247.0	13.9	32.9	32.6
x_{max}	886.0	893.8	1014.0	999.0	889.1	829.0	1058.0	910.6	958.0	107.0	72.4	106.0
x_{min}	0.0	0.0	0.0	0.0	0.0	0.0	0.0	0.0	0.0	0.0	0.0	0.0
\bar{D}		-81.6	48.7		-34.2	125.3		-30.7	112.4		-24.6	-26.9
D_{max}		331.7	482.0		389.9	669.0		349.0	643.0		72.4	106.0
D_{min}		0.0	0.0		0.0	0.0		0.0	0.0		0.0	0.0
$ D $		89.2	69.8		71.3	130.7		82.0	124.2		25.6	27.2
D_{rms}		129.8	125.3		108.1	207.4		122.2	201.8		40.7	40.9
SE		-20.7	18.5		-8.8	54.7		-7.7	44.1		-91.2	-91.9
IE		22.6	26.4		18.3	57.0		20.6	48.7		94.8	92.9

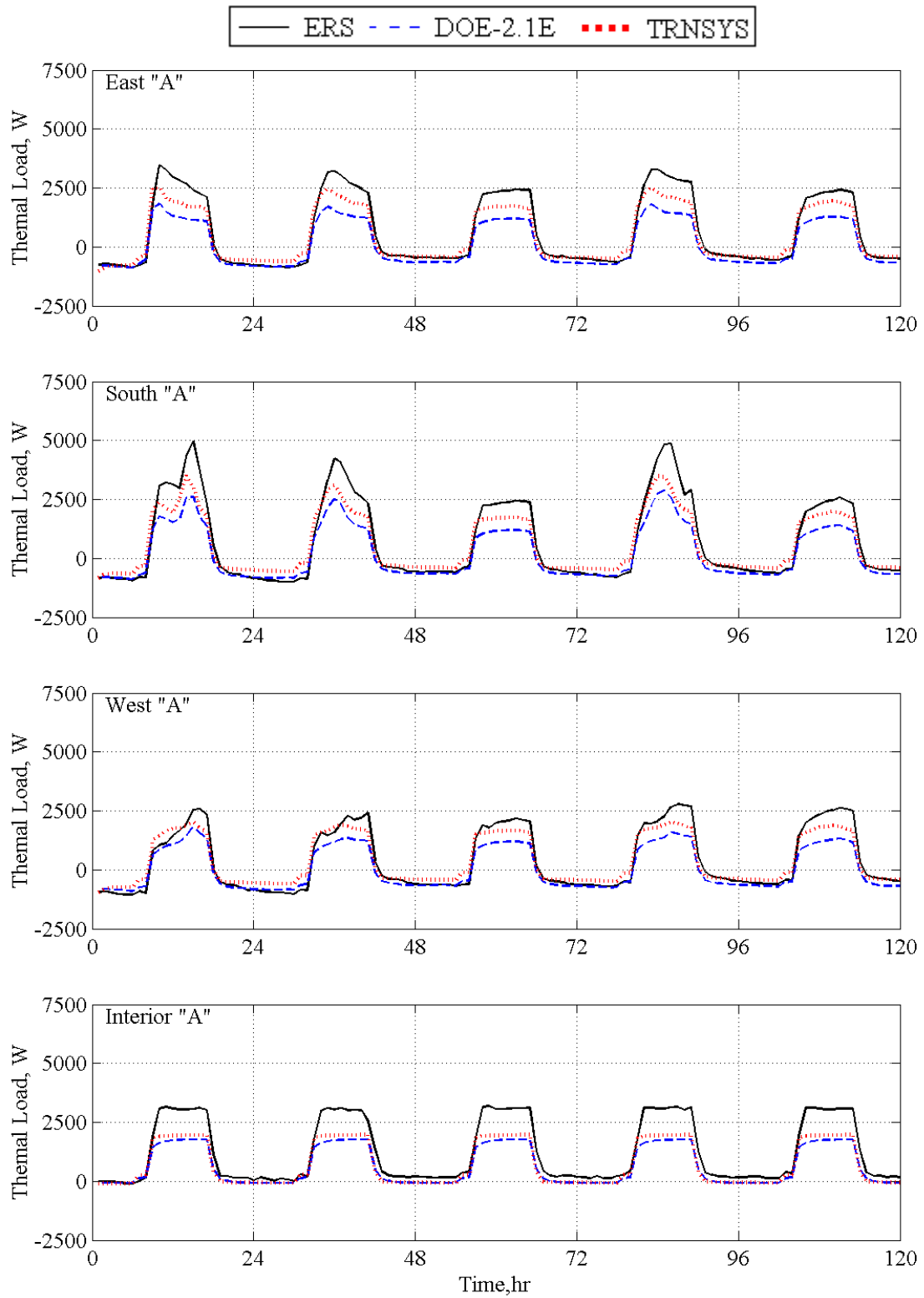


Figure 3.13 Thermal loads for the "A" test rooms

3.2.3 Comparison with daylight controlled “B” test rooms

As discussed in Section 3.1, the “B” test rooms used daylight controls. Modelers simulated this condition, and in this section the results from the models are compared to the experimental values.

3.2.3.1 System level results for the “B” system

Air handling unit “B” supplies air to the “B” test rooms. As was shown Table 1.2, the parameters generally used for system-level comparison are the supply airflow rate, the outside airflow rate, the temperature of air entering cooling coil, the temperature of air leaving cooling coil, the temperature of return air, and the cooling coil energy. However, for this test, the outside airflow rate was specified to equal zero; therefore, the air temperature entering the cooling coil equals the return air temperature. Table 3.12 provides a statistical summary of the air handling unit parameter comparison. The results show reasonable agreement for all parameters except for the TRNSYS supply airflow rates and cooling coil loads. The internal heat generation rates may be too large for the TRNSYS model.

Table 3.12 Statistical comparison of AHU-B parameters

Statistical Parameter	Supply airflow rate, m ³ /hr			Return air temperature, °C			Leaving coil air temperature, °C			Cooling coil heat transfer rate, kW		
	ERS	DOE2.1E	TRNSYS	ERS	DOE2.1E	TRNSYS	ERS	DOE2.1E	TRNSYS	ERS	DOE2.1E	TRNSYS
\bar{x}	1648.8	1669.9	1847.6	22.3	22.8	22.7	13.3	13.3	13.3	4.9	5.3	5.3
σ	112.0			0.2			0.2			1.6		
s	600.9	682.7	838.4	0.4	0.4	0.2	0.3	0.5	0.0	1.9	2.0	2.6
x_{\max}	3044.0	3435.0	3479.0	23.1	23.7	23.1	14.7	14.4	13.3	9.8	10.1	10.4
x_{\min}	1206.0	1211.0	1211.0	21.7	22.0	22.3	12.6	12.9	13.3	3.0	3.7	3.3
\bar{D}		-21.1	-198.7		-0.5	-0.4		0.0	0.0		-0.4	-0.4
D_{\max}		437.0	1120.0		1.4	0.8		1.5	1.4		1.5	3.9
D_{\min}		0.0	0.0		0.0	0.0		0.0	0.0		0.0	0.0
$ D $		68.3	209.5		0.6	0.4		0.4	0.2		0.4	0.8
D_{rms}		131.7	359.0		0.6	0.4		0.5	0.3		0.6	1.1
SE		-1.3	-10.8		-2.2	-1.6		-0.3	-0.3		-6.7	-7.4
IE		4.1	11.3		2.5	1.7		3.2	1.5		8.5	14.2

Figure 3.14 shows the graphical results of the AHU-B system parameters during the five days of the test.

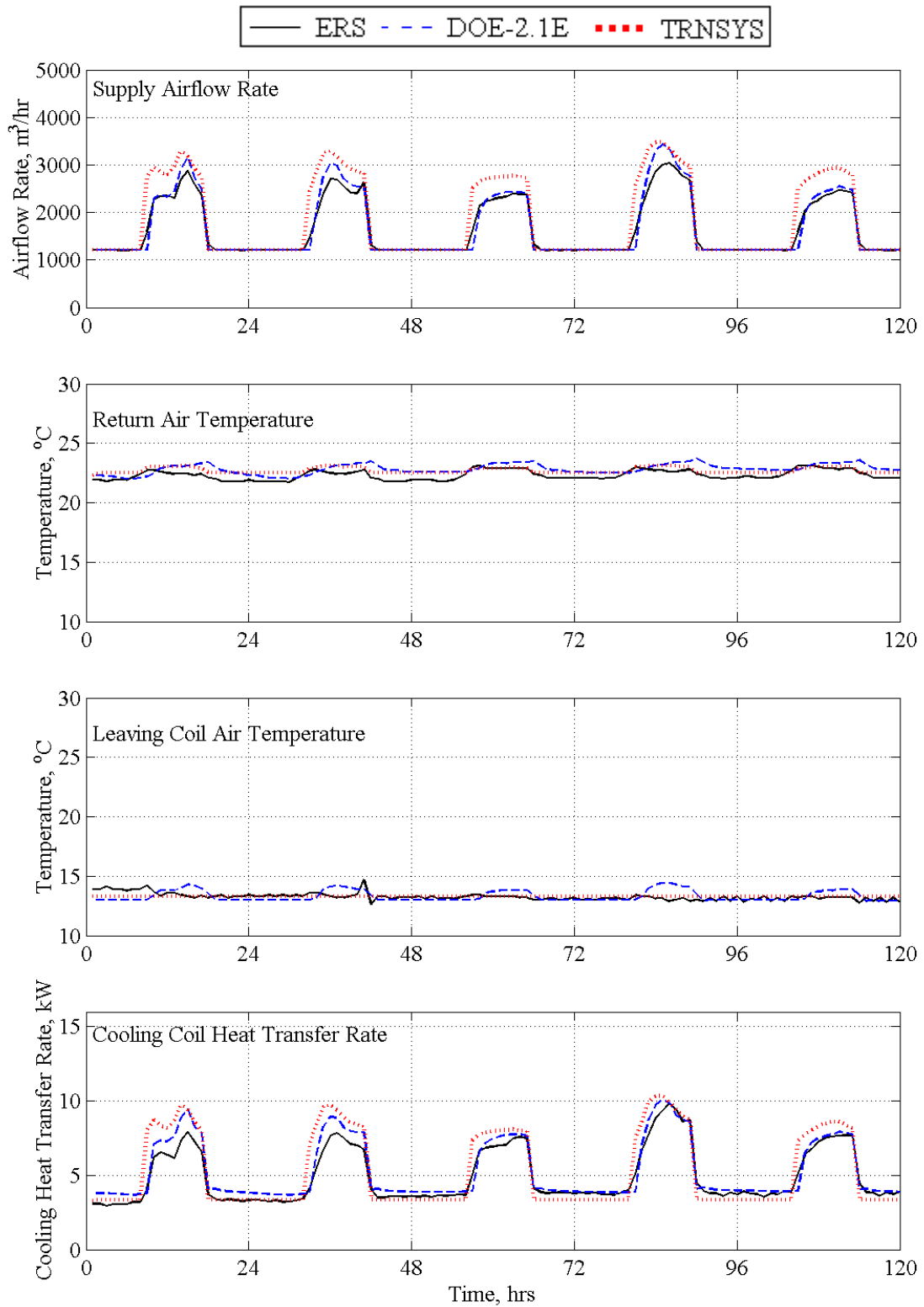


Figure 3.14 AHU-B parameters

3.2.3.2 Zone level results for the “B” test rooms

In this section, comparisons are made for the zone-level parameters. As was shown in Table 1.2, the zone-level parameters used for comparison are: the lighting electrical power, the luminance level at the reference point, the zone temperature, the supply airflow rate, the reheat energy, and the thermal load (without ventilation).

3.2.3.2.1 Lighting electrical power

Because daylighting controls were used for the “B” test rooms, the lighting electrical power reduces as the amount of available daylight enters the space. The control algorithm allowed for the lights to be turned off if sufficient daylight was available. Figure 3.15 shows the graphical results of the lighting electrical power. Because there is no daylight available for the interior test room, the interior room lights remain at 100% power while they are scheduled on. Table 3.13 provides a statistical summary of the lighting electrical power comparison. The overall results show a reasonable comparison for most of the daylight hours.

Table 3.13 Statistical comparison of lighting electrical power in the “B” test rooms, W

Statistical Parameter	East “B”			South “B”			West “B”			Interior “B”		
	ERS	DOE2.1E	TRNSYS	ERS	DOE2.1E	TRNSYS	ERS	DOE2.1E	TRNSYS	ERS	DOE2.1E	TRNSYS
\bar{x}	121.7	127.7	128.3	110.5	98.5	117.8	136.3	139.5	142.8	179.9	179.0	179.0
σ	0.1			0.1			0.1			0.1		
s	148.5	149.4	150.2	150.4	142.1	152.2	151.3	151.7	151.9	180.1	179.8	179.8
x_{max}	354.0	350.3	351.0	361.0	356.8	359.0	358.0	356.8	357.0	362.0	358.0	358.0
x_{min}	0.0	0.0	0.0	0.0	0.0	0.0	0.0	0.0	0.0	0.0	0.0	0.0
\bar{D}		-6.0	-6.6		11.9	-7.3		-3.2	-6.5		0.9	0.9
D_{max}		164.1	188.0		193.0	187.0		163.6	152.0		6.0	6.0
D_{min}		0.0	0.0		0.0	0.0		0.0	0.0		0.0	0.0
$ D $		12.9	12.1		13.9	14.3		14.2	12.7		1.2	1.2
D_{rms}		31.9	31.5		32.4	36.8		32.1	28.5		2.0	2.0
SE		-4.7	-5.1		12.1	-6.2		-2.3	-4.5		0.5	0.5
IE		10.1	9.4		14.1	12.2		10.2	8.9		0.7	0.7

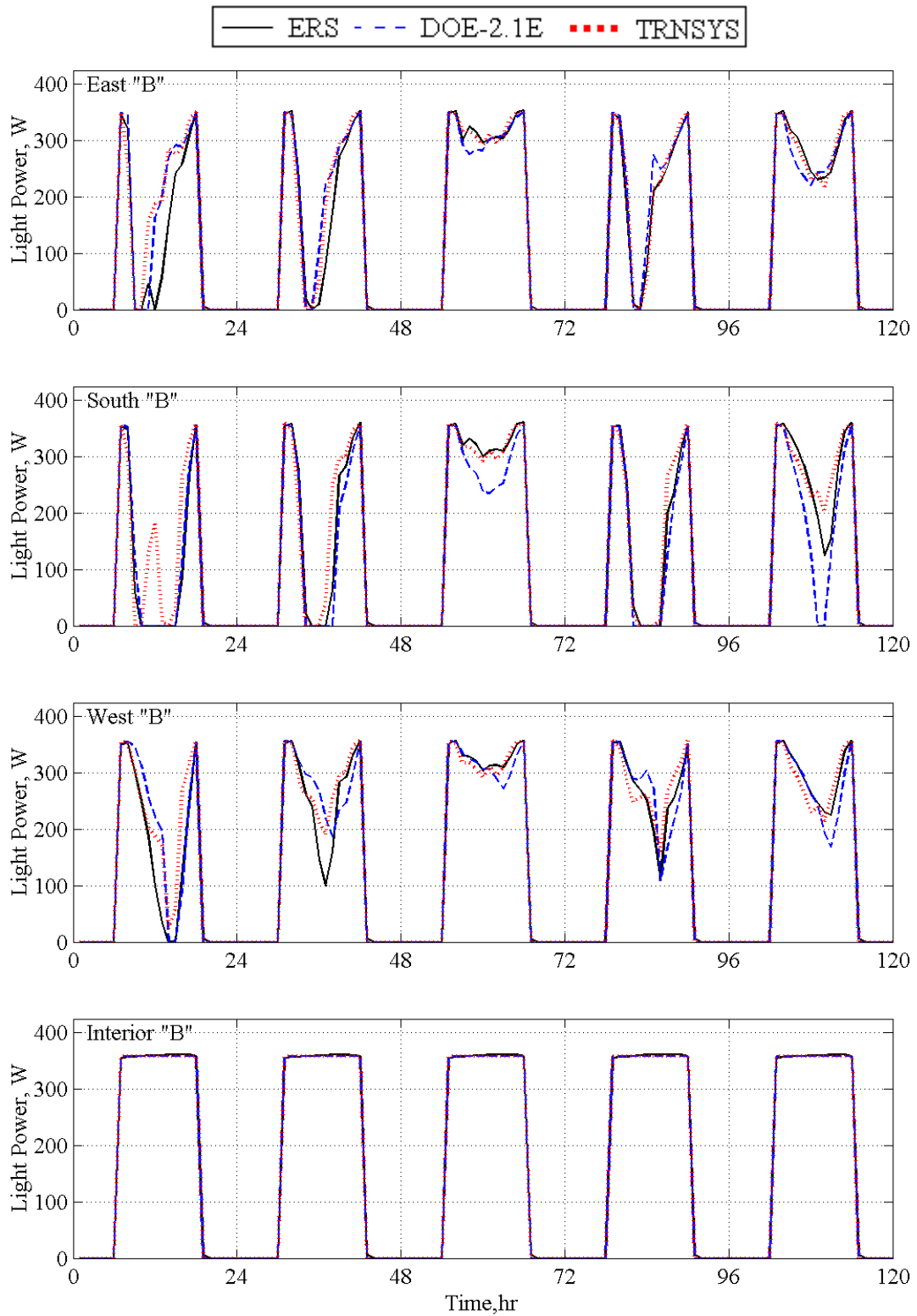


Figure 3.15 Lighting electrical power values for the "B" test rooms

3.2.3.2.2 Reference point illuminance

Figure 3.16 shows the graphical results of the illuminance values at the reference point. It is important to note that the values shown in the plots are illuminance values from daylight only since each model only accounts for daylight illuminance in the space. Light level measurements made during the experiment were modified to account for the illuminance from the overhead fluorescent lights. Because the interior test rooms have no exterior windows, the illuminance due to daylight is zero. Table 3.14 provides a statistical summary of the daylighting illuminance comparison. These results are similar to those seen for the “A” test rooms.

Table 3.14 Statistical comparison of the daylighting illuminance in the “B” test rooms, Lux

Statistical Parameter	East "B"			South "B"			West "B"		
	ERS	DOE2.1E	TRNSYS	ERS	DOE2.1E	TRNSYS	ERS	DOE2.1E	TRNSYS
\bar{x}	170.9	128.6	142.1	353.3	263.0	220.9	114.6	100.9	92.5
σ	4.1			5.9			3.9		
s	348.1	253.6	284.1	805.1	497.3	461.2	213.8	191.3	159.0
x_{\max}	2024.0	1381.1	1650.7	3510.0	2012.7	2271.9	1377.0	1327.9	840.8
x_{\min}	0.0	0.0	0.0	0.0	0.0	0.0	0.0	0.0	-4.8
\bar{D}		42.3	28.5		90.4	132.3		13.6	22.1
D_{\max}		643.4	942.7		1497.3	2094.4		308.2	589.1
D_{\min}		0.0	0.0		3.0	0.0		0.0	0.0
$ D $		50.4	40.2		140.3	153.5		35.3	33.6
D_{rms}		117.9	113.9		345.4	416.8		75.2	83.9
SE		32.9	20.1		34.4	59.9		13.5	23.9
IE		39.2	28.3		53.4	69.5		35.0	36.3

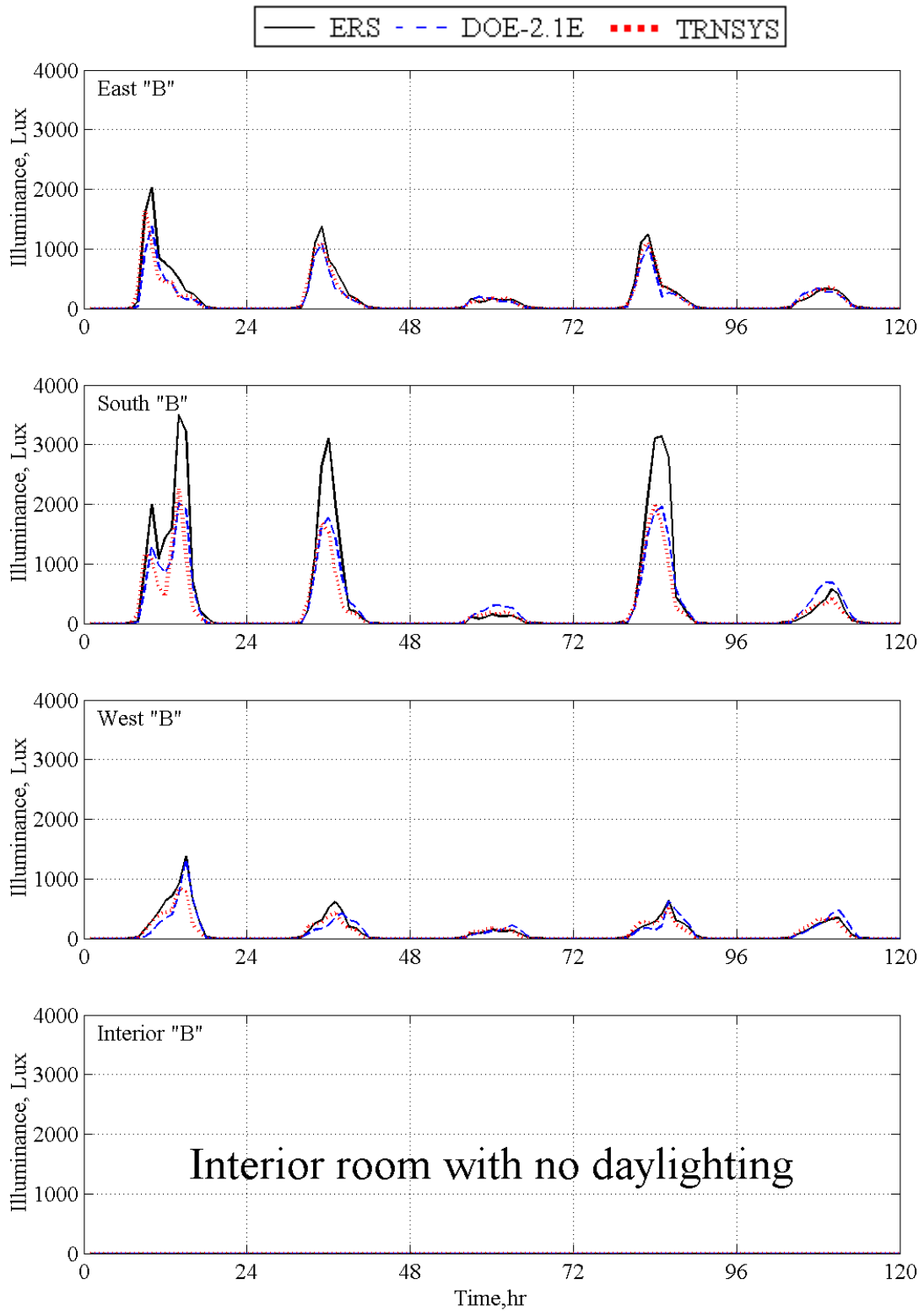


Figure 3.16 Reference point illuminance values due to daylight in the “B” test rooms

3.2.3.2.3 Zone temperatures

Figure 3.17 illustrates the zone temperatures for the “B” test rooms. The thermostat schedule called for a fixed heating set-point temperature of 22.2 °C and a fixed cooling set-point temperature of 22.8 °C. Table 3.15 provides a statistical summary of the room temperature. Good comparisons are seen between the empirical results and the models.

Table 3.15 Statistical comparison of the room temperature in the “B” test rooms, °C

Statistical Parameter	East "B"			South "B"			West "B"			Interior "B"		
	ERS	DOE2.1E	TRNSYS	ERS	DOE2.1E	TRNSYS	ERS	DOE2.1E	TRNSYS	ERS	DOE2.1E	TRNSYS
\bar{x}	22.4	22.4	22.4	22.4	22.4	22.4	22.4	22.4	22.4	22.4	22.4	22.4
σ	0.2			0.2			0.2			0.2		
s	0.5	0.3	0.3	0.5	0.4	0.3	0.5	0.3	0.3	0.5	0.3	0.3
x_{\max}	23.0	22.8	22.8	23.0	22.8	22.8	23.0	22.8	22.8	23.0	22.8	22.8
x_{\min}	22.0	21.9	22.1	22.0	21.4	22.2	22.0	21.6	22.1	22.0	22.2	22.2
\bar{D}		0.0	0.0		0.0	-0.1		0.0	0.0		-0.1	-0.1
D_{\max}		0.2	0.2		0.6	0.2		0.8	0.2		0.2	0.2
D_{\min}		0.0	0.1		0.0	0.2		0.0	0.1		0.2	0.2
$ D $		0.2	0.2		0.2	0.2		0.2	0.2		0.2	0.2
D_{rms}		0.2	0.2		0.2	0.2		0.2	0.2		0.2	0.2
SE		-0.2	-0.2		0.0	-0.2		-0.1	-0.2		-0.2	-0.2
IE		0.9	0.9		0.9	0.9		0.9	0.9		0.9	0.9

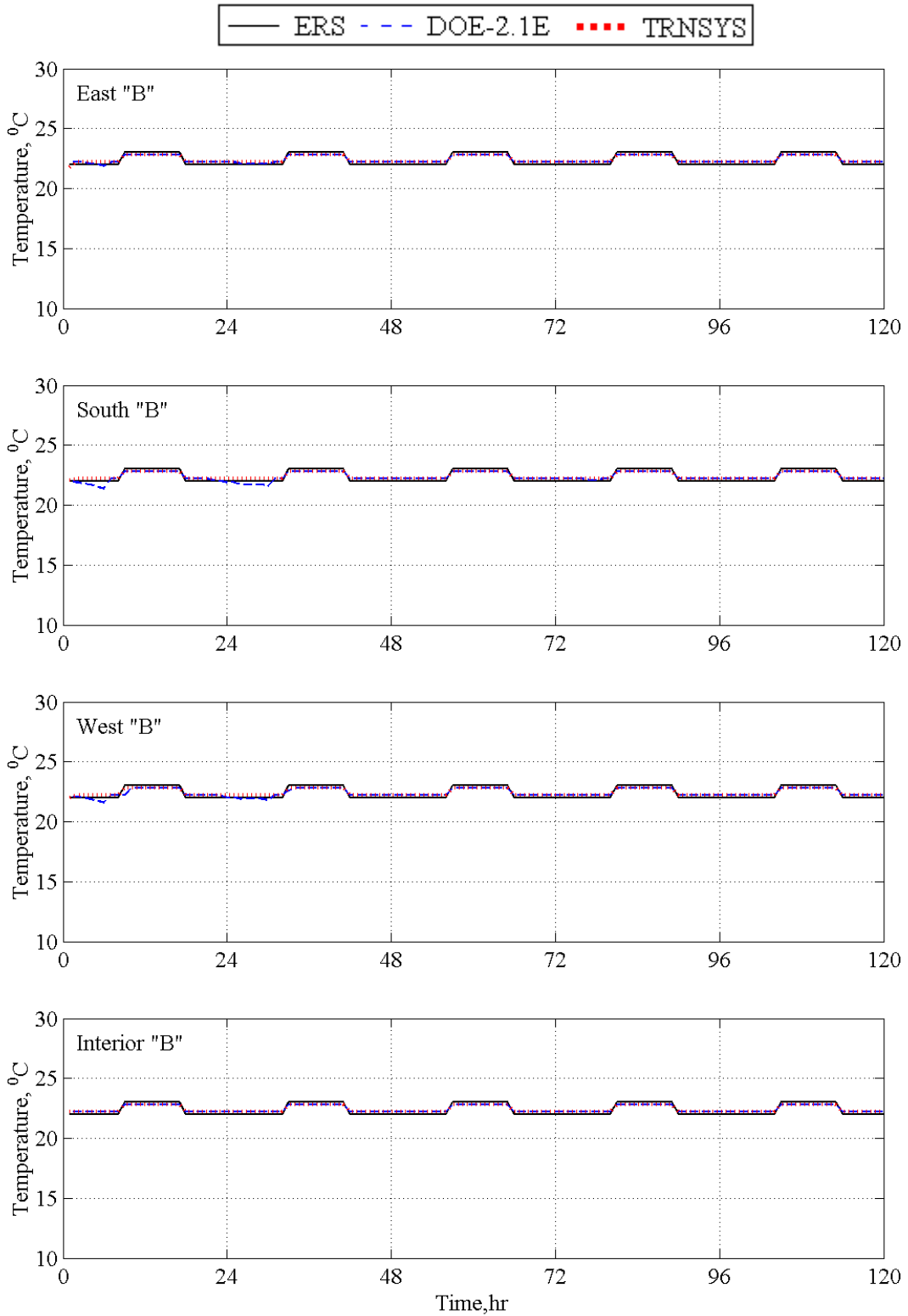


Figure 3.17 Room temperature values for the “B” test rooms

3.2.3.2.4 Zone airflow rates

Figure 3.18 illustrates the zone airflow rates for the “B” test rooms. For this test, the specified minimum supply airflow rates varied slightly from room to room (refer to Table 3.4). Table 3.16 provides a statistical summary of the room supply airflow rate comparison. The results for the DOE2 are within the 95% uncertainty intervals. TRNSYS over-predicts the airflow rate for the test rooms.

Table 3.16 Statistical comparison of the supply airflow rates in the “B” test rooms, m³/hr

Statistical Parameter	East "B"			South "B"			West "B"			Interior "B"		
	ERS	DOE2.1E	TRNSYS	ERS	DOE2.1E	TRNSYS	ERS	DOE2.1E	TRNSYS	ERS	DOE2.1E	TRNSYS
\bar{x}	415.9	405.2	459.3	407.9	416.4	465.6	380.1	386.3	446.6	444.9	462.2	476.1
σ	20.7			41.7			32.4			89.1		
s	128.5	123.1	181.1	199.3	228.7	259.8	105.9	123.9	183.7	193.3	234.0	230.6
x_{\max}	719.0	706.0	842.0	1065.0	1267.0	1227.0	631.0	745.0	778.0	764.0	840.0	787.0
x_{\min}	318.0	323.0	323.0	281.0	283.0	283.0	306.0	307.0	307.0	293.0	298.0	298.0
\bar{D}		10.7	-43.4		-8.4	-57.6		-6.2	-66.5		-17.2	-31.2
D_{\max}		166.0	332.0		239.0	347.0		140.0	261.0		175.0	261.0
D_{\min}		0.0	0.0		0.0	0.0		0.0	0.0		0.0	0.0
$ D $		16.5	45.4		23.1	61.9		18.4	68.3		36.8	35.9
D_{rms}		34.2	79.3		50.8	114.2		35.8	113.8		60.7	69.6
SE		2.6	-9.4		-2.0	-12.4		-1.6	-14.9		-3.7	-6.5
IE		4.1	9.9		5.5	13.3		4.8	15.3		8.0	7.5

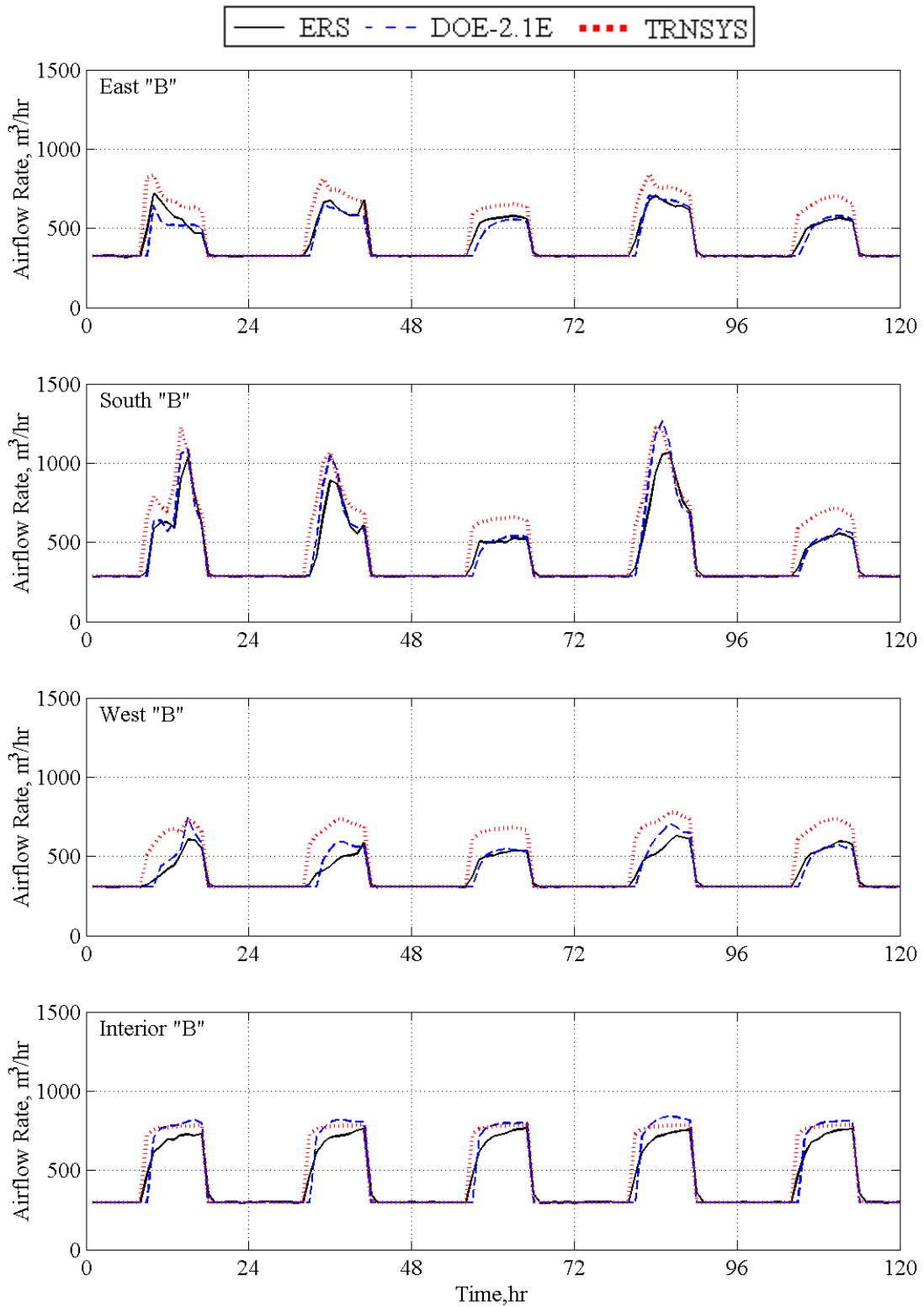


Figure 3.18 Supply airflow rates to the "B" test rooms

3.2.3.2.5 Zone reheat power

Figure 3.19 illustrates the zone reheat power for the “B” test rooms. The zone reheat power was calculated using Equation 2.2 (Section 2.2.2.2.5). Table 3.17 provides a statistical summary of the zone reheat power comparison. The results are similar to those seen for the “A” test rooms.

Table 3.17 Statistical comparison of the reheat power in the “B” test rooms, W

Statistical Parameter	East "B"			South "B"			West "B"			Interior "B"		
	ERS	DOE2.1E	TRNSYS	ERS	DOE2.1E	TRNSYS	ERS	DOE2.1E	TRNSYS	ERS	DOE2.1E	TRNSYS
\bar{x}	973.6	773.3	706.8	927.4	708.7	628.8	987.1	752.7	669.1	532.8	374.8	416.8
σ	402.7			426.6			331.7			499.3		
s	758.5	663.7	569.9	737.9	607.1	510.4	778.9	645.0	541.4	382.3	326.8	345.4
x_{\max}	1897.0	1521.0	1660.0	2021.0	1335.0	1501.0	2072.0	1446.0	1615.0	1000.0	709.0	798.0
x_{\min}	0.0	0.0	0.0	0.0	0.0	0.0	0.0	0.0	0.0	35.0	0.0	0.0
\bar{D}		200.3	266.9		218.7	298.6		234.3	317.9		158.0	116.0
D_{\max}		1028.0	790.0		744.0	1074.0		1079.0	959.0		402.0	409.0
D_{\min}		0.0	0.0		0.0	0.0		0.0	0.0		35.0	2.0
$ D $		200.3	266.9		220.2	303.7		234.3	317.9		158.0	116.7
D_{rms}		279.4	346.5		303.6	403.1		328.3	417.1		184.6	146.8
SE		25.9	37.8		30.9	47.5		31.1	47.5		42.2	27.8
IE		25.9	37.8		31.1	48.3		31.1	47.5		42.2	28.0

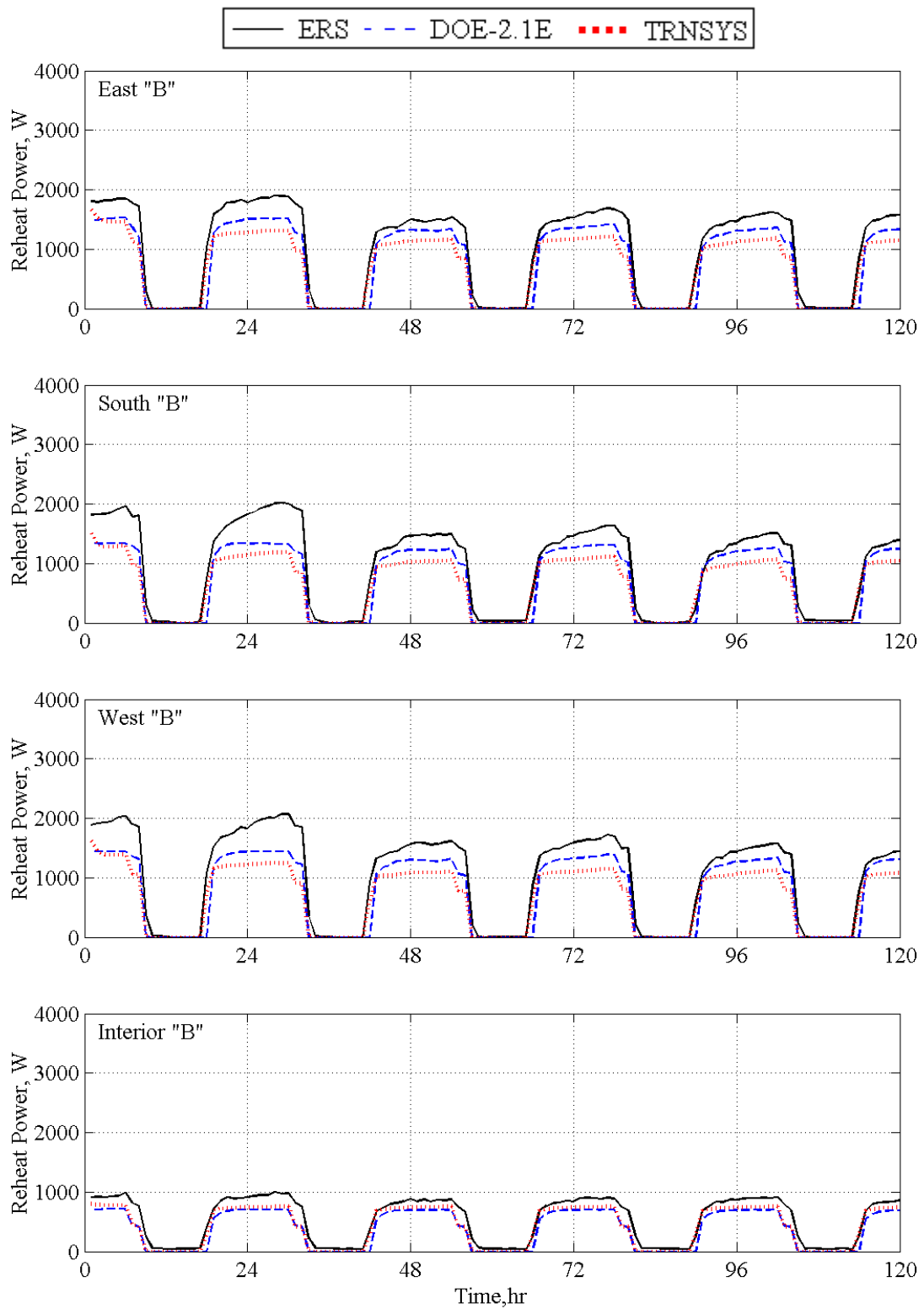


Figure 3.19 Reheat power values for the “B” test rooms

3.2.3.2.6 Zone thermal load

Figure 3.20 illustrates the thermal load for each of the “B” test rooms. The zone thermal load was calculated using Equation 2.3 (Section 2.2.2.2.6). Table 3.18 provides a statistical summary of the room thermal load comparison. The results show that overall the models are predicting the heating loads and under predicting the cooling loads. The uncertainty in the thermal load calculations makes it difficult for quantitative comparisons.

Table 3.18 Statistical comparison of the room thermal loads in the “B” test rooms, W

Statistical Parameter	East "B"			South "B"			West "B"			Interior "B"		
	ERS	DOE2.1E	TRNSYS	ERS	DOE2.1E	TRNSYS	ERS	DOE2.1E	TRNSYS	ERS	DOE2.1E	TRNSYS
Cooling Loads												
\bar{x}	870.9	445.3	665.0	933.7	528.1	743.2	715.0	419.8	630.1	1207.0	690.1	785.7
σ	294.4			330.8			262.5			685.9		
s	1128.0	587.2	862.9	1302.8	744.6	993.5	946.0	556.3	815.8	1286.4	830.2	941.3
x_{max}	3117.0	1593.4	2166.0	4580.0	2636.3	3140.0	2532.0	1606.4	1918.0	3164.0	1797.4	2024.0
x_{min}	0.0	0.0	0.0	0.0	0.0	0.0	0.0	0.0	0.0	52.0	0.0	0.0
\bar{D}		425.6	205.9		405.5	190.4		295.2	84.9		516.9	421.3
D_{max}		1665.9	1062.0		2259.6	1953.0		1138.8	715.0		1366.6	1140.0
D_{min}		0.0	0.0		0.0	0.0		0.0	0.0		41.9	8.0
$ D $		425.6	227.9		411.1	247.7		295.2	135.8		516.9	436.6
D_{rms}		697.0	378.3		713.5	471.1		498.1	240.9		704.4	581.8
SE		95.6	31.0		76.8	25.6		70.3	13.5		74.9	53.6
IE		95.6	34.3		77.8	33.3		70.3	21.6		74.9	55.6
Heating Load												
\bar{x}	290.9	394.9	250.0	360.2	389.9	232.9	406.0	398.7	255.3	0.0	28.7	26.8
σ	294.4			330.8			385.6			0.0		
s	279.3	336.4	243.2	364.1	334.2	226.2	386.9	339.7	246.2	0.0	33.2	31.6
x_{max}	810.0	893.8	927.0	1134.0	889.1	839.0	1163.0	910.6	937.0	0.0	72.4	110.0
x_{min}	0.0	0.0	0.0	0.0	0.0	0.0	0.0	0.0	0.0	0.0	0.0	0.0
\bar{D}		-104.1	40.9		-29.7	127.3		7.3	150.7		-28.7	-26.8
D_{max}		358.8	444.0		415.2	826.0		332.0	721.0		72.4	110.0
D_{min}		0.0	0.0		0.0	0.0		0.0	0.0		0.0	0.0
$ D $		106.4	67.1		94.1	135.7		73.5	154.6		28.7	26.8
D_{rms}		151.1	117.5		140.6	227.1		117.5	238.9		43.8	41.3
SE		-26.3	16.4		-7.6	54.6		1.8	59.0		-100.0	-100.0
IE		26.9	26.9		24.1	58.3		18.4	60.6		100.0	100.0

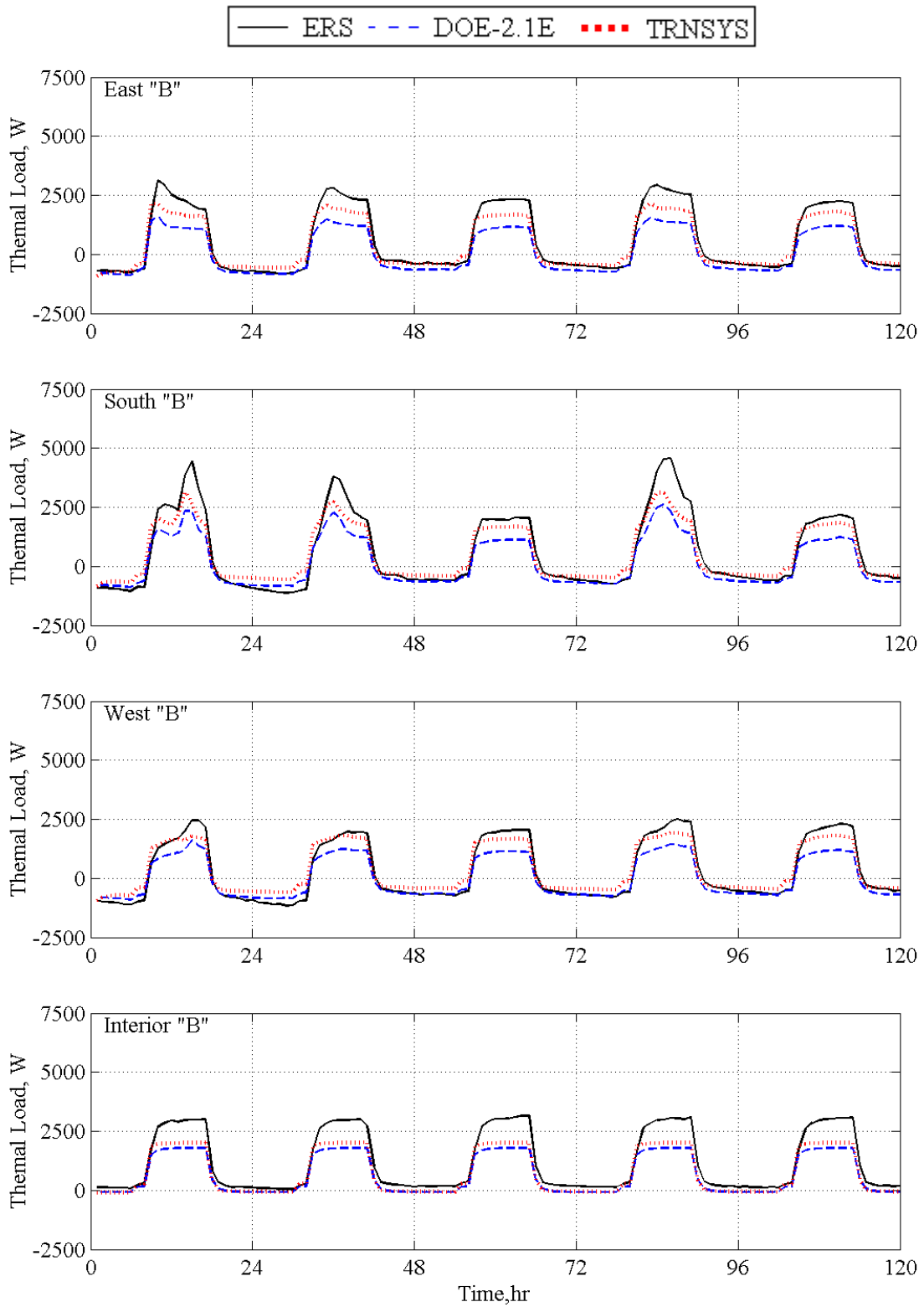


Figure 3.20 Thermal load values for the “B” test rooms

4 Summary

4.1 Thermal stratification

A significant finding of this work showed that thermal stratification within a room does affect the heating energy requirements to maintain the space temperature. Because many simulation programs do not account for spatial temperature variation within the space, differences will occur between model predictions and actual energy usage. This can be shown by examining the data in Tables 2.17 and 3.17. Specifically, the simulation errors for the models can be compared between the two test cases. Based on the results from the tests, an improvement in the agreement between the models and the experimental results of at least 150% was seen. Modelers and designers need to be aware of the affects of temperature stratification on the energy requirements as well as the thermal comfort for the occupants.

4.2 Energy usage with and without daylight

Results from this work show that energy savings are possible through daylighting controls. Energy can be saved directly from the reduced lighting power and indirectly through a reduction in cooling load. Table 4.1 shows the total light energy used in the exterior test rooms during the five days of Test 2, and compares the daylighting controlled “B” test rooms with the non-daylighting controlled “A” test rooms. The table also includes the model results. For the test, the actual lighting energy saved was 16.4 kWh. The predicted energy savings from DOE2 and TRNSYS was 16.1 and 10.9 kWh, respectively.

Table 4.1 Lighting energy comparison for the daylighting test, in kWh

	ERS	DOE2	TRNSYS
"A" rooms	51.7	51.2	51.2
"B" rooms	35.4	35.1	40.3
Difference	16.4	16.1	10.9

The reduction in cooling energy for the five-day test is shown in Table 4.2. Because of the large experimental uncertainty in the cooling energy calculation and the inherent difference in the AHU-A and AHU-B systems, the actual cooling energy savings may not be accurately represented by the value in the table.

Table 4.2 Cooling energy comparison for the daylighting test, in kWh

	ERS	DOE2	TRNSYS
AHU-A	508.8+115.2	518.4	508.8
AHU-B	470.4+153.6	508.8	499.2
Difference	38.4	9.6	9.6

4.3 Experimental error

Experimental error played a significant role in the interpretation of the results. Large uncertainties in airflow rate measurements and water flow rate measurements are the primary cause of the experimental error. Flow rate measurements play a significant role in the heating and cooling energy calculations. In the case of the room thermal stratification, a large uncertainty exists for the room temperature measurement. This error is diminished when the

temperature gradient in the room is reduced. Future experiments need to reduce the uncertainties in flow rate measurements in order to improve the quality of the results.

4.4 Future work

Empirical validation plays a key role in building simulation software validation. By comparing simulation results to actual building performance, modelers can examine the affects of assumptions often used to simplify the physical systems and determine the short comings of the models. A comprehensive set of tests can provide a standard of comparison for future model development and validation.

Appendix A Energy Resource Station Specification

This appendix contains information about the Energy Resource Station (ERS) which should provide sufficient detail to allow building energy simulation modelers to develop their own models for use in the validation exercises. The information is organized in a format similar to a DOE2 input file.

Section A.1 contains information necessary to describe the building. This information has been obtained from the architectural drawings and construction documents available from the ERS manager. AutoCad drawings of the ERS are located on the CD that accompanies this report. While information about the entire ERS is provided, it is the “A” and “B” test rooms that were modeled for the empirical validation exercises. Data from the exercises are only available for the HVAC systems AHU-A and AHU-B, the “A” and “B” test rooms and the ERS weather station.

Section A.2 contains information about the HVAC systems in the ERS. The information presented is generic since specific system parameters differ from one validation exercise to another. The detailed system specifications are presented along with the description of each exercise.

A.1 INPUT FOR LOAD CALCULATION

A.1.1 RUN-PERIOD

For each validation exercise, the starting and ending dates are specified. The run period is used to specify the initial and final dates of the desired simulation period. It is important that the run period coincide with the dates of the exercise so that the appropriate weather data are used in the simulation.

A.1.2 WEATHER-DATA

During the dates of a validation exercise, weather and solar measurements are recorded. These data are post-processed into TMY format. The TMY data created from the ERS weather replace specific fields in an original DESMOINE.TMY file. Of the 8,760 days of data in the original file, only the days that correspond to the dates of the exercise have modified values. A TMY data file contains many meteorological parameters which may or may not be used in building simulation software. The only data fields which are modified with ERS data include the following:

- Dry bulb temperature
- Dew point temperature
- Barometric pressure
- Total horizontal solar irradiation
- Direct normal solar irradiation
- Wind direction
- Wind speed

The weather files created for the empirical validation exercises are named according to the year in which the test was conducted. For example the file “IEA2002.tmy” contains modified data for

validation tests that were conducted in 2002. TMY weather files for the validation exercises are provided on the CD provided with this report.

A.1.3. BUILDING-LOCATION

This specifies the location of the building and information about the time zone.

LATITUDE: 41.71 degree north

LONGITUDE: 93.61 degree west

ALTITUDE: 938.0 feet above sea level

TIME-ZONE: 6, central time zone in the US

DAYLIGHT-SAVINGS: YES/NO. Depending on the time of year this parameter is YES or NO. Generally daylight-saving time is in effect from early April until mid-October. This parameter is specified for each exercise. The parameter affects the relationship between the local time and solar time and is significant when defining time-based events such as light schedules, thermostat schedules, etc.

A.1.4. BUILDING-SHADE:

There are no surrounding objects that significantly block solar irradiation on the ERS. A monument located south and east of the building does cast a small shadow on the east-facing test rooms during the early morning hours of clear days for the months from October to March. The shadow only occurs for a few minutes shortly after sunrise when solar irradiation is small. Because the shadow is small and does not remain in the same location for any significant time, the affect of the shadow on the solar irradiation striking the wall or glass is assumed to be insignificant. The shadow would have an impact on daylighting validation exercises if the shadow affected the amount of ambient light entering the test room. The surrounding ground cover is nearly all grass with a limited amount of concrete walkways approaching the doors.

A.1.5. FLOOR-PLAN

The floor plan is used to identify each space for the building model. Figure A.1 is a simplified floor plan. Details of the floor plan are available on the CD.



Figure A.1 A floor plan of the Energy Resource station

A.1.6 CONSTRUCTION LAYER DESCRIPTION

This specifies the material layers of each construction element in the model. These include; the cross section of an exterior wall, interior wall, ceiling, door, slab on grade floor and roof.

A.1.6.1 LAYER TYPE IDENTIFICATION

There are fifteen (15) different construction layers used to describe the construction of the ERS. Table A.1 identifies the layer name and description/location for each layer.

A.1.6.2 LAYER DESCRIPTION

Each construction layer is composed of materials. The description of each material, the material thermal properties and the material thickness is described in Table A.2. The properties are given in terms of the following symbols:

- T: thickness, in inches
- K: conductivity, in Btu/(hr-ft-°F)
- D: density, in lb/ft²
- Cp: specific heat, in Btu/(lb-°F)
- R: resistance, in (hr-ft²-°F)/Btu.

Table A.1 Identification of construction layers used in the ERS building

Layer type	Description
LAY-R1	Layers for the roof of all spaces except for the classroom.
LAY-R2	Layers for the roof of the classroom.
LAY-W1	Layers for the lower portion of the exterior wall of the test rooms
LAY-W2	Layers for the upper portion of the exterior wall of the test rooms
LAY-W3	Layers for the spandrel wall in the lower portion of the computer room and office
LAY-W4	Layers for the upper portion of the exterior wall in the computer room and office
LAY-W5	Layers for the exterior wall of the classroom
LAY-W6	Layers for the lower portion of the exterior wall of other spaces
LAY-W7	Layers for the upper portion of the exterior wall of other spaces
LAY-P1	Layers for the 6-inch interior partition wall of all spaces
LAY-P2	Layers for the 4-inch interior partition wall of all spaces
LAY-P3	Layers for the 1/8-inch interior glass partition wall of test rooms
LAY-P4	Layers for the door of all spaces
LAY-C1	Layers for the ceiling of all spaces
LAY-F1	Layers for the slab on grade floor of all spaces

Table A.2 Thickness and thermal properties used for construction layers

Layer type	Description	T	K	D	Cp	R
LAY-R1	Inside surface					
	2 in heavy weight concrete	2.00	0.7576	140	0.2	0.22
	4 in horizontal air space	4.00	-	-	-	0.87
	2 in heavy weight concrete	2.00	0.7576	140	0.2	0.22
	Vapor barrier	-	-	-	-	0.06
	4 in insulation	4.00	0.0133	1.5	0.38	25.06
	Single-ply membrane	-	-	70	0.35	0.44
	Washed river rock	1.00	0.8340	55	0.4	0.10
Outside surface						
LAY-R2	Inside surface					
	22 gage steel deck	0.034	26.0	480	0.1	
	4 in insulation	4.00	0.0133	1.5	0.38	25.06
	Single-ply membrane	-	-	70	0.35	0.44
	Washed river rock	1.00	0.8340	55	0.4	0.10
Outside surface						
LAY-W1	Inside surface					
	5/8 in gypsum board	0.63	0.0926	50	0.2	0.56
	Vapor barrier	-	-	-	-	0.06
	3/8 in vertical air space	0.38	-	-	-	0.90
	1.5 in rigid insulation with foil face	1.50	0.0133	1.5	0.38	9.39
	4 in pre-cast conc.	4.00	0.7576	140	0.2	0.44
Outside surface						
LAY-W2	Inside surface					
	5/8 in gypsum board	0.63	0.0926	50	0.2	0.56
	3/8 in vertical air space	0.38	-	-	-	0.90
	1 in rigid insulation with foil face	1.00	0.0133	1.5	0.38	6.26
	6 in pre-cast conc.	6.00	0.7576	140	0.2	0.66
Outside surface						
LAY-W3	Inside surface					
	5/8 in gypsum board	0.63	0.0926	50	0.2	0.56
	Vapor barrier	-	-	-	-	0.06
	Metal stud framing with R13 batt insulation with foil face	3.50	0.0250	0.6	0.2	12.96
	1 in rigid insulation	1.00	0.0133	1.5	0.38	6.26
	4.75 in vertical air space	4.75	-	-	-	0.92
	1 in spandrel glass	1.00	-	-	-	2.08
Outside surface						

Table A.2 (continued)

Layer type	Description	T	K	D	Cp	R
LAY-W4	Inside surface					
	Metal stud framing with R13 batt insulation with foil face	3.50	0.0250	0.6	0.2	12.96
	3/4 in vertical air space	0.75	-	-	-	0.90
	1 in rigid insulation	1.00	0.0133	1.5	0.38	6.26
	6 in pre-cast conc.	6.00	0.7576	140	0.2	0.66
	Outside surface					
LAY-W5	Inside surface					
	3/4 in gypsum board	0.75	0.0926	50	0.2	0.67
	Vapor barrier	-	-	-	-	0.06
	Metal stud framing with R13 batt insulation with foil face	3.50	0.0250	0.6	0.2	12.96
	1 3/8 in vertical air space	1.38	-	-	-	0.89
	1 in rigid insulation	1.00	0.0133	1.5	0.38	6.26
	6 in pre-cast conc.	6.00	0.7576	140	0.2	0.66
	Outside surface					
LAY-W6	Inside surface					
	5/8 in gypsum board	0.63	0.0926	50	0.2	0.56
	Vapor barrier	-	-	-	-	0.06
	Metal stud framing with R13 batt insulation with foil face	3.50	0.0250	0.6	0.2	12.96
	3/4 in vertical air space	0.75	-	-	-	0.90
	1 in rigid insulation	1.00	0.0133	1.5	0.38	6.26
	4 in pre-cast conc.	4.00	0.7576	140	0.2	0.44
	Outside surface					
LAY-W7	Inside surface					
	5/8 in gypsum board	0.63	0.0926	50	0.2	0.56
	Metal stud framing with R13 batt insulation with foil face	3.50	0.0250	0.6	0.2	12.96
	3/4 in vertical air space	0.75	-	-	-	0.90
	1 in rigid insulation	1.00	0.0133	1.5	0.38	6.26
	6 in pre-cast conc.	6.00	0.7576	140	0.2	0.66
	Outside surface					
LAY-P1	5/8 in gypsum board	0.63	0.0926	50	0.2	0.56
	Metal stud framing with fiberglass fill, insulation	3.50	0.0225	3.0	0.33	12.96
	5/8 in gypsum board	0.63	0.0926	50	0.2	0.56
LAY-P2	5/8 in gypsum board	0.63	0.0926	50	0.2	0.56
	Metal stud framing with fiberglass fill, insulation	2.37	0.0225	3.0	0.33	8.78
	5/8 in gypsum board	0.63	0.0926	50	0.2	0.56

Table A.2 (continued)

Layer type	Description	T	K	D	Cp	R
LAY-P3	1/8 in glass with steel frame	1/8	0.797	138	0.18	0.013
LAY-P4	Door	1.75	-	-	-	4.16
LAY-C1	Ceiling	0.75	0.033	18	0.32	1.89
LAY-F1	Carpet	-	-	-	0.34	1.23
	4 in heavy weight conc.	4.00	0.7576	140	0.20	0.44
	Perimeter insulation, 2-inch width	-	-	-	-	5.00

A combined radiative and convective inside film resistance of 0.68 (hr-ft²-°F)/Btu is assumed for all interior surfaces (both vertical and horizontal). The outside film resistance should be based on the wind speed obtained from the TMY weather data. The assumed values for solar absorptances for the exterior walls and roofs are 0.6 and 0.29, respectively.

A.1.7 WINDOW TYPE AND DESCRIPTION

This section specifies the fenestration for the building. Three types of window glazing are used throughout the building. All of the test rooms have double-pane clear glass while the remaining windows have double-pane tinted glass. A skylight is located above the media center which contains a translucent glass. The bottom of all windows located on an exterior wall is 3.5 feet (1.07 m) above the floor.

Table A.3 summarizes the fenestration for the ERS. For each type of window information is provided about the number of panes, shading coefficient, heat conductance of the total window (except for the outside film coefficient), width and height of the window. The glass conductance does not include the outside film coefficient but does include the frame.

A.1.8 SPACE DESCRIPTION

This section identifies each space. Once all spaces have been identified, then each surface of the space is described in terms of orientation, width and height, and construction layer. Gross surface areas are presented in this section. Thus the areas include door and/or window areas. The size of a door is 3 feet (0.91 m) wide and 7 feet (2.13 m) high.

A.1.8.1 SPACE IDENTIFICATION

All of the test rooms and most of the rooms in the remainder of the building have a plenum space and a conditioned space. The mechanical room and storage room do not have plenum spaces. The ceiling height of most rooms is 8.5 feet (2.59 m), and the plenum height is 5.5 feet (1.68 m). Detailed information about the size is illustrated in Section A.1.8.2. Since the “A” and “B” test rooms are matched pairs, information provided on each orientation applies to either room. Table A.4 identifies a space as either plenum space or conditioned space. Plenum space is designated with the prefix “P.”

Table A.3 Window identification and its characteristics with size

Type	Location	W	H	P	S	C
WIN-TEST	Exterior wall in test rooms	14.0	5	2	0.85	0.55
WIN-TYP1	Exterior wall east in the office	11.8	5	2	0.31	0.30
WIN-TYP2	Exterior wall south in the office	15.3	5	2	0.31	0.30
WIN-TYP3	Exterior wall south in the computer room	15.3	5	2	0.31	0.30
WIN-TYP4	Exterior wall west in the computer room	24.0	5	2	0.31	0.30
WIN-TYP5	Exterior wall south in the classroom	3.5	5	2	0.31	0.30
WIN-TYP6	Exterior wall west in the classroom	7.0	5	2	0.31	0.30
WIN-TYP7	Exterior wall north in the classroom	3.5	5	2	0.31	0.30
WIN-TYP8	Exterior wall east in the reception room	7.9	5	2	0.31	0.30
WIN-TYP9	Door in vest east and west	3.0	7.0	2	0.31	0.30
WIN-SKY	Roof of the media center	10.0	10	1	0.35	0.24

W: width, in feet H: height, in feet P: number of panes S: shading coefficient
 C: heat conductance of the total window, in Btu/(hr-ft²-°F)

Table A.4. Identification of plenum and conditioned space

Space-ID	Description
P-EAST	Plenum in the East test room
P-SOUTH	Plenum in the South test room
P-WEST	Plenum in the West test room
P-INTE	Plenum in the Interior test room
P-BREAK	Plenum in the break room, restrooms of women and men
P-RECEPT	Plenum in the reception room
P-OFFICE	Plenum in the office
P-COMPUTE	Plenum in the computer center
P-CLASS	Plenum in the classroom
P-DISPLAY	Plenum in the display room
P-MEDIA	Plenum in the media center
EASTROOM	Conditioned space in the East test room
SOUTHROOM	Conditioned space in the South test room
WESTROOM	Conditioned space in the West test room
INTEROOM	Conditioned space in the Interior test room
BREAKROOM	Conditioned space in the break room, restrooms of women and men
RECEPTION-RM	Conditioned space in the reception room
OFFICE	Conditioned space in the office
COMPUTE-RM	Conditioned space in the computer center
CLASSROOM	Conditioned space in the classroom
DISPLAY-RM	Conditioned space in the display room
STORAGE-RM	Conditioned space in the storage room, elec./comm. room
MEDIA-CENTER	Conditioned space in the media center
MECH-ROOM	Conditioned space in the mechanical room

A.1.8.2 SPACE DESCRIPTION

From the ERS floor plan (Figure A.1) one sees that the test rooms are not rectangular in shape. However, for simplification the rooms are assumed to be rectangular. Therefore, each test room has six surfaces: 4 walls, a ceiling (above) and a floor (below). Above each test room is a plenum space. The plenum space is also assumed to have six surfaces: 4 walls, a roof (above) and a ceiling (below). For a better understanding of the surface geometry, a capital letter representing the position of the surface is used. Refer to Figures A.2(a) and A.2(b) which illustrate the surface arrangements.

- C: a horizontal surface used for the *ceiling*
- E: a vertical surface used for the *wall east*
- F: a horizontal surface used for the *floor*
- N: a vertical surface used for the *wall north*
- R: a horizontal surface used for the *roof*
- S: a vertical surface used for the *wall south*
- W: a vertical surface used for the *wall west*

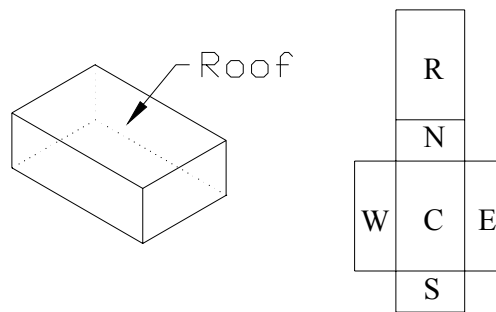


Figure A.2(a) Geometry presentation for plenum spaces

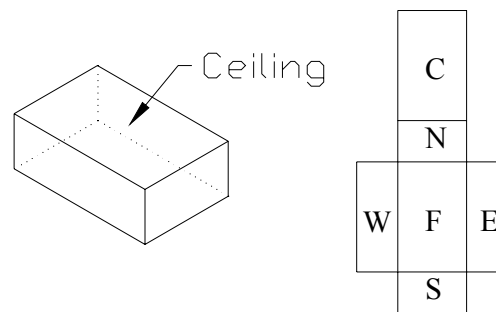


Figure A.2(b) Geometry presentation for conditioned spaces

Table A.5 describes the spaces with detailed information about the surfaces. The ERS is oriented with respect to true north/south. In the same way, the spaces identified in Table A.5 are described by surface orientation such as north, east, south and west. For example, consider the space “P-EAST” that defines the plenum space above the East test room. P-EAST is located on the east side of the building at an elevation of 8.5 feet (2.59 m) above the floor level. The space

is surrounded by six surfaces: one east-facing exterior wall, one interior north-facing wall, one interior south-facing wall, one interior west-facing wall, one ceiling and one roof. Once the surface orientations are specified, detailed information about the six surfaces which make up “P-EAST” must be provided. This includes the dimensions of the surface, the construction layer of the surface, and any windows or doors, if present.

As another example, consider the conditioned space called “SOUTHROOM” that is located on the south side of the building at the floor level. This space also is surrounded by six surfaces: one south-facing exterior wall that has a window, one north-facing interior wall that has a door, one east-facing interior wall, one west-facing interior wall that is adjacent to the computer room, one ceiling that is adjacent to the plenum space called “P-SOUTH”, and one floor.

Table A.5. Description of the space and details of its six surfaces

Space	Orientation	Width (ft)	Height (ft)	Layer	Window	Door
P-EAST	R	17.74	15.50	LAY-R1	-	-
	C	17.74	15.50	LAY-C1	-	-
	N	17.74	5.50	LAY-P2	-	-
	E	15.50	5.50	LAY-W2	-	-
	S	17.74	5.50	LAY-P2	-	-
P-SOUTH	W	15.50	5.50	LAY-P1	-	-
	R	15.50	17.74	LAY-R1	-	-
	C	15.50	17.74	LAY-C1	-	-
	N	15.50	5.50	LAY-P2	-	-
	E	17.74	5.50	LAY-P2	-	-
P-WEST	S	15.50	5.50	LAY-W2	-	-
	W	17.74	5.50	LAY-P1	-	-
	R	17.74	15.50	LAY-R1	-	-
	C	17.74	15.50	LAY-C1	-	-
	N	17.74	5.50	LAY-P2	-	-
P-INTE	E	15.50	5.50	LAY-P1	-	-
	S	17.74	5.50	LAY-P2	-	-
	W	15.50	5.50	LAY-W2	-	-
	R	15.50	17.74	LAY-R1	-	-
	C	15.50	17.74	LAY-C1	-	-
P-BREAK	N	15.50	5.50	LAY-P2	-	-
	E	17.74	5.50	LAY-P2	-	-
	S	15.50	5.50	LAY-P2	-	-
	W	17.74	5.50	LAY-P1	-	-
	R	10.66	36.60	LAY-R1	-	-
P-RECEPT	C	10.66	36.60	LAY-C1	-	-
	N	10.66	6.00	LAY-P2	-	-
	E	36.60	6.00	LAY-W7	-	-
	S	10.66	6.00	LAY-P2	-	-
	W	36.60	6.00	LAY-P2	-	-
P-OFFICE	R	17.74	13.00	LAY-R1	-	-
	C	17.74	13.00	LAY-C1	-	-
	N	17.74	5.50	LAY-P2	-	-
	E	13.00	5.50	LAY-W4	-	-
	S	-	-	-	-	-
P-OFFICE	W	-	-	-	-	-
	R	16.40	12.10	LAY-R1	-	-
	C	16.40	12.10	LAY-C1	-	-
	N	-	-	-	-	-
	E	12.10	5.50	LAY-W4	-	-
P-OFFICE	S	16.40	5.50	LAY-W4	-	-
	W	12.10	5.50	LAY-P1	-	-

Table A.5. (continued)

Space	Orientation	Width (ft)	Height (ft)	Layer	Window	Door
P-COMPUTE	R	16.30	25.10	LAY-R1	-	-
	C	16.30	25.10	LAY-C1	-	-
	N	16.30	5.50	LAY-P2	-	-
	E	25.10	5.50	LAY-P1	-	-
	S	16.30	5.50	LAY-W4	-	-
P-CLASS	W	25.10	5.50	LAY-W4	-	-
	R	22.20	34.67	LAY-R2	-	-
	C	22.20	34.67	LAY-C1	-	-
	N	22.20	1.00	LAY-W5	-	-
	E	-	-	-	-	-
P-DISPLAY	S	22.20	1.00	LAY-W5	-	-
	W	34.67	1.00	LAY-W5	-	-
	R	17.83	17.74	LAY-R1	-	-
	C	17.83	17.74	LAY-C1	-	-
	N	17.83	5.50	LAY-P2	-	-
P-MEDIA	E	17.74	5.50	LAY-P1	-	-
	S	-	-	-	-	-
	W	-	-	-	-	-
	R	30.00	60.80	LAY-R1	-	-
	C	30.00	57.20	LAY-C1	-	-
EASTROOM	N	-	-	-	-	-
	E	-	-	-	-	-
	S	-	-	-	-	-
	W	6.00	5.50	LAY-W7	-	-
	C	17.74	15.50	LAY-C1	-	-
SOUTHROOM	F	17.74	15.50	LAY-F1	-	-
	N	17.74	8.50	LAY-P2	-	-
	E	15.50	8.50	LAY-W1	WIN-TEST	-
	S	17.74	8.50	LAY-P2	-	-
	W	15.50	8.50	LAY-P3	-	LAY-P4
WESTROOM	C	15.50	17.74	LAY-C1	-	-
	F	15.50	17.74	LAY-F1	-	-
	N	15.50	8.50	LAY-P3	-	LAY-P4
	E	17.74	8.50	LAY-P2	-	-
	S	15.50	8.50	LAY-W1	WIN-TEST	-
INTERROOM	W	17.74	8.50	LAY-P1	-	-
	C	17.74	15.50	LAY-C1	-	-
	F	17.74	15.50	LAY-F1	-	-
	N	17.74	8.50	LAY-P2	-	-
	E	15.50	8.50	LAY-P3	-	LAY-P4
BREAKROOM	S	17.74	8.50	LAY-P2	-	-
	W	15.50	8.50	LAY-W1	WIN-TEST	-
	C	15.50	17.74	LAY-C1	-	-
	F	15.50	17.74	LAY-F1	-	-
	N	15.50	8.50	LAY-P2	-	-
RECEPTION-RM	E	17.74	8.50	LAY-P2	-	-
	S	15.50	8.50	LAY-P3	-	LAY-P4
	W	17.74	8.50	LAY-P1	-	-
	C	10.66	36.60	LAY-C1	-	-
	F	10.66	36.60	LAY-F1	-	-
RECEPTION-RM	N	10.66	8.00	LAY-P2	-	-
	E	36.60	8.00	LAY-W6	-	-
	S	10.66	8.00	LAY-P2	-	-
	W	36.60	8.00	LAY-P2	-	LAY-P4
	C	17.74	13.00	LAY-C1	-	-
RECEPTION-RM	F	17.74	13.00	LAY-F1	-	-
	N	17.74	8.500	LAY-P2	-	-
	E	13.00	8.50	LAY-W4	WIN-TYP8	-
	S	17.74	8.50	LAY-P2	-	-
	W	-	-	-	-	-

Table A.5 (continued)

Space	Orientation	Width (ft)	Height (ft)	Layer	Window	Door
OFFICE	C	16.40	12.10	LAY-C1	-	-
	F	16.40	12.10	LAY-F1	-	-
	N	16.40	8.50	LAY-P2	-	LAY-P4
	E	12.10	8.50	LAY-W3	WIN-TYP1	-
	S	16.40	8.50	LAY-W3	WIN-TYP2	-
	W	12.10	8.50	LAY-P1	-	-
COMPUTER-RM	C	16.30	25.10	LAY-C1	-	-
	F	16.30	25.10	LAY-F1	-	-
	N	16.30	8.50	LAY-P2	-	-
	E	25.10	8.50	LAY-P1	-	LAY-P4
	S	16.30	8.50	LAY-W3	WIN-TYP3	-
	W	25.10	8.50	LAY-W3	WIN-TYP4	-
CLASSROOM	C	22.20	34.67	LAY-C1	-	-
	F	22.20	34.67	LAY-F1	-	-
	N	22.20	9.00	LAY-W5	WIN-TYP7	-
	E	34.16	9.00	LAY-P1	-	LAY-P4
	S	22.20	9.00	LAY-W5	WIN-TYP5	-
	W	34.67	9.00	LAY-W5	WIN-TYP6	-
DISPLAY-RM	C	17.83	17.74	LAY-C1	-	-
	F	17.83	17.74	LAY-F1	-	-
	N	17.83	8.50	LAY-P2	-	-
	E	17.74	8.50	LAY-P1	-	-
	S	17.83	8.50	LAY-P2	-	LAY-P4
	W	17.74	8.50	LAY-P2	-	-
STORAGE-RM	C	10.55	25.30	LAY-C1	-	-
	F	10.55	25.30	LAY-F1	-	-
	N	10.55	14.00	LAY-W6	-	-
	E	25.30	14.00	LAY-W6	-	-
	S	10.55	14.00	LAY-P2	-	-
	W	15.30	14.00	LAY-P2	-	LAY-P4
MEDIA-CENTER	R	10.50	10.50	LAY-R1	WIN-SKY	-
	C	30.00	57.20	LAY-C1	-	-
	F	30.00	60.80	LAY-F1	-	-
	N	-	-	-	-	-
	E	-	-	-	-	-
	S	-	-	-	-	-
MECH-ROOM	W	6.00	8.50	LAY-W6	WIN-TYP9	-
	R	66.30	30.60	LAY-R1	-	-
	F	66.30	30.60	LAY-F1	-	-
	N	57.80	14.00	LAY-W7	-	-
	E	25.30	14.00	LAY-P2	-	-
	S	57.80	14.00	LAY-P2	-	LAY-P4
W	25.30	14.00	LAY-W7	-	-	

A.1.9. TEST ROOMS OPERATION

The operation of the test rooms is specified for each validation exercise. The operational parameters includes: lighting, internal loads, thermostat schedules, special window coverings, etc.

A.2 INPUT FOR SYSTEM MODEL

Information in this section provides an over view of the HVAC air-side system used for conditioning the test rooms. A dedicated air-distribution system is used to condition the “A” test rooms while a second dedicated air-distribution system is used to condition the “B” test rooms. The air handling units are referred to as AHU-A and AHU-B. The remaining spaces in the ERS are conditioned from a third air-distribution system referred to as AHU-1. The focus on the information presented here is for the HVAC systems that serve the “A” and “B” test rooms.

The air handling units contain chilled water coils and heating water coils. Chilled water can be provided from an air-cooled chiller or from district chilled water provided by the campus facility. Heating water is provided by a natural gas-fired boiler. Each air handling unit is equipped with a supply fan and a return fan, both of which have variable frequency drives, and each unit is instrumented to provide operational data such as temperatures and flow rates. Figure A.3 illustrates the air-handling unit and sensors

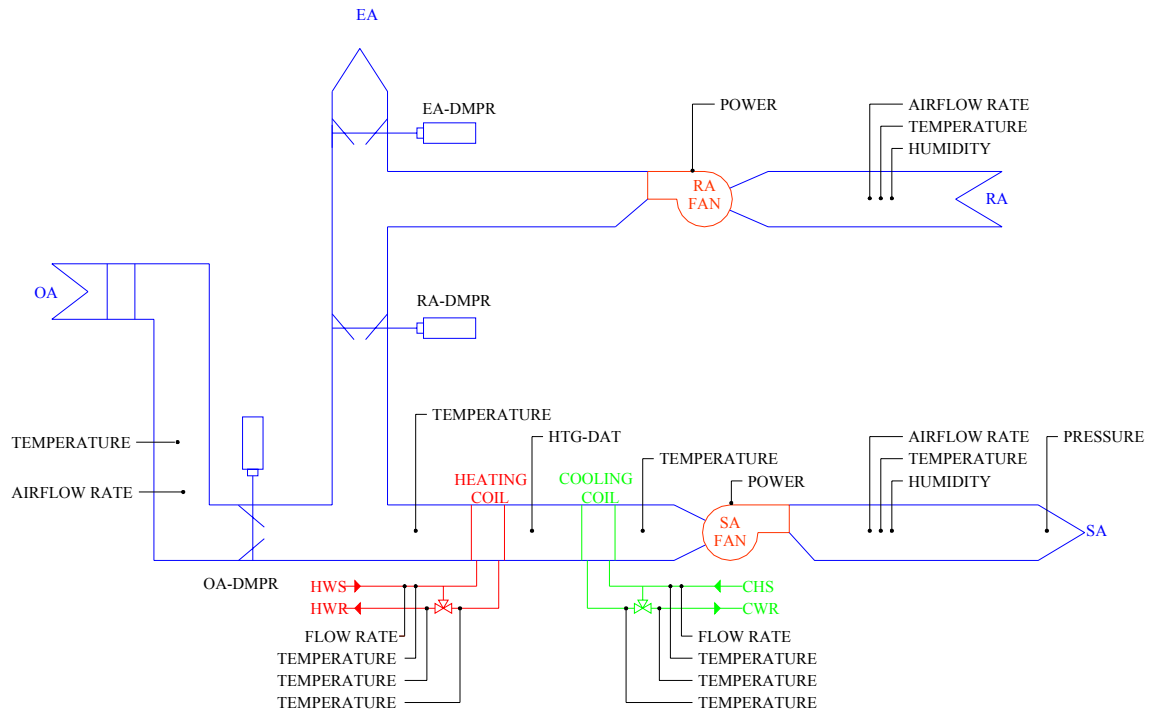


Figure A.3 Air handling unit

The building automation system provides for a great variety of system operational modes and parameter control. Each validation exercise requires a complete control and operational specification to assure the system is properly configured for the desired test.

The air-distribution system for the test rooms is illustrated in Figure A.4. The figure illustrates some of the flexibility available for testing. Again, the building automation system provides for flexibility in the specification of the operational and control parameters for each test room. For example, reheat can be provided either from an electrical resistance coil or a hydronic coil. Although not shown in the figure, another zone level system that can be used for space conditioning includes a four-pipe fan coil unit. Each validation exercise requires a complete control and operational specification to assure the zone level systems are configured properly.

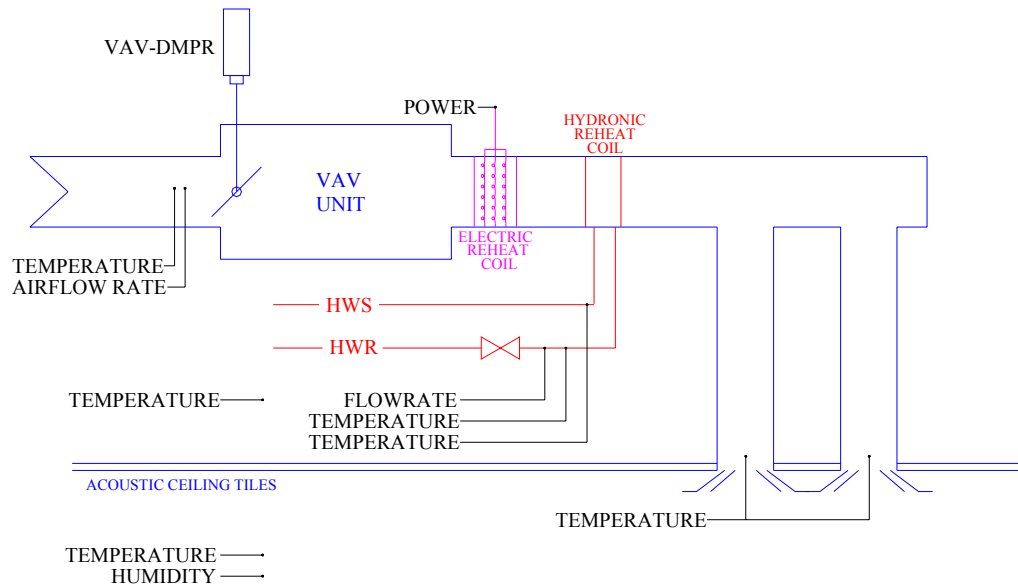


Figure A.4 Zone level HVAC system

Appendix B Uncertainty Analysis

For every experiment, there are errors that are associated with the measured parameters. Experimental error is the variation among observations and measurements that are treated alike. The errors for the experimental parameters measured at the ERS were quantified using information obtained from calibrations and corrections, manufacturer information, and current literature. The error values were used to estimate the experimental error for calculated quantities in the experiment. This was done using a Propagation of Error formulation.

B.1 Calibration Information

An extensive set of calibrations was performed at the ERS for the resistant temperature devices (RTD) at the ERS (Wen and Smith, 2001). In this procedure, the measurements from the individual RTDs were compared with a Hart 1522 thermometer, the so-called gold standard. The calibration results from this endeavor were used to quantify the portion of the error for the RTDs. A sample of the temperatures used for the final calibration check was used for regression to perform a regression analysis. Ninety-five percent uncertainty bands were calculated to quantify the part experimental error linked to the calibration. Figure B1 shows the plot with a linear regression analysis and the uncertainty bands for the mixed air temperature for the “A” system.

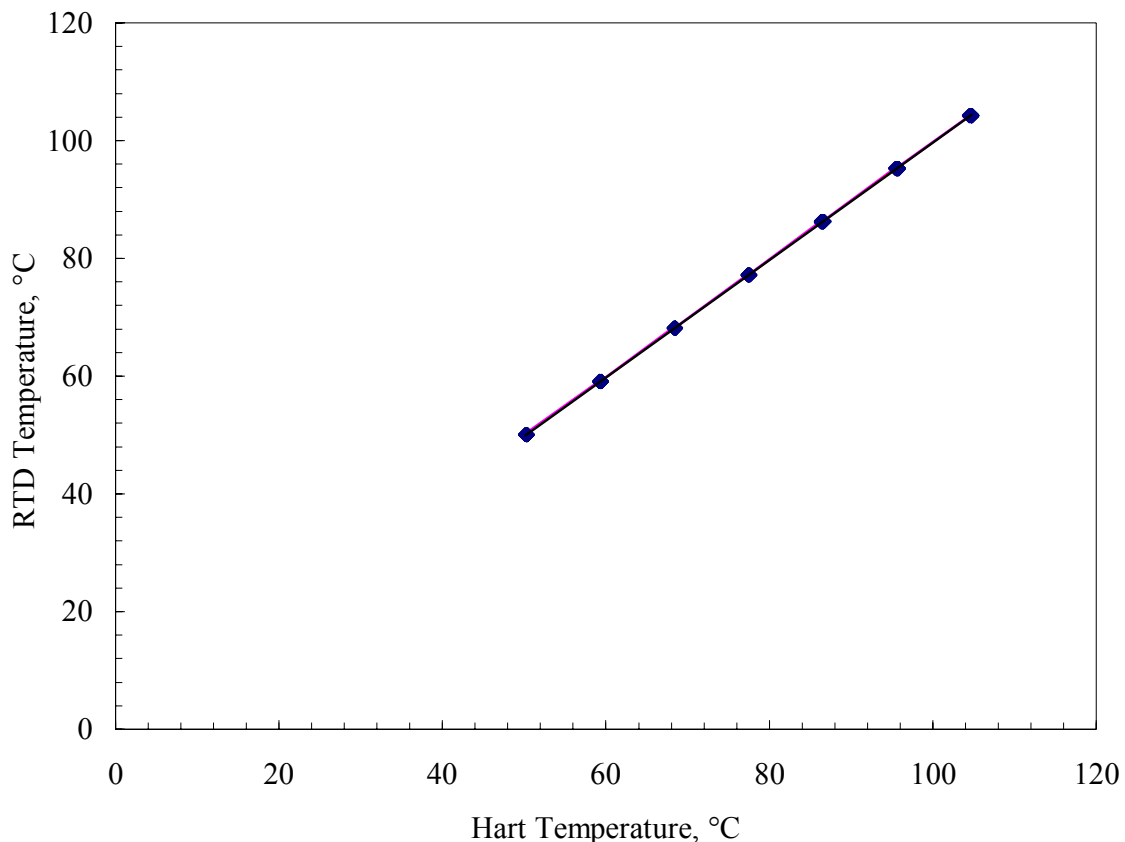


Figure B.1 Hart temperature versus RTD temperature with 95% uncertainty bounds.

From Figure B1, the uncertainty bands are small, primarily due to good correlations. The linear relationship between the Hart and the RTD temperatures is shown in Equation B1. Tables B1, B2, and B3 contain information from the regression analysis for the temperatures.

$$T_{RDT} = 0.9967529 T_{HART} - 0.063006 \quad (B1)$$

where

T_{RDT} is the temperature of the RTD, in °C.

T_{HART} is the temperature of the Hart thermometer, in °C.

Table B.1 Summary of the fit for the temperature calibration.

Term	Estimate
R-Square	0.999975
R-Square Adjusted	0.999974
Root Mean Square Error	0.091288
Mean of Response	77.29286
Observations	216

Table B.2: Analysis of variance for the temperature calibration.

Source	Degrees of Freedom	Sum of Squares	Mean Square
Model	1	70,050	70,150.21
Error	214	1.781	0.0083823
Corrected Total	215	70,152	

Table B.3: Parameter estimates for the temperature calibrations.

Term	Estimate	Standard Error	t Ratio	Prob> t
Intercept	-0.063006	0.027358	-2.30	0.0222
X-Component	0.9967529	0.000343	2903.2	0.0000

The associated error from the RTD was calculated from a 95% uncertainty bands. The temperature variance with respect to the gold standard was calculated using Equation B2.

$$\sigma_{Hart} = \frac{\pm N \sqrt{MSE}}{\beta_1} \quad (B2)$$

where

N is the Gaussian distribution quantity for a 97.5% quantile.

MSE is the mean squared error value.

β_1 is the slope of the line from the regression analysis.

There were also small measurement errors for the Hart thermometer quantifies by the manufacturer. The manufacture error values are for the ERS are shown in Table B7. To assign a 95% interval of uncertainty for the temperature parameter, Gleser (1998) proposed a method for dealing with different types of errors variances, which is shown in Equation B3.

$$\sigma_{Total} = \sqrt{\sigma_{Hart}^2 + 1.96^2 \sigma_{Hart,error}^2} / 3 \quad (B3)$$

where

$\sigma_{Hart,error}$ is the error bounds for the Hart thermometer provided by the manufacture.

Similar analyses for two additional RTDs were performed. There were very minute discrepancies. Therefore, the relationship developed for the mixed air RTD for the “A” system was used for the all the RTDs in the experiments.

B.2 Corrected Data

Immediately following the Daylighting Test 2 experiment, discrepancies were realized for the room airflow rates. An experimental apparatus was assembled to measure the airflow rates in the duct using a pitot tube traverse at low airflow rates and a flow hood for high airflow rates. These values were compared with the building control’s airflow rate measurements. A correlation with building control measurements and a regression analysis was performed to correct measurement errors. The linear relation from the regression analysis was used to post-process the room airflow measurements. Figure B2 shows the results of the regression analysis for the East “A” airflow rates. Ninety-five percent uncertainty bounds were used for the error calculations.

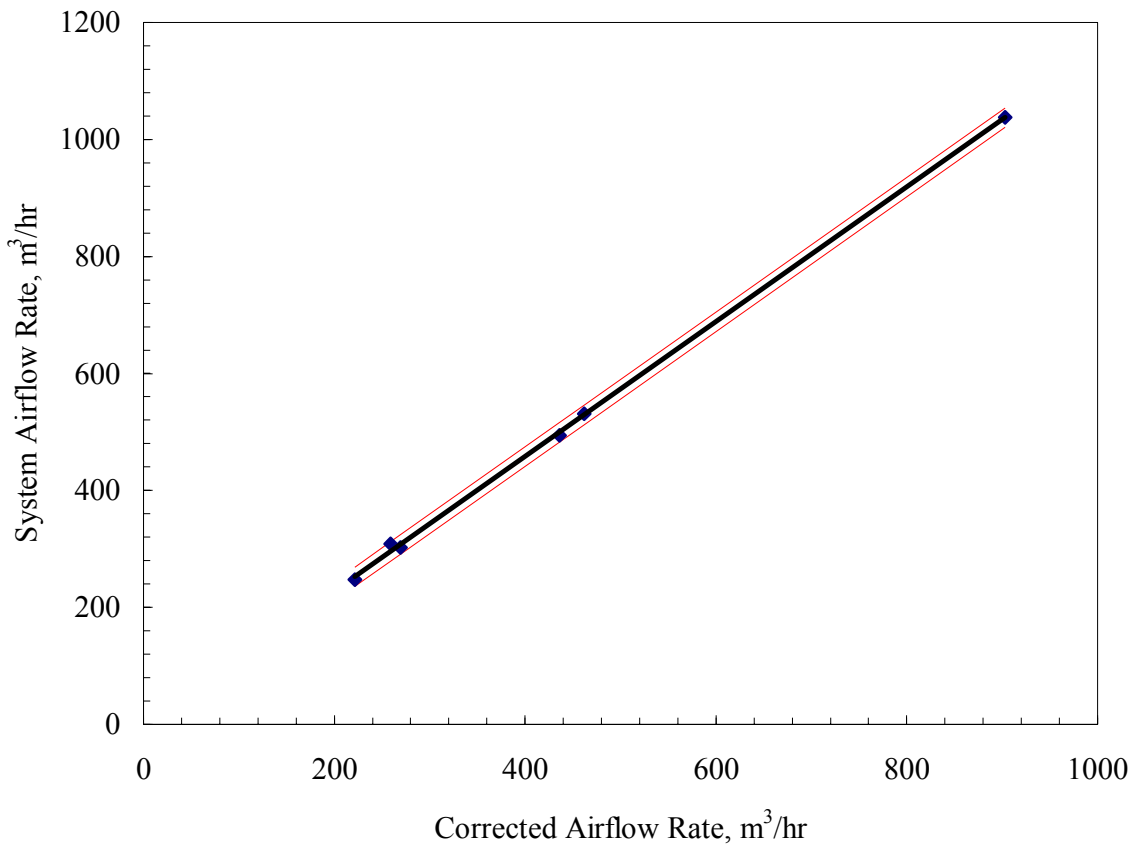


Figure B.2 East “A” test room airflow rate correction curve.

Equation B4 is the linear fit from the regression analysis. Tables B4, B5, and B6 contain the results from the regression analysis.

$$Q_{system} = -2.565086 + 1.151116 Q_{Cor} \quad (B4)$$

where

Q_{Cor} is the airflow rate measured by the system in m³/hr.

Table B.4 Summary of the fit for the airflow rate correction.

Term	Estimate
R-Square	0.999361
R-Square Adjusted	0.999201
Root Mean Square Error	8.276338
Mean of Response	486.8506
Observations	6

Table B.5 Analysis of variance for the airflow correction.

Source	Degrees of Freedom	Sum of Squares	Mean Square
Model	1	428,496.32	428,496
Error	4	273.99	68
Corrected Total	5	428,770.32	

Table B.6 Parameter estimates for the airflow correction.

Term	Estimate	Standard Error	t Ratio	Prob> t
Intercept	-2.565086	7.05027	-0.36	0.7344
X-Component	1.151116	0.014554	79.09	<.0001

Similar regressions analyses were performed to correct the airflow rates for the other test rooms. The error from post-processing of the data is estimated by Equation B5. A 95% uncertainty bound was used to calculate the error value.

$$\sigma_{Flow} = \frac{\pm t\sqrt{MSE}}{\beta_1} \quad (B5)$$

where

t is the student distribution quantity for a 97.5% quantile.

MSE is the mean squared error value.

β_1 is the slope of the line from the regression analysis.

Base on literature about airflow rate measurement with a pitot tube traverse and flow hoods, the error is 1-5% of the measured value (Schroeder et al, 2000). Therefore, the total error for the airflow rates for Daylight Case II was estimated in a similar manner as the temperatures. This relationship is shown in Equation B6.

$$\sigma_{Total Flow} = \sqrt{\sigma_{Flow}^2 + (1.96(0.01Q_0))^2} \quad (B6)$$

The statistical parameter used to calculate the 95% uncertainty bounds for the test rooms are shown in Table B7.

Table B.7 Statistical parameters for uncertainty bound calculations for zone airflow rates.

Location	n	MSE	β_l
East "A"	6	68	1.151116
East "B"	6	342	1.2283747
South "A"	6	279	1.1173097
South "B"	5	218	1.108725
West "A"	6	178	1.1540728
West "B"	5	144	1.1849076
Interior "A"	6	408	1.0939741
Interior "B"	6	1319	1.1321554

B.3 Propagation of Error

Several parameters that were compared with output from the building simulation software were not measured directly during the experiment. These values were later calculated as functions of measured experimental parameters. The calculated quantities included: room reheat power and cooling heat transfer rate. The calculations for the reheat power and the cooling heat transfer rate are described in Equations 5.2.1 and 5.2.2, respectively.

The reheat energy for the zone was calculated using the propagation of error. Equation B7 describes how the error was calculated.

$$\sigma_{reheat}^2 = \left(\frac{\partial q_{zone}}{\partial p} \sigma_p \right)^2 + \left(\frac{\partial q_{zone}}{\partial Q_{zone}} \sigma_{Q_{zone}} \right)^2 + \left(\frac{\partial q_{zone}}{\partial T_{EAT}} \sigma_{T_{EAT}} \right)^2 + \left(\frac{\partial q_{zone}}{\partial p} \sigma_p \right)^2 + \left(\frac{\partial q_{zone}}{\partial c_p} \sigma_{c_p} \right)^2 + \left(\frac{\partial q_{zone}}{\partial T_{DAT}} \sigma_{T_{DAT}} \right)^2 + \left(\frac{\partial q_{zone}}{\partial T_{EAT}} \sigma_{T_{EAT}} \right)^2 \quad (B7)$$

Similar calculations were made for the cooling heat transfer rate. The system airflow rate was calculated by summing the room airflow rates. Thus the errors associated with the rooms impacted the system airflow rate calculation.

The average error for a given experiment was calculated by taking the arithmetic mean of the hourly errors. These values are provided in the comparison tables from the results section of each compared parameter contained within the main body of the report. For many quantities, it was impossible to perform statistical analyses and estimate of uncertainty. Therefore, many error values were estimated using manufactures information or information from current literature. This information is contained in Table B8.

Table B.8 Accuracy of ERS instrumentation.

Name	Units	Uncertainty
HART 1522 Thermometer	°C	± 0.0025
Outside Airflow Rate	ft ³ /min	$\pm 2\%$ of Reading (> 500 ft ³ /min) $\pm 10\%$ of Reading (< 500 ft ³ /min)
Room Airflow Rates	ft ³ /min	$\pm 2\%$ of Reading
Room Light Power	W	$\pm 0.2\%$ of Reading
Barometric Pressure	millibars	± 0.75 millibars
Outside air humidity	% RH	$\pm 2\%$ of RH
Pyranometer	Btu/(hr-ft ²)	$\pm 0.5\%$ of Reading
Pyrheliometer	Btu/(hr-ft ²)	$\pm 0.5\%$ of Reading
Wind Direction	°	$\pm 1^\circ$
Wind Speed	mph	± 1 mph
Constant Specific Heat for Air	J/kg-K	$\pm 2\%$ of Reading

Appendix C Hourly Averaged Experimental Data

This appendix describes the data found on the CD-ROM that accompanies this report. The data can be used by modelers who wish to make comparisons with the daylighting tests conducted in IEA Task 22 Subtask D. The CD contains two ASCII text files, two Microsoft Excel files and a pdf version of this report.

C.1 Weather Data

The ASCII text files are TMY weather files that contain the processed weather information collected at the Energy Resource Station during the tests. The test dates for Daylighting Case 1 were: April 19, 2002 through April 23, 2002. The weather file is called “IEA2002.TMY”. The test dates for Daylighting Case 2 were: January 29, 2003 through February 2, 2003. The weather file is called “IEA2003.TMY”. Although each TMY file is for a full year, only the specified test dates contain data based on weather measured at the ERS. The remainder of the TMY file is from a standard Des Moines, IA TMY file.

It is important to note that ERS modified weather information included in the TMY file does not replace all weather related data. For example, the sky conditions, amount of rain fall, etc. are not altered from their original values. The only TMY fields that are modified to reflect weather data measured at the ERS are shown in Table C.1

Table C.1 Fields modified in the TMY weather files

Field Number	Position	Element
003	006 - 015	Solar Time
102	024 – 028	Direct Radiation
108	054 – 058	Total Horizontal Radiation
206	099 – 103	Station Pressure
207	104 – 111	Temperature
208	112 – 118	Wind

C.2 Hourly averaged data

The Microsoft Excel files contain hourly averaged values of data collected during each daylighting test. During a test, information is recorded on a one-minute time interval. For comparison purposes, the data are averaged over a one-hour period. The graphs in this report illustrating ERS results are based on the hourly-averaged values found in these files. The Excel file names for the two tests are called “Daylighting Case1.xls” and “Daylighting Case2.xls”, respectively.

The two Excel spreadsheet files are organized using tabs. Each tab is a worksheet that contains values for a particular air handling unit system or a particular test room. One additional tab includes measured visible light levels on the outside of the ERS.

C.3 Air Handling Unit Data

Figure C.1 is a schematic of an air handling unit that serves the test rooms at the ERS. The “point names” in the figure represent locations where measurements are made; however, not all of these measurements are relevant for the daylighting tests. Table C.2 provides a list of the point names and their description that are relevant for the daylighting tests. These names appear as column headings for the spreadsheets labeled as “System A” and “System B” in the Excel files.

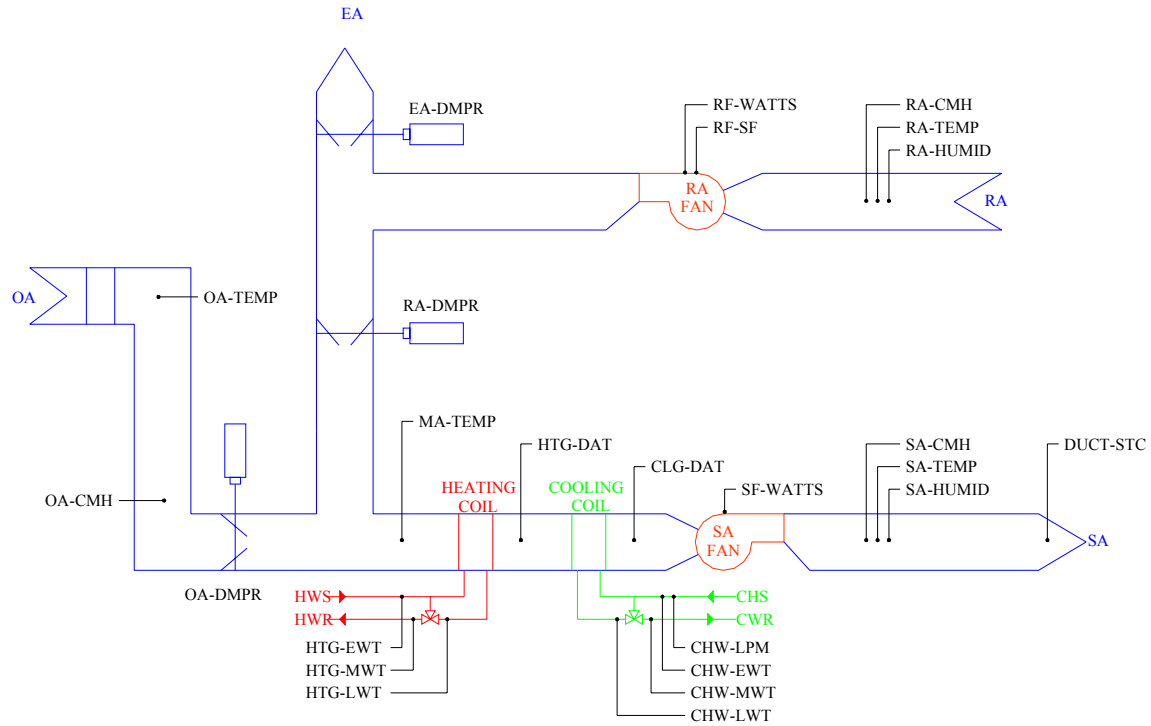


Figure C.1 Air handling unit schematic

Table C.2 AHU System A and System B Nomenclature

OA-CMH	Outside air flow rate [m ³ /hr]
OA-TEMP	Outside air temperature [°C]
OA-DMPR	Outside air damper position [% open]
CHW-LPM	Cooling coil water flow rate [liter/min]
CHW-EWT	Cooling coil entering water temperature [°C]
CHW-MWT	Cooling coil mixed water temperature [°C]
CHW-LWT	Cooling coil leaving water temperature [°C]
CLG-DAT	Cooling coil discharged air temperature [°C]
RA-TEMP	Return air temperature [°C]
RA-HUMID	Return air humidity [%]
RF-WATTS	Return fan power [Watts]
RF-SF	Return fan speed as a percent of supply fan speed
RA-DMPR	Return air damper position [% open]
EA-DMPR	Exhaust air damper position [% open]
MA-TEMP	Mixing air temperature [°C]
SA-CMH	Supply air flow rate [m ³ /hr]
SA-TEMP	Supply air temperature (after supply fan) [°C]
SA-HUMID	Supply air relative humidity (after supply fan) [%]
SF-WATTS	Supply fan power [Watts]
DUCT-STC	Supply duct static pressure [kPa]

C.4 Test Room Data

Figure C.2 is an HVAC schematic of a test room at the ERS. The “point names” in the figure represent locations where measurements are made; however, not all of these measurements are relevant for the daylighting tests. Table C.3 provides a list of the point names and their description that are relevant for the daylighting tests. These names appear as column headings for the spreadsheets labeled as test rooms in the Excel files. The spreadsheet tab names for the test rooms are East A, East B, Interior A, Interior B, South A, South B, West A and West B.

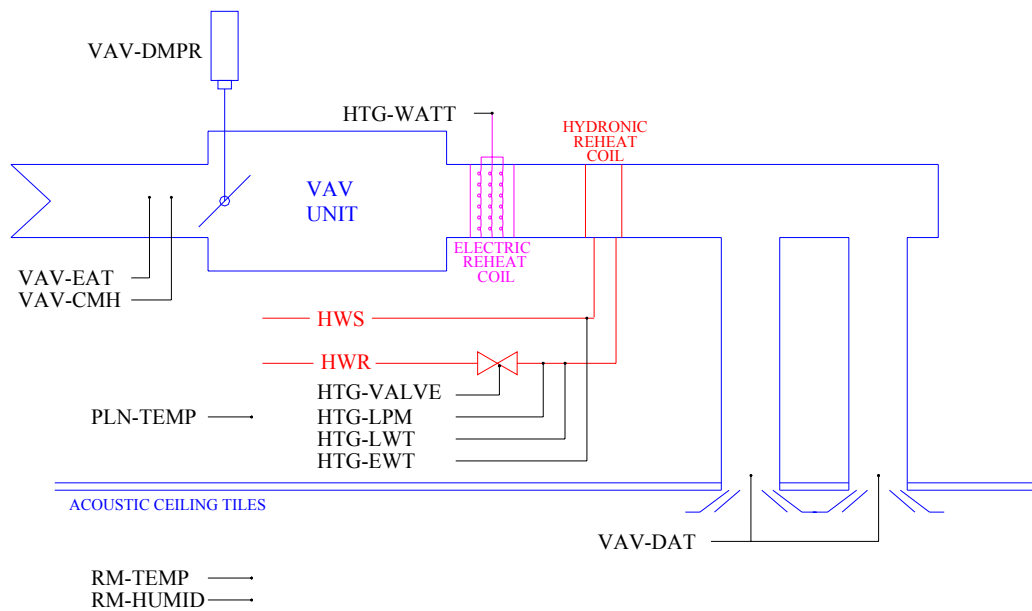


Figure C.2 Test Room HVAC Schematic

C.5 Exterior Illuminance Data

The ERS is equipped with four light sensors located on the outside of the building. These sensors measure visible light levels in a hemispherical field of view. One sensor is located on the roof and is oriented to measure the visible light falling on a horizontal plane from the entire sky. The other three sensors are vertically mounted just above the windows on the East, South and West walls of the building. The exterior illuminance values, in Lux, are on the spreadsheet tab labeled “Outside Light Level”.

Table C.3 Test rooms (East, South, West, Interior) nomenclature

HTG-VALVE	Hydronic reheat coil control valve position [% closed]
HTG-LPM	Hydronic reheat coil water flow rate [liter/min]
HTG-LWT	Hydronic reheat coil entering water temperature [°C]
HTG-EWT	Hydronic reheat coil leaving water temperature [°C]
VAV-CMH	VAV air flow rate [m ³ /hr]
VAV-EAT	VAV discharge air temperature [°C]
VAV-DAT	VAV entering air temperature [°C]
VAV-DMPR	VAV damper position [% open]
PLN-TEMP	Room plenum temperature [°C]
RM-TEMP	Room temperature [°C]
LIGHT-LVL	Illuminance at the reference point [lux]
LIGHT-WATT	Room electric light power [Watts]

Appendix D Modelers Reports

This appendix presents the Modeler Reports from the organizations that participated in IEA Task 22 Subtask D. These reports address any information that the modelers wish to share which explains or clarifies their model validation results.

Modeler's Report
Clemens Felsmann
Technical University of Dresden
felsmann@tga.tu-dresden.de
May 2003

1. Model and simulation program

All the tests were done with TRNSYS TUD a modified and rewritten version of TRNSYS 14.2. At the Dresden university the original TRNSYS program source code was subjected to a lot of changes as well as additions to create a tool characterized by very specific properties in regard to the simulation and analysis of both operation and control of HVAC-systems in buildings.

The building model is the standard TRNSYS multizone model. All information (zone dimensions, orientations, materials etc.) that are required to build a TRNSYS model of the ERS were taken from a large set of architect's plans. It is a time consuming procedure to get all the data from the plans and put them into the model.

The model of the HVAC system consists of a series of energy and mass flow balance equations dealing with heat and moisture transfer. The components (chiller, cooling coil, hydronic reheat) are not described in physical detail. Due to the simplified modeling it is also not necessary calculate the pressure drops in the duct system.

With the assumption that the cooling load always can be served the chiller leaving temperature was set to a fixed value. This fixed value was calculated from the supply air set point temperature minus the temperature rise caused by the supply fan.

Both building and HVAC system model already were validated during former empirical tests conducted at the ERS.

Normally a daylighting model in TRNSYS does not exist. Nevertheless, a simple daylight calculation algorithm was implemented into TRNSYS to run the daylight tests. The calculation method used bases on the daylight factor method. The daylight factor is the ratio of the illuminance at a point on a given plane due to the light received from the sky, to the illuminance on a horizontal plane due to an unobstructed hemisphere of this sky. The contribution of direct sunlight to both values are excluded. The influences of glazing, dirt effects, etc. are included. These definitions are in accordance with the situation at the ERS building where white muslin drapes were used to internally shade the windows. By this way no direct solar radiation has to be taken into considerations. The radiation entering the room is treated as totally diffuse.

The light sensors were always located at the work plane. The daylight factor for these reference points were calculated with geometric data of the rooms.

In the Daylight Tests the luminous efficacy of radiation was used to estimate the illuminance at the outside. The luminous efficacy of radiation is the quotient of the luminous flux, by the corresponding radiant flux. In the simulation runs a constant value of 115 lm/W was used.

The simulation time step is fixed to 0.005 h. This low value is caused by the PI-control strategies for the VAV boxes (air flow and hydronic reheater).

2. Test Cases

There are two daylight test cases that are detailed in the appropriate specifications. Once the models of the building and the HVAC system are created it is not very difficult to get complete simulation models according to specific test parameters.

The parameters of test cases 1 and 2 mainly differ in the schedule for artificial lighting. There are also some minor differences in minimum airflow rates as well as in the ranges of the lighting power.

3. Results

Three different types of output information were analyzed: global, system and zone data. All output data required to fill out the pre-formatted data sheets are available in TRNSYS-TUD.

The calculated light power profile matches the experiment with a sufficient accuracy.

In general the differences between simulation and experimental data are less for Daylight Test 2 compared to Daylight Test 1.

Especially there were big difficulties to predict air flow rates and reheat energy in a right way. For Daylight Test 1 this may be caused by strong stratification effects in the test rooms. Different supply air temperatures due to different heat gains from the duct system as well as from the fan could be another reason for data mismatch. In Daylight Test 2 the reduction of the supply air temperature by less than 1K leads to a reduction of the supply air flow rate by 10-15%. At the same time the reheat energy increases by round about 10%. The supply air temperature is influenced by the air temperature leaving the cooling coil and the duct heat gains including the heat gain from the supply fan.

The comparison of loads from simulation against experiment is not very meaningful since the load can not be measured but only recalculated from experimental data. Unfortunately these data by them self underlay measurement uncertainties.

Transmission loads depend from surface temperatures and film coefficients, too. The effect of the operation of the destratification fan on the film coefficients was neglected.

4. Summary

The simple daylight calculation method that was implemented seems to be accurate enough to simulate the interaction between natural and artificial lighting and how do they influence thermal loads.

Regardless the simulations do not completely match the experiments the daylight tests are excellent examples to study and analyze real physical effects and how to incorporate them in the simulation model.

The tests were also very useful to gain first experiences in simple daylighting simulation with TRNSYS-TUD.

Modeler's Report

Peter Loutzenhiser and Gregory Maxwell

Iowa State University

gmaxwell@iastate.edu

May 2003

The main objective of this report was to describe the modeling strategy used for the empirical validation exercise developed at the Iowa Energy Resource Station (ERS) by Iowa State University, Ames, Iowa, using DOE-2.1E.

The LOADS model was developed for the matched set of test rooms at the ERS. A system model was created for the "A" and "B" test rooms. Building construction documentation was used to obtain information about the wall, roof, and slab construction layers as well as windows. The walls separating the test rooms from the remainder of the ERS were modeled as adiabatic.

The thermal mass of the test rooms presented a problem for the first iterations of the daylighting tests for the baseboard heat load. The best results were obtained when the load was modeled as an instantaneous convective load. Information from the window manufacturer coupled with the DOE-2.1E windows library helped create a more sophisticated window model. Many default values provided by the program were used when specific values could not be obtained.

References

- Gleser, G.L. 1998, "Assessing Uncertainty in Measurement", *Statistical Science*, Vol. 13, No.3:277-290
- Schroeder, C.C., Moncef, K., Brandemehl, M.J., 2000, "Error Analysis of Measurements and Control Techniques of Outside Air Intake Rates in VAV Systems", *ASHRAE Transactions*, Vol. 106, Part 2:26-38
- Wen, J., Smith, T.F., 2001, *Calibration and Check Procedures for Temperature Sensors at the Iowa Energy Center Energy Resource Station*, Department of Mechanical Engineering, University of Iowa, Technical Report: ME-TFS-01-009